6-24-2010

Evaluation of selected airport pavements in New Mexico

Raju Bisht

Raju Bisht
Candidate

Civil Engineering
Department

This thesis is approved, and it is acceptable in quality and form for publication:

Approved by the Thesis Committee:

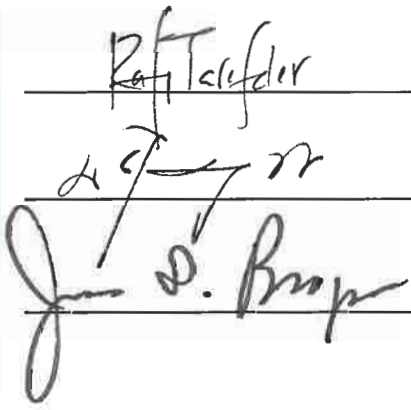

, Chairperson

EVALUATION OF SELECTED AIRPORT PAVEMENTS IN NEW MEXICO

BY

RAJU BISHT

M.SC.,CIVIL ENGINEERING, TASHKENT AUTOMOBILE AND ROAD CONSTRUCTION INSTITUTE, TASHKENT,UZBEKISTAN, 1987

THESIS

Submitted in Partial Fulfillment of the
Requirements for the Degree of

Master of Science

Civil Engineering

The University of New Mexico
Albuquerque, New Mexico

May, 2010

DEDICATION

To family and friends

AKNOWLEDGEMENTS

I would like to thank Dr. Rafiqul A. Tarefder, my advisor and thesis committee chair, for his support, time and encouragement for this study. His guidance and professional style will always remain with me.

I would like to thank my thesis committee members: Dr. James D. Brogan and Dr. Tang-Tat Ng for their valuable recommendations pertaining to this study and assistance in my professional development.

Gratitude is extended to the New Mexico Department of Transportation - Aviation Division (NMDOT-AD) for the funding to pursue this research. I also thank Ms. Jane Lucero, Airport Development Administrator of NMDOT, Mr. Robert McCoy, Head of the Pavement Exploration Section of NMDOT, and the Field Exploration Crew of NMDOT for their assistance in field testing and materials collection.

Special thanks go to Mr. Mesbah Uddin Ahmed, Graduate Research Assistant at UNM and Ryan Webb, Undergraduate Research Assistant at UNM who helped me with the laboratory testing.

EVALUATION OF SELECTED AIRPORT PAVEMENTS IN NEW MEXICO

BY

RAJU BISHT

ABSTRACT OF THESIS

Submitted in Partial Fulfillment of the
Requirements for the Degree of

Master of Science

Civil Engineering

The University of New Mexico
Albuquerque, New Mexico

May, 2010

EVALUATION OF SELECTED AIRPORT PAVEMENTS IN NEW MEXICO

by

Raju Bisht

M. Sc., Civil Engineering, University of New Mexico

Albuquerque, NM, USA 2010

M. Sc., Civil Engineering, Tashkent Automobile and Road Construction Institute,

Tashkent, Uzbekistan 1987

ABSTRACT

Rehabilitation of poor conditioned airport pavements can be very expensive compared to the rehabilitation of relatively good conditioned airport pavements. Determining the conditions of airport pavements is a first step to determine appropriate rehabilitation method and timing. In this study, the conditions of 10 airport pavements in New Mexico are evaluated. Those airports include a total of 19 runway pavements. The major goal is to rank these airport pavements based on their functional and structural conditions. The functional conditions of the pavements are evaluated based on the field collected surface distress data and skid resistance. Field collected distress data such as rutting, cracking, and shoving are processed using MicroPaver, a commercial pavement management software, to calculate the Pavement Condition Index (PCI). Field collected skid resistance test data are processed to obtain a single value Skid Number (SN). Drilling and field coring are performed to collect samples of asphalt cores, base aggregate, and soils. These

samples are then transferred to the Pavement Laboratory at the University of New Mexico for testing. Soil tests include index properties, moisture, and classification tests. Using these laboratory test results, a strength parameter called the California Bearing Ratio (CBR) value of the subgrade soils is determined. Also, the CBR value of base aggregate is determined. These CBR values are used to rank the airport pavements according to the FAA's Advisory Circular 150/5320 – 6D. Asphalt concrete cores are tested for parameters such as resilient modulus (M_R), indirect tensile strength (ITS), void ratio, asphalt content, and aggregate gradation. These parameters are used to determine the structural strength of a pavement in this study.

Based on the PCI value, 5 out of 19 runway pavements are found to be in poor condition. These pavements have a PCI value of less than 55. The PCI value is used in pavement rehabilitation design. Based on the SN value, 6 out of 18 runway pavements are found to be in poor condition. Their SN values are below the minimum required value of 50. Low skid resistance can pose a threat to the safe operation of aircrafts on pavements during wet weather conditions. When PCI and SN values are combined to estimate the overall functional condition, 7 runway pavements are shown to be in poor condition, 7 in fair condition, and 4 in good condition.

Based on the subgrade CBR value, all the runway pavements look good because they passed the minimum required CBR value of 15 for subgrade. Based on the base course CBR value, all the pavements can be considered to have a fair to good base course. Ranking based on subgrade and base course CBR is important. A subgrade with a poor CBR value may need expensive rehabilitation measures because it requires removing the surface and base course in order to fix the subgrade. CBR value is useful for Aircraft

Classification Number – Pavement Classification Number (ACN-PCN) based rating of pavements. Based on the resilient modulus of asphalt concrete ($M_{R)}$, only one runway has shown to have poor performance with a value of 183.6 ksi, 3 runways have fair M_R values, and 10 runways have satisfactory M_R values. An indirect tension modulus of 300 ksi is considered to be good for existing surface course. The M_R value is used in mechanistic design of roadway pavements, however, it has not been adopted in airport pavement design yet. Based on the ITS value, all the pavements are in good condition. A pavement having an ITS value of greater than 100 psi is considered to be in good condition in this study. A pavement with a low ITS value is more likely to develop low temperature cracks during winter seasons. In addition to strength and modulus of asphalt cores, mix design parameters such as asphalt content, air voids, and aggregate gradation of surface course are determined. Five runways have over 7% air voids, 7 runways have between 4-7% air voids, and 2 runways have less than 3% air voids. A high percent of air voids can lead to higher permeability and moisture damage problems. Low air voids can lead to rutting problems. Five runways have more than 7% asphalt content, and nine runways have 5-7% asphalt content. Low asphalt content (2-3%) can be a problem in terms of pavement durability. Based on the structural strength calculated using CBR, M_R, and ITS, 1 runway is in poor condition, 9 in satisfactory condition, and 4 in good condition.

Overall, based on combined functional and structural strength, 2 runways are in poor condition, 6 runways in fair condition, 4 runways in satisfactory condition, and 2 runways in good condition. It is hoped that this ranking will help design the future alternative rehabilitations when it is time to apply such rehabilitation alternatives.

TABLE OF CONTENTS

LIST OF TABLES

LIST OF FIGURES

CHAPTER 1

INTRODUCTION

1.1 Problem Statement

Airports have pavements in the form of runways, taxiways, and aprons. The main function of these pavements is to serve the air-traffic safely, comfortably, and efficiently. With time and under repetitive air-traffic loading, the conditions of the airfield pavements deteriorate and one or more of the functions are compromised. As the reconstruction cost of a pavement is high, they must be protected through periodic rehabilitation and maintenance. Rehabilitating airport pavements in very poor condition can be up to three times more expensive than rehabilitating pavements in fair condition (USGAO 1998). Preventive maintenance is the best way to eliminate expensive rehabilitation. Therefore, these pavements should be evaluated through laboratory and field testing to determine their conditions accurately in order to build efficient and timely maintenance and rehabilitation strategies.

According to Haas et al. (1994), the condition of the pavement can be defined using four key measures: 1) Roughness (as related to serviceability or ride comfort), 2) Surface distress, 3) Surface friction (as related to safety), and 4) Deflection (as related to structural adequacy). Roughness is derived from the longitudinal profile of the pavement surface and affects the ride quality. Since the pavements are constructed for the users, roughness defines the functional response of the pavement and is the primary operating characteristic affecting the users. Distress is the deterioration of the surface, such as cracking and rutting. Although safety of the pavement surface is mainly related to surface friction or skid resistance, it is also affected by severe rutting or potholes. Structural

adequacy is the ability of the pavement to carry loads without resulting in undue distress. Structural evaluation can be used to estimate the future response of the pavement to load. The focus of this study is to rank airport pavements of 10 selected airports in New Mexico based on functional and structural strength.

It is beneficial to develop a database of the condition of the existing airport pavements at both the state and national level. In that way, the investments in airport pavements can be allocated in a timely manner. A database can help forecast the future condition of the pavements as well as provide pavement management personnel with sufficient time to plan for maintenance and/or rehabilitation. Timely maintenance can prolong major maintenance works and reduce the overall cost over time. The United States General Accounting Office (USGAO) recommended that the Federal Aviation Agency (FAA) improve existing runway condition information to create a database for forecasting anticipated maintenance needs. A runway condition database can help ensure that airports are funded in a timely manner to reduce reconstruction cost in the long run. In this study, data from a total of ten airport pavements are entered into a mini-database over the past two years. These data can be used to determine the future conditions and remedy using MicroPaver software.

In New Mexico, there are about 47 privately and government owned airports that had not been evaluated recently. A map of New Mexico with all the airports is shown in Figure 1.1. In 2006 and 2007, a distress survey was carried out. The distress data are analyzed using MicroPaver, a pavement management software, to determine the Pavement Condition Index (PCI). The PCI value is used to determine the functional conditions of the pavements of the 10 airports. Field and laboratory tests are performed to determine

the structural conditions. Field tests include the Falling Weight Deflectometer (FWD) test, skid test, and coring. Cores and underlying base, subbase, and subgrade materials are collected and tested in the laboratory. These data are used to populate the database, and engineering analyses are carried out to gain a comprehensive understanding of the remaining service life of airport pavements and their past performance.

1.2 Hypothesis

Airport pavements can be evaluated using the surface distress data. However, this is not sufficient since surface data does not provide enough information about the structural strength of pavements. A pavement may show an adequate surface roughness, but its structural condition may not be good at all. So far, there is no symmetric study of both functional and structural health of a network of airport pavements. A complete evaluation requires analyzing both the functional and the structural health of the pavements. If the functional and structural health conditions can be combined, it will provide the overall condition of the airport pavements. In this study, it is hypothesized that the functional and structural strength can be combined to rank airport pavements.

1.3 Objectives

The objectives are to:

1. Determine the functional conditions of 10 airport pavements using surface distress data collected through field survey. In particular, determine Pavement Condition

Index (PCI) using the distress data and Skid Number (SN) using the skid resistance data.

2. Determine the structural strength of 10 airport pavements. Characterize asphalt core, soil, and base aggregate materials from each runway. Soil tests include gradation, Plasticity Index (PI), moisture, and classification test. Base aggregate is tested for gradation and classification only. Asphalt cores are tested for resilient modulus (M_R), indirect tensile strength (ITS), void ratio, asphalt content and gradation.

3. Combine the structural and functional condition of the pavements in a single index value. Using this combined index, rank the pavements of the 10 airports.

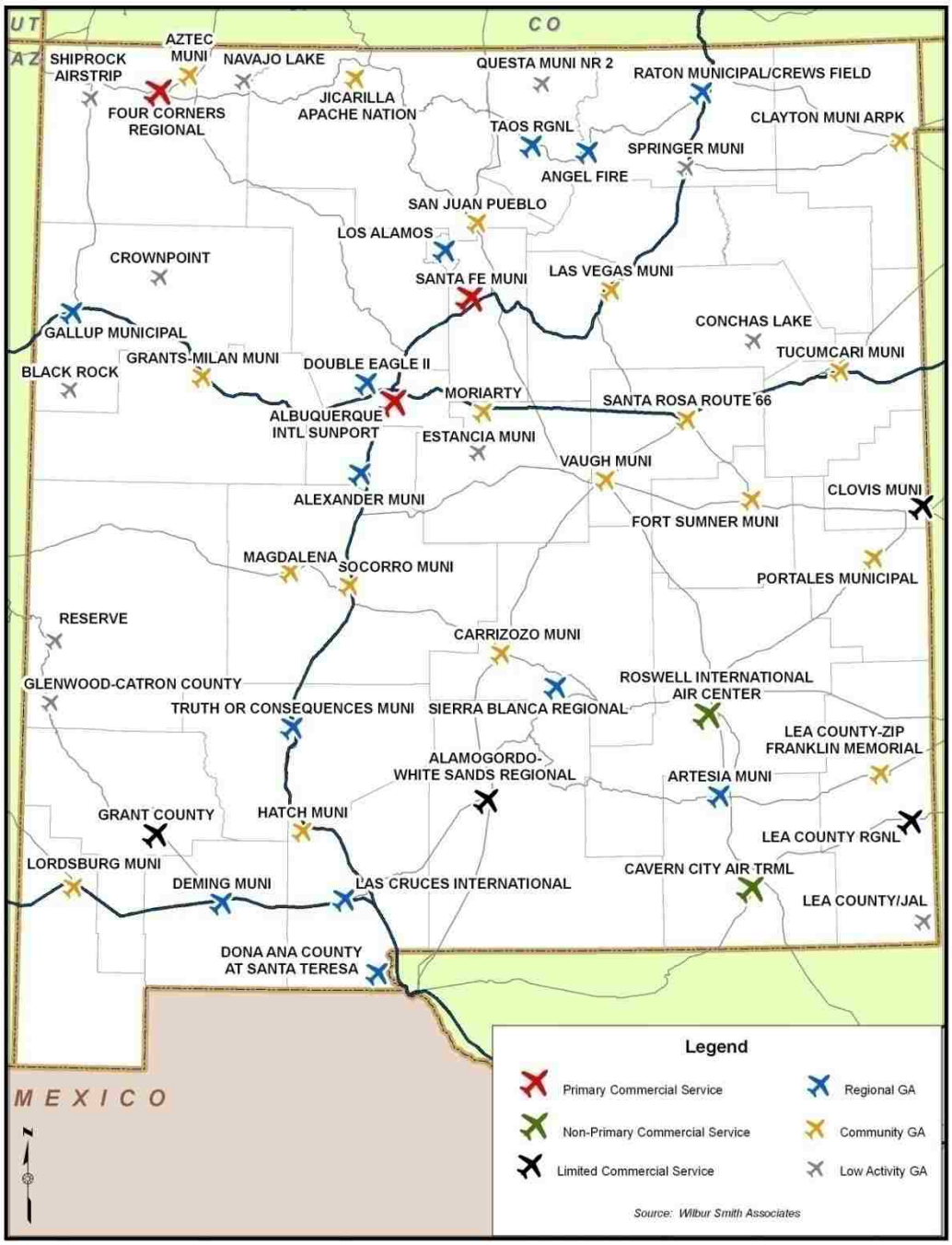

Figure 1.1 Map of New Mexico Airports

CHAPTER 2

LITERATURE REVIEW

2.1 Recent Evaluation of Airport Pavements

Buttlar et al. (1999) conducted a study on the rehabilitation alternatives for runway 18-36 at Rantoul Airport in Champaign, Illinois. The evaluation of the pavement system included a visual survey, a full-scale Pavement Condition Index (PCI) Survey, Falling Weight Deflectometer (FWD) Testing, and Dynamic Cone Penetrometer (DCP) Testing. The PCI survey provides the type, extent and severity of distresses over a section. PCI analysis was performed using the ASTM method to manually determine the numerical index. There are sixteen types of distresses for asphalt concrete pavements with three levels of severity – low, medium and high. PCI calculation involves interpreting deduct values from deduct curves for each of the sixteen types of distresses. The deduct curve for alligator cracking is shown in Figure 2.1. As it can be seen in Figure 2.1, a deduct value of 0 means that the distress has no effect on the pavement structural integrity whereas a deduct value of 100 indicates an extremely serious distress. Deduct values for all the distresses are obtained. In this project, an automated PCI analysis program MicroPaver was used. MicroPaver can not only perform a quantitative assessment of the pavement condition but also design maintenance and rehabilitation strategies. The PCI values were as low as 17. Runway 18-36 was in a very poor or failed condition according to the PCI rating.

DCP values were converted to California Bearing Ratio (CBR) using an algorithm developed by Kleyn (1975) as follows:

$$\log(CBR) = 0.84 - 1.26\log(N_f) \tag{2.1}$$

where N_f is the number of blows per inch of DCP penetration.

The upper 12 inches of subgrade under runway 18-36 had an average CBR value of 3.5 and was evaluated as weak cohesive soil.

Bell et al. (2008) carried out a study for the US Army Corps of Engineers which involved evaluation of four Army airfield pavements in different states to develop a method for predicting the performance of aged Asphalt concrete (AC) surfaces in situ. The seismic modulus was measured on site using the Portable Seismic Pavement Analyzer (PSPA) and adjusted to find the AC design modulus at a temperature of 77 ^{o}F and design frequency of 15 Hz using the formula (Nazarian et al. 2005):

$$E_{77^{o}F} = \frac{E_{PSPA}}{\left[\left\{-0.0109\left[(T-32)\frac{5}{9}\right]+1.2627\right\}(3.2)\right]} \tag{2.2}$$

where $E_{77^{o}F}$ = AC design modulus in ksi, E_{PSPA} = modulus measured by the PSPA in ksi and T = pavement temperature in $^{\circ}$F.

Bell et al. (2008) established a correlation between Indirect Tension Strength (ITS) peak stress and AC design modulus as follows:

$$E = 1581(\sigma_{ITS}) + 219{,}200 \tag{2.3}$$

with root mean square error of 105,000 psi and $R^2 = 0.55$. Here, σ_{ITS} is the peak stress in indirect tension strength test. Results of their tests and calculations are presented in Table 2.1. It can be seen that the AC modulus varies from 355 to 763 ksi, whereas the indirect tensile strength varies from 118 to 358 psi. The peak value of ITS does not confirm that it is peak modulus. This is expected as the former is strength and the latter is stiffness. Stiffness and strength are different parameters of a material.

2.2 Pavement Condition Index

Shahin et al. (1978) summarized the concepts and theory that led to the development of the Pavement Condition Index (PCI). Pavement Condition Index (PCI) is a numerical value of pavement condition based on visual survey information. The PCI varies from 0 and 100, with 100 being excellent condition of pavements. The PCI for airport pavements was developed by the United States Army Corps of Engineers (ASTM D 5340 – 03). Determination of the PCI requires three pavement distress characteristics: type of distress, severity of distress, and amount of distress. The development of acceptable distress definitions and deduct values required extensive field testing, improvements and revisions. The process required having three experienced pavements engineers evaluate the airfield pavements to come up with the mean Pavement Condition Rating ($\overline{\text{PCR}}$). The Mean Deduct Value ($\overline{\text{DV}}$) is then calculated using the formula:

$$\overline{DV} = 100 - \overline{PCR} \tag{2.4}$$

In Shahin et al. (1978), the procedure was repeated for 16 distress types. It was found that the PCIs for sections with several distress types were lower than the PCRs. Since the deduct values were developed for different distress types, they cannot just simply be

added together. All deduct values less than five were omitted as they have little effect on the pavement condition. Further a graph (Figure 2.2) for the Corrected Deduct Value (CDV) was developed. CDV is obtained using the sum of the deduct values greater than five and the corresponding number of distresses. PCI for the section is calculated using the formula:

$$PCI = 100 - CDV \tag{2.5}$$

Shahin et al. (1978) evaluated the PCI of 38 sections from five airfields using the above procedure and found it correlated closely with the mean subjective Pavement Condition Rating ($\overline{PCR}$) of experienced pavement engineers.

Greene et al. (2004) studied the methodology used by the U.S. Air Force for assessing and rating airfield pavements condition. The factors addressed in the ratings include PCI, Structural Index (ratio of aircraft classification number to the pavement classification number), friction characteristics, and foreign-object damage (FOD) potential. According to Greene et al. (2004) study, the standard PCI rating has seven categories as shown in Table 2.2. The seven categories are Good (PCI = 86-100), Satisfactory (PCI = 71-85), Fair (PCI = 56-70), Poor (PCI = 41-55), Very Poor (PCI = 26-40), Serious (PCI = 11-25), and Failed (PCI = 0-10). However, for simplicity of presentation, the categories may be reduced to three: Good (PCI = 71-100), Fair (PCI = 56-70), and Poor (PCI = 0-55).

Muntasir (2006) collected airport pavement management data of over 1360 airports from 22 states and stored them in a MicroPaver database. Forty two states have successfully established the Airport Pavement Management System (APMS) and 75 percent of them use MicroPaver. Muntasir (2006) database includes four major types of pavement surface

such as Asphalt concrete (AC) pavement, Asphalt concrete over asphalt concrete (AAC) pavement, Portland cement concrete (PCC) pavement, and Asphalt concrete over portland cement concrete (APC) pavement. Muntasir (2006) reported that 81 percent of the pavements were initially constructed with an AC surface as opposed to 17 percent PCC. The area-weighted age of AC, AAC, PCC and APC is 12, 10, 25 and 13 years respectively. Muntasir (2006) study includes airports from four regions: Central, North Atlantic, Southern and Western. It is reported that even though the area-weighted age of PCC is twice that of AC, PCC is not the frequent choice of airport construction in any of the regions. Of the total pavement area, 42 percent was runway, 36 percent taxiway, 21 percent apron, and less than 1 percent helipad.

The study by Muntasir (2006) reported that AAC with a PCI value of 81 performed the best while APC with a PCI value of 70 performed the worst. Also, the taxiway in all of the regions was found to be in a better condition as compared to the other facilities. The pavement condition with age for different regions is shown in Table 2.3. It can be seen that pavement performance was slightly better in the Western region for the first 20 years whereas it was worst in the Southern region. The data suggested that the performance of AC pavement was better than that of AAC pavement for the first ten years with the exception of the Southern region. After ten years, the condition of the AC pavement deteriorates faster than that of AAC pavement. The performance of PCC pavement was better than that of the APC pavement in all age categories with the exception of 0-5 years in the Western region and 21-30 years in the Northern and Southern regions.

Garg et al. (2004) analyzed the pavement data of 30 airports from 10 states. Sixteen distresses defined in ASTM D 5340 were used for determining the PCI of HMA

pavements. The authors divided the distresses into five groups: i) Cracking – includes longitudinal and transverse cracks, alligator or fatigue cracking, block cracking, slippage cracking, and reflection cracking, ii) Disintegration – includes raveling and weathering, iii) Distortion – includes rutting, corrugation, shoving, depression, and swelling, iv) loss of skid resistance – includes bleeding, polished aggregate, and fuel spillage and v) Others – includes jet blast and patching distresses. The accumulated deduct values due to distresses in a group are defined as the reduction of PCI for the group as shown in Table 2.4. It can be seen that group I is responsible for higher PCI reduction value for runways as compared to taxiways and aprons suggesting that runways have more cracks. On the other hand, group III is responsible for higher PCI reduction values for taxiways and aprons as compared to runways suggesting that the taxiways and aprons have more distortion distresses such as rutting. Garg et al. (2004) also developed a formula to calculate the Structural Condition Index (SCI):

$$SCI = 100 - (100 - PCI) \times \frac{DSCI(\%)}{100} \tag{2.6}$$

where PCI = Pavement Condition Index, DSCI(%) is deduct SCI and is equal to the sum of the deduct values due to load related distresses.

Only the load-related distresses, alligator cracking and rutting, were considered for computing the SCI of flexible pavements. Higher values of SCI are desirable and the minimum required value is 80. Garg et al. (2004) reported that the SCI of runways is higher than the SCIs of taxiways and aprons. The slow speed of the aircraft on the taxiways and aprons and longer load durations are the contributing factors as both of them are related to HMA fatigue (alligator cracking) and pavement rutting.

2.3 California Bearing Ratio (CBR)

2.3.1 CBR Test

CBR test was developed by the California Department of Transportation. It is a strength test for evaluation of the strength of subgrades and basecourses. The procedure for finding the CBR value in the laboratory is described in ASTM D 1883. In the CBR test, a standard piston having an area of 3 $in.^2$ is used to penetrate the soil at a standard rate of 0.05 in. per minute. The pressure at each 0.1-in. penetration up to 0.5 in. is recorded and its ratio to the bearing value of a standard crushed rock is termed as the CBR:

$$CBR = \frac{P_1}{P_2} \times 100 \qquad (2.7)$$

where P_1 = unit load on piston for 0.1 or 0.2 inches penetration, P_2 = standard unit load for standard crushed rock (1000 psi and 1500 psi for 0.1 inches and 0.2 inches penetration respectively).

2.3.2 Correlation of CBR with Soil Index Properties

CBR is correlated to D_{60} (Sieve size through which 60 % passes), Passing #200 sieve (P_{200}), and Plasticity Index (PI) (NCHRP 1-37). Materials are divided into two groups: (i) coarse, clean and non-plastic soils and (ii) soils containing more than 12% fines and exhibiting some plasticity. For the first group i.e. non-plastic soils, the CBR value is correlated with to the D_{60} using the following equation:

$$CBR = 28.09(D_{60})^{0.358} \qquad \text{for PI} = 0 \qquad (2.8)$$

where D_{60} = sieve size through which 60 % materials pass. Equation 2.8 is limited to D_{60} values greater than 0.01 mm and less than 30 mm. For D_{60} less than 0.01 mm, the recommended value of CBR is 5. For D_{60} greater than 30 mm, the recommended value of CBR is 95. For soils containing more than 12 % fines and exhibiting some plasticity, the CBR value is correlated to the weighted Plasticity Index (wPI) using the equation:

$$CBR = \frac{75}{1 + 0.728(wPI)} \qquad \text{for PI} > 0 \qquad (2.9)$$

where wPI is the weighted Plasticity Index = Passing # 200 * Plasticity Index.

2.3.3 Correlation of CBR with M_R

Gopalakrishnan and Thompson (2006) evaluated and compared the subgrade characterization test results obtained from the pre-traffic and post-traffic test pit at the National Airport Pavement Test Facility (NAPTF) located at the Atlantic City International Airport, New Jersey. Their study developed the following correlations between CBR and M_R:

(i) Pre-traffic condition:

$$M_R = 1268\, CBR, \qquad R^2 = 0.80 \qquad (2.10)$$

(ii) Post-traffic condition:

$$M_R = 2596 CBR^{0.7564}, \qquad R^2 = 0.92 \qquad (2.11)$$

Gopalakrishnan and Thompson (2006) reported that the low-strength subgrade CBR increased while medium-strength subgrade CBR decreased as a result of trafficking. Also, backcalculated moduli are higher than their laboratory counterparts for low-strength soils and the reverse is true for medium-strength soils.

Walston et al. (2000) carried out the field tests at three General Aviation (GA) airports in 1997 to address the loading conditions at these airports. The soil types varied and included clays, silts, and granular materials with in-situ CBR values ranging from 6 to 50. Back-calculated FWD subgrade moduli ranged from 4000 psi to 50,000 psi. The condition survey indicated that most pavement distresses were related to weather and not load induced. The PCI values ranged from 50 to 90. Walston et al. (2000) developed the following relationship for the subgrade soils of GA airports in North Carolina:

$$E = 1000(CBR) \tag{2.12}$$

E is in psi unit. This equation results in a more conservative subgrade strain criteria for GA airport pavement analysis.

The resilient modulus of fine-grained soils can also be estimated using the relationship developed by Heukelom and Klomp (1962):

$$M_R = 1500(CBR) \tag{2.13}$$

Rahim (2005) proposed the following correlation equations to predict resilient modulus (M_R) for fine- and coarse-grained (sandy) soils. For fine-grained soil:

$$M_R = 17.29\left[\left(\frac{LL}{w_c + 1} \times \gamma_{dr}\right)^{2.18} + \left(\frac{\#200}{100}\right)^{-0.609}\right] \tag{2.14}$$

with $R^2 = 0.70$.

For coarse-grained (sandy) soil:

$$M_R = 324.14\left(\frac{\gamma_d}{w_c + 1}\right)^{0.8998}\left(\frac{\#200}{\log C_u}\right)^{-0.4652} \quad (2.15)$$

with $R^2 = 0.72$

where M_R = resilient modulus (MPa), LL = liquid limit (%), # 200 = passing # 200 sieve (%), γ_{dr} = maximum dry density (kN/m^3), γ_d = dry density (kN/m^3), C_u = uniformity coefficient, R^2 = coefficient of determination.

2.4 Structural Capacity of Airfield Pavements

Structural Number (SN) expresses the capacity of the pavement to carry loads for a given combination of soil support, estimated traffic, terminal serviceability, and environment. SN has been related to the Falling Weight Deflectometer (FWD) data by different researchers. Romanoschi and Metcalf (1999) developed the following relationship to calculate the SN of the flexible pavement where the surface layer material is much stiffer than the underlying base layer material:

$$SN = 6.96 - 0.196[(AREA) - 450(D_{1200})]^{0.5} \quad (2.16)$$

$$AREA = 25.4[4DEF_0 + 6D_{200} + 5D_{300} + 3D_{450}] \quad (2.17)$$

where D_{1200}, D_{450}, D_{300}, D_{200} = extrapolated values of the deflection at an offset of 1200, 450, 300 and 200 mm. from the center of the FWD ball drop and DEF_0 = temperature-corrected deflection under the ball drop (microns) and is calculated using the formula:

$$DEF_0 = (D_0)(DAF) \tag{2.18}$$

and DAF is calculated from the relationship:

$$\log(DAF) = 3.65\times10^{-4}(68 - T_{mac})AC_t^{1.4635} \tag{2.19}$$

where DAF=deflection adjustment factor, AC_t = thickness of asphalt (in.), and T_{mac} = asphalt concrete layer mid-depth temperature (^oF) at testing time.

Jameson (1993) developed the following formula for calculating the subgrade CBR from FWD data:

$$\log(CBR) = 3.264 - 1.018\log(D_{900}) \tag{2.20}$$

where D_{900} = normalized deflection at 900 mm offset (microns).

The deflection normalization is the process of correcting the deflection measured at load P to a standard load P_0 and calculated as:

$$D_i = D_{mi}\left(\frac{P_0}{P}\right) \tag{2.21}$$

where D_i is the normalized deflection, D_{mi} is the measured deflection, P is the measured load and P_o is the standard load.

2.5 Skid Resistance

Skid resistance is an important pavement evaluation parameter. Inadequate skid resistance may lead to higher incidences of skid related accidents. Most agencies have an obligation to provide users with airport pavements that is reasonably safe. Skid resistance measurements can be used to evaluate the effects of various types of materials and construction practices contributing to safety.

It is a common fact that the lower the skid resistance value, the higher the percentage of accidents, especially during the wet seasons. A low value of skid resistance value on an asphalt concrete surface can be attributed to the following reasons: (i) use of higher asphalt content than recommended by the mix design procedure, (ii) mix design procedure itself, (iii) used aggregate gradation, and (iv) aggregate quality (Asi 2007). Good skid resistance on asphalt pavement surface could be achieved by controlling both microtexture and macrotexture. Microtexture is affected by polish-resistant, hard, coarse, angular aggregates composed of minerals capable of differential wearing. Macrotexture depends on the type of mix (dense or open graded). Microtexture controls contact between tire and surface and depends on coarse aggregate properties. Macrotexture controls the escape of water from under the tire and depends on the arrangement of the aggregate particles. Design procedures focus on controlling aggregate quality, i.e. the microtexture. However, research shows that macrotexture plays a significant role in determining skid behavior at higher speeds and wet pavement conditions (Bazlamit and Reza 2005).

Skidding is usually a wet weather concern. At low speeds, the water is usually squeezed out from underneath the tire. At higher speeds, the water has less time to escape. A layer

of water gets trapped between the surface and the tire resulting in significant reduction in friction with the possibility of hydroplaning. Macrotexture plays a significant role here in absorbing and transporting the water away. The coefficient of friction is multiplied by 100 to obtain the skid number:

$$SN = 100\mu = 100\left(\frac{F}{W}\right) \tag{2.22}$$

where μ = coefficient of friction, F = the tractive force applied to the tire, W = dynamic vertical load on tire. Skid number deteriorates with increasing traffic until it reaches a level of equilibrium. There is no specific value at which it levels off (Shahin, 2005).

Surface friction is defined as the force developed when a tire that is prevented from rotating slides along the pavement surface. Figure 2.3 shows that the force required to drag a locked wheel along the surface depends on the vertical load on the wheel and the coefficient of friction between the pavement surface and the wheel. It is computed as:

$$F = \mu \times W \tag{2.23}$$

In general, friction coefficient decreases with increases in speed, significantly so on wet pavement. Slip is the relation between the angular wheel speed at free rolling and at time of measurement. When brake is applied, it increases until it reaches 100. It can be seen from Figure 2.3 that the friction factor increases with slip until it reaches a maximum value at critical slip (usually 10 – 15 %) and then it decreases. SN is calculated when the test wheel is fully locked, that is at 100 % slip.

2.5.1 Variation of Skid Resistance with Temperature

The general trend is that during seasons with warmer temperature, skid resistance decreases and during seasons with colder temperatures, skid resistance increases. Since the temperature varies each time a measurement is made, it is important to relate skid number obtained at some arbitrary temperature to an effective skid number at a reference temperature. Bazlamit et al. (2005) carried out a research in the laboratory using the British pendulum tester to examine the effect of temperature on friction and developed the following relationships:

$$BPN_T = 125.2508 - 0.232T \tag{2.24}$$

where T = temperature in Kelvin, BPN_T = value of British pendulum number at temperature T.

$$\Delta BPN_T = 68.0108 - 0.232T \tag{2.25}$$

where ΔBPN_T = number to be added to the BPN reading at T = 293.15 K. (68° F).

Kissoff (1988) developed the following correlation between SN and BPN:

$$SN = 0.862(BPN) - 9.69 \tag{2.26}$$

$$\Delta SN_T = 58.453 - 0.1994T \tag{2.27}$$

where ΔSN_T = number to be added to the SN reading obtained at T = 293.15 K. The equation (2.25) yields positive values for T < 293.15 and negative values for T > 293.15.

2.5.2 SN Measurement Equipments

There are a number of equipment types that measure skid resistance. Al-Qadi et al. (1991) studied the various technologies available to determine the pavement condition.

Table 2.5 lists some of the equipment in use. The technologies used are the slip test, locked wheel and side force. Most of the states including New Mexico perform skid resistance test in accordance with the ASTM E 274. It can be seen from Table 2.5 that ASTM E 274 is a locked wheel test.

Table 2.1 Test Results of Various Army Airfield Pavements (Bell et al., 2008)

Sample	Name of Army Airfield	Age, yrs	PCI	T , °F	PSPA Modulus, ksi	AC Design Modulus, ksi	ITS Peak Stress, psi
LM-2	Lab sample	0	No data	72	1160	355	118
P-1	Polk	22	8	72	1625	498	237
P-2	Polk	7	82	79	1948	622	358
R-1	Redstone	21	43	62	2388	690	262
R-2	Redstone	41	47	86	1765	589	188
S-1	Simmons	14	57	59	2388	679	256
S-2	Simmons	14	53	74	1840	570	263
S-3	Simmons	14	48	91	1780	614	258
F-1	Forney	27	43	59	2683	763	232
F-2	Forney	27	59	69	1526	459	164
F-3	Forney	7	66	89	1260	429	191

Table 2.2 Standard PCI Rating Scale (Greene et al., 2004)

PCI	Rating
86 – 100	Good
71 – 85	Satisfactory
56 – 70	Fair
41 – 55	Poor
26 – 40	Very Poor
11 – 25	Serious
0 – 10	Failed

Table 2.3 PCI Value by Surface Type, Region, and Age Group (Muntasir, 2006)

Surface / Age	Central		Northern		Southern		Western	
	AAC	AC	AAC	AC	AAC	AC	AAC	AC
0 – 5	93.4	94.3	93.0	96.1	93.9	88.2	94.9	95.4
6 – 10	77.0	78.1	82.8	85.6	77.9	74.2	85.3	86.3
11 – 15	69.2	73.1	78.9	76.6	66.6	71.0	84.3	77.5
16 – 20	68.8	65.7	69.2	67.0	67.1	57.0	69.1	71.2
21 – 30	63.6	67.0	64.4	61.4	61.9	53.3	66.6	60.4
31 – 40	40.4	62.7	61.9	56.0	38.3	50.9	65.9	53.0
>40	60.4	49.2	71.2	50.2	-	35.1	71.8	53.8

Table 2.4 Pavement Condition Index Reduction by Group (Garg et al., 2004)

Group	Location	PCI Reduction, %
I	Runways	82.2
	Taxiways	71.8
	Aprons	72.0
II	Runways	6.6
	Taxiways	5.4
	Aprons	6.6
III	Runways	8.1
	Taxiways	17.1
	Aprons	16.9
IV	Runways	1.6
	Taxiways	3.1
	Aprons	1.9
V	Runways	1.5
	Taxiways	2.6
	Aprons	2.6

Table 2.5 List of In-Use and Underdevelopment Equipment to Measure Skid Resistance Based on Technology Used (Al-Qadi et al., 1991)

Locked Wheel	Slip Test	Side Force
ASTM E 274	Runway Tester	Mu Meter (U.K.)
Diagonal Braking	BV 8 (Sweden)	Stradograph (Denmark)
Cobiert Trailer (Poland)	BV 11 (Sweden)	Skid Tester ST-1(Finland)
LCPC Trailer (France)	BV 12 (Sweden)	Odoliograph (Belgium)
SCRIM (U.K.)	RWL Trailer (Netherlands)	DF Tester (Japan)
COMTUCI CS-130 (Hungary)	SAAB Friction Tester (Sweden)	Australian Road Evaluation Vehicle (Australia)
Stuttgarder Reibungnesser (Germany)	Spin-up/Spin-down	British Pendulum Tester (U.K.)
Belgium Tester (Belgium)	Portable Friction Tester (Sweden, Germany, France, U.K.)	
Portable Skid Resistance Tester (U.K.)		
Friction Measuring Device (Finland)		
SUMMS Italy (Italy, U.K.)		
Grip Tester (U.K.)		
SRT (France)		
Danish Stradograph (Denmark)		
Yandell-Mee Texture Friction Meter (Australia)		
Road Surface Analyzer		

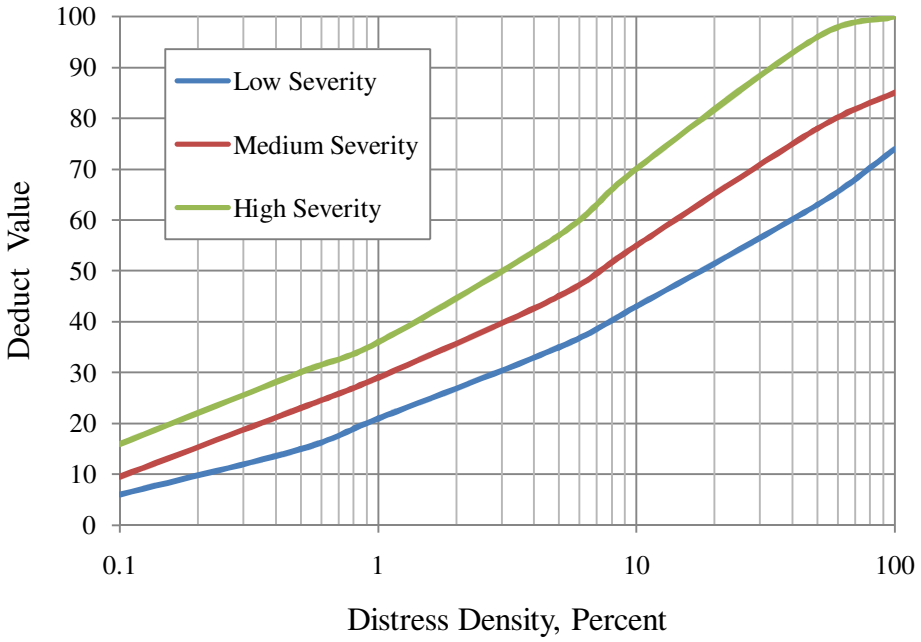

Figure 2.1 Distress Deduct Value Curve for Alligator Cracking

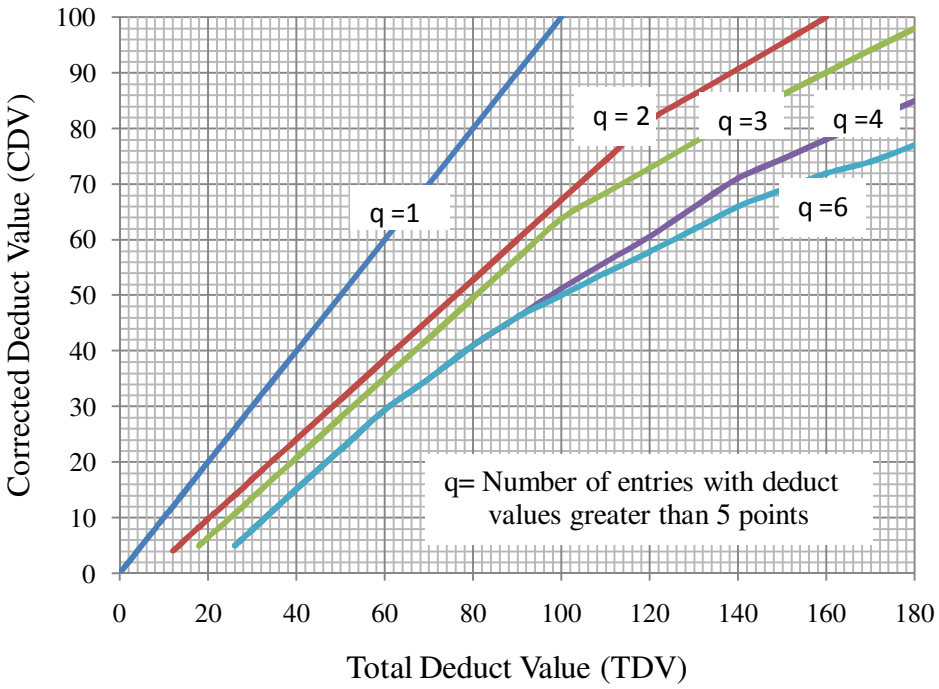

Figure 2.2 Corrected Deduct Values for Flexible Airfield Pavement

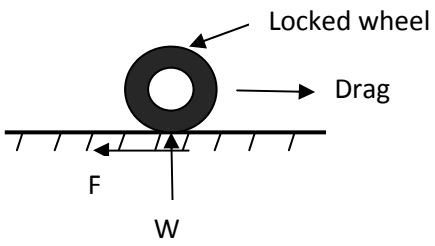

Figure 2.3 Forces Acting on the Locked Wheel

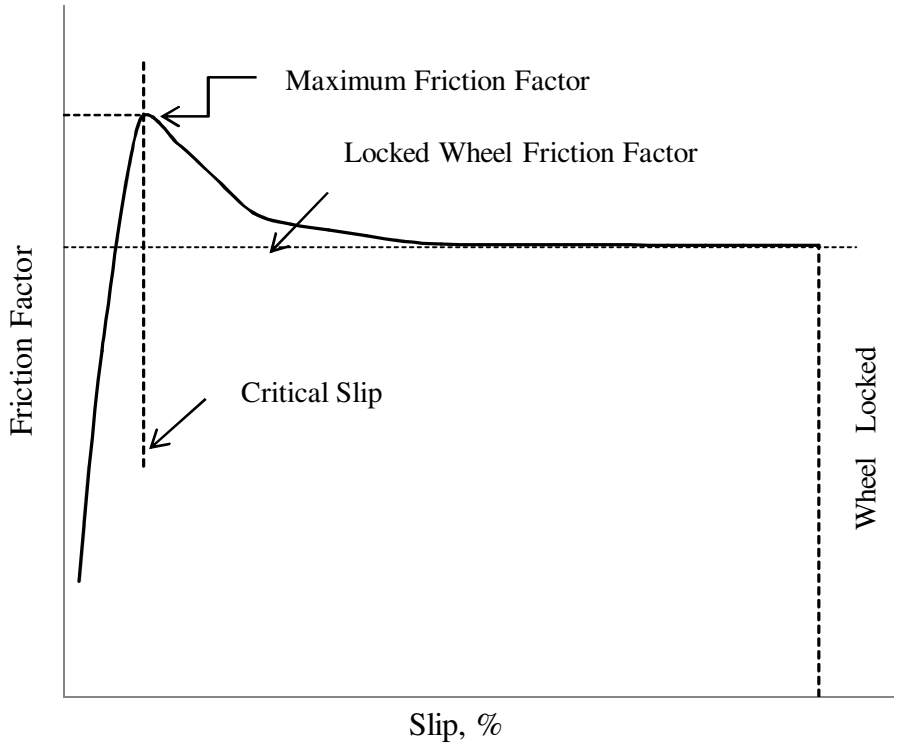

Federal Aviation Administration (1971)

Figure 2.4 Friction Factor as a Function of Slip

CHAPTER 3

FIELD AND LABORATORY TESTING

3.1 Distress Data

Ten airports evaluated in this study are: (1) Double Eagle II, (2) Sierra Blanca Regional, (3) Raton Municipal, (4) Moriarty Municipal, (5) Las Cruces International, (6) Grant County, (7) Deming Municipal, (8) Roswell International Air Center, (9) Belen Alexander, and (10) Clayton Municipal Airports. Figure 3.1 shows the locations of these airports in New Mexico. The airport pavements are divided into three branches according to their functions. These branches are runway, taxiway, and apron. A runway is a pavement on which an aircraft can take off and land. A taxiway is a path that connects runways with ramps, hangars, terminals, and other facilities. Aprons are parking areas for aircraft.

Each of the runway, taxiway, and apron areas was subdivided into sample units of 5000 square feet plus-minus 2000 square feet if the pavement was not evenly divisible by 5000. Distress data was collected for 10 – 20 % of the total sample units. Figure 3.2 shows longitudinal and transverse cracking on runway 4-22 of Double Eagle II airport. Distress data collection was done in accordance with the ASTM 5340-03 for the 16 distresses and three severity levels: low, medium, and high. Sample Condition Survey Data Sheet for Las Cruces International Airport, Runway 12-30 is shown in Figure 3.3. It can be seen from Figure 3.3 that for sample unit 4, there is 1000 square feet of low severity block cracking, 210 square feet of low severity, and 10 square feet of medium severity alligator cracking, and 75 feet of low severity and 146 feet of medium severity longitudinal and transverse cracking. These distress data were used in MicroPaver as

inputs to determine the PCI value for each of the runway, taxiway and apron. The PCI values obtained for all the 10 airports are shown in Table 3.1. It can be seen that the PCI values range from 28 to 98. Asphalt cores and soil samples were collected from pavements with low PCI values. Although Runway 4-22 at Las Cruces International Airport has a low PCI value of 28, no coring was carried out here as this runway is not funded by the State. Also, coring was terminated at Runway 17-35 of Roswell International Air Center upon encountering concrete. The PCI values for the runways, taxiways and aprons at Double Eagle II are shown in Figure 3.4. It can be seen from Figure 3.4 that Runway 4-22 and Taxiway 02 are in poor condition whereas Runway 17-35 and Taxiway 01 are in good condition. The PCI figures for all the ten airports are shown in Appendix I.

3.2 Field Testing Plan

Falling Weight Deflectometer (FWD) and Skid tests were conducted on all the runways and taxiways. The field testing plan for sample collection was developed based on the results of the PCI values. No coring was done on runways and taxiways with good PCI values. Coring was carried out to collect asphalt samples and boreholes were drilled to a depth of 5 feet to collect base course and subgrade samples. Samples were collected from selected boreholes at approximately 1000 feet intervals along the runways, three locations on the taxiways, and two locations on the aprons.

3.2.1 FWD Data

The FWD testing plan is shown in Figure 3.5. The tests were done at 200 foot intervals 5 feet on either side of the centerline along the length of the runway, at 400 feet interval 20

feet on either side of the centerline, and at 600 feet interval 30 or 40 feet (depending on the width of the runway) on either side of the centerline. In general, FAA requires the test to be done at 200 feet interval (FAA AC 150/5370-11A). However, due to time constraints, test spacing was increased. In the FWD test, an impulse load is applied by dropping a weight (ball) on the pavement and the resulting deflections are measured at specified distances from the point of load application by the sensors. These sensors are geophones. The number of load applications is called the drop number. Field data of north bound lane, 5 feet from the centerline of Runway 17-35 of Double Eagle II airport is presented in Table 3.2. Three weights or loads such as 9, 12, and 16 kips were used. The responses are measured using seven sensors spaced at 0, 8, 12, 18, 24, 36 and 60 inches from the point of impact as shown in Figure 3.6. Using these deflections, the moduli of elasticity of the different layers can be determined by back calculation. The tests were carried out using the Jills FWD equipment.

3.2.2 Skid Data

Skid resistance was carried out according to ASTM E 274 – 06. The Dynatest vehicle and trailer used is shown in Figure 3.7. A standard smooth tire with tire inflation pressure of 24 psi was used. The test speed was 40 mph and the quantity of water applied to the pavement ahead of the test tire was 4.0 gallons ± 10 % /min.in. of wetted width. The vehicle is brought to the desired speed of 40 mph. With the press of a switch on board the vehicle, water is delivered and the braking system is actuated to lock the test tire. The resulting friction force, speed, temperature and the effective wheel load are automatically recorded for an interval of 1 to 3 seconds. The mean value in the interval is used to calculate the skid number (SN) according to Eq. (2-22) and displayed on the screen. The

skid test plan is presented in Figure 3.8. The tests were done at 5 feet, 20 feet, and 30 or 40 feet (depending on the width of the runway) on either side of the centerline. The average test interval was about 200 feet. The results of the skid test for runway 4-22 at Double Eagle II Airport is shown in Table 3.3. Test results for all of the airports are presented in Appendix II.

3.2.3 Coring and Drilling

Coring was carried out to collect asphalt surface core samples from selected borehole locations across the runway, taxiway and apron. Figure 3.9 shows the borehole locations at Sierra Blanca Regional Airport. Four samples, each of 4 inches diameter, were collected from each borehole location. The cores were inspected, numbered, and the thickness measured and recorded in the Field Log. Figure 3.10 shows Borehole Log of Runway 3-21 at Belen Airport. It can be seen from Figure 3.10 that the thickness of the asphalt surface at Runway 3-21 is 2.25 inches. The cores were then bagged for further testing in the laboratory.

The boreholes were drilled approximately to a depth of five feet to collect aggregate and soil samples as shown in Figure 3.11. The samples were extracted every nine inches, visually examined, classified and the details entered into the Field Log. Table 3.4 shows the field log of Runway 2-20 at Raton Municipal Airport. The first column shows the coring location from the start point and the distances are in feet. The second column shows the identification number of the sack. Samples were collected in sacks. The third column shows the identification number of borehole. The asphalt cores, base, and subgrade materials were collected from each of these boreholes. At each borehole, the

layer identification is obtained from the fourth column. The fifth and sixth columns show the layer thickness information. The seventh column shows the source of the materials such as the surface, base, or subgrade. In the last column, the soil type information is recorded. The process was repeated every time there was any change in the soil properties. The sample was then bagged and numbered as shown in Figure 3.12 for further laboratory testing. The sacks are numbered so that the source of the material is easily identified.

3.3 Laboratory Testing

The soil samples, base aggregates and asphalt cores were transferred to the Pavement Materials Laboratory at the University of New Mexico for further testing.

3.3.1 Soil Testing

Soil samples from the field were split as shown in Figure 3.13. The sample is passed through the splitter which splits it into two halves in two separate pans. The process is repeated until the amount of material in one pan is about 800 grams. The split sample was oven dried for the particle size analysis and air dried for the Atterberg limits tests. After sieve analysis, the hydrometer analysis was carried out for the portion passing the no. 200 sieve if it was in excess of 10 % of the total mass. This was done in accordance with ASTM D 2487-00 and ASTM D 422-63 (Reapproved 1998). Figure 3.14 shows hydrometer test in progress. The hydrometer readings were taken for 24 hours since there was no significant change in the readings after that. Atterberg limit tests followed the procedures outlined in ASTM D 4318-00. Figure 3.15 shows the Liquid Limit test apparatus with the soil sample. Motorized testing device was used to obtain uniform

testing with greater degree of accuracy. The sieve analysis results were used to plot the cumulative particle-size distribution curve as shown in Figure 3.16. It is a log normal distribution. We can obtain D_{60}, $D_{30,}$ and D_{10} which are the particle sizes corresponding to 60, 30, and 10 % passing from Figure 3.16. The coefficient of curvature (C_c) was calculated as follows:

$$C_c = \frac{(D_{30})^2}{(D_{10} \times D_{60})} \quad (3.1)$$

The coefficient of uniformity (Cu) was calculated using the formula:

$$C_u = \frac{D_{60}}{D_{10}} \quad (3.2)$$

Based on the results of the particle size distribution, the soil was classified according to the Unified Soil Classification System. The CBR value is calculated according to Eq. (2-8) for non-plastic soils and Eq. (2-9) for plastic soils. The results of the CBR calculations and soil profile for Runway 4-22 at Double Eagle II airport is shown in Table 3.5. The thickness of each layer is listed in column 5 of Table 3.5. From column 6 and column 7 of Table 3.5, we can obtain the soil classification and CBR value. Figure 3.16 shows the layer thickness and the CBR value for each layer for all the eight boreholes of Runway 4-22 at double Eagle II Airport. We can see from Figure 3.17 that the CBR values for the base course range from 50 to 64. The range for the subgrade CBR is from 18 to 29. The results for all the airports are shown in Appendix III.

Direct shear test was carried out for selected soil samples underneath the base course. The test followed the procedures outlined in ASTM D 3080-98. Figure 3.18 shows the sheared sample in the shear box. The results of the tests for Ottowa sand is plotted to obtain the friction angle as shown in Figure 3.18. Figure 3.18 is a plot of shear stress versus normal stress. The Direct Shear equipment was calibrated using Ottowa sand

whose friction angle is known to be 31° (Duncan 2004). Samples from three locations across each runway were tested and the average friction angle was calculated. The results of the friction angle for all the airports are shown in Table 3.6. Table 3.6 shows that the friction angle values range from 35° to 42°.

3.3.2 Aggregate Testing

About 1500 grams of the base course sample from the field was taken and oven dried for the particle size analysis. Based on the results of the particle size distribution, the coefficient of curvature (C_c) and the coefficient of uniformity (Cu) were calculated using Eq. (3-1) and Eq. (3-2). The sample was then classified according to the Unified Soil Classification System. The CBR value is calculated according to Eq. (2-8). The thickness of the base course and results of the CBR calculations for Runway 4-22 at Double Eagle II airport can be seen in Table 3.5 and Figure 3.17 with the subgrade data. The results for all the airports are shown in Appendix III.

3.3.3 Asphalt Testing

3.3.3.1 Resilient modulus (M_R)

Asphalt cores were tested to determine the resilient modulus using the Resilient Modulus Testing Device of Retsina Company. The equipment is shown in Figure 3.20. The sample thickness was measured at four points and the average was determined. The samples were subjected to a repeated load of about 30 lb along the sample diametral axis. The tests were performed according to the guidelines of ASTM D 4123-82 and carried out at

ambient room temperature (23 ± 0.3°C). The repeated load and the recoverable horizontal deflection were recorded. The resilient modulus was calculated using the formula (Heinicke and Vinson 1989):

$$M_R = \left(\frac{P}{Ht}\right) \times (\nu + 0.27) \qquad (3.3)$$

where M_R = resilient modulus (psi), P = repeated load (lbs), H = total recoverable horizontal deflection (inches), T = specimen thickness (inches), and ν = Poisson's ratio. Poisson's ratio for asphalt concrete was assumed to be 0.35 (Huang 2004). The result of the tests of the asphalt cores from runway 4-22 of Double Eagle II airport is presented in Table 3.7. It can be seen from Table 3.7 that the values for runway 4-22 of Double Eagle II airport range from 230,056 to 285,254 psi. The results for all the airports are presented in Appendix IV.

3.3.3.2 Indirect Tensile Strength (IDT)

Indirect Tensile Strength (IDT) of the asphalt cores were determined using the Humboldt equipment and the data was collected using Labview. The tests were carried out at ambient room temperature (23 ± 0.3°C). As shown in Figure 3.21, the sample is loaded across its vertical diametral plane and the rate of loading is 50 mm/minute (2 inches per minute). This test was carried out in accordance with ASTM D 4123-82. The maximum load at failure is noted and the IDT is calculated using the formula:

$$S_t = \frac{2 \times P}{\pi \times t \times D} \qquad (3.4)$$

where S_t = IDT strength (psi), P = maximum load (lbf), T = specimen height (inches), and D = specimen diameter (inches). The result of the tests of the asphalt cores from runway 4-22 of Double Eagle II airport is presented in Table 3.8. It can be seen from Table 3.8 that the values for runway 4-22 of Double Eagle II airport range from 230.4 to 249.8 psi. The results for all the airports are presented in Appendix IV.

3.3.3.3 Bulk Specific Gravity of Core

Bulk Specific Gravity (G_{mb}) of the asphalt cores was determined according to AASHTO T 166. In this procedure, core is weighed in air and then immersed in water for 3 to 3.5 minutes suspended beneath a balance and the mass under water is recorded as shown in Figure 3.22. The sample is removed and surface dried using a damp towel and weighed as quickly as possible in air. This weight is the saturated surface dry weight of a sample. The bulk specific gravity is calculated using the formula:

$$G_{mb} = \frac{A}{B-C} \qquad (3.5)$$

where G_{mb} = bulk specific gravity to the nearest 0.001, A = weight in grams of the specimen in air, B = weight in grams, surface dry, and C = weight in grams, in water. The result of the tests of the asphalt cores from runway 4-22 of Double Eagle II airport is presented in Table 3.9. The results for all the airports are presented in Appendix IV.

Theoretical Maximum Specific Gravity (G_{mm}) of the mix is determined according to AASHTO T 209. This is the same as bulk specific gravity test but of loose mix. The cores are placed in the oven in a large pan. The pan is removed from the oven and the particles are loosened so that the clumps of fine aggregate portion are no longer larger

than 6.3 mm. The flask is filled with water and the weight is recorded. The empty flask is placed on the scale and the scale is tared. Half of the loose material is poured into the flask, weighed and recorded. Water is poured into the flask to cover the sample completely. The entrapped air is removed using partial vacuum of 30 mm Hg for 15 minutes as shown in Figure 3.23. The flask with the material is then filled with water and the weight is recorded. The procedure is repeated using the other half of the loose material. The theoretical maximum specific gravity is calculated using the formula:

$$G_{mm} = \frac{A}{(A+D-E)} \tag{3.6}$$

where G_{mm} = theoretical maximum specific gravity to the nearest 0.001, A = mass of oven-dry sample in air, D = mass of flask filled with water, and E = mass of flask filled with sample and water. If the difference in results of the two tests exceeded 0.011, the tests were rerun. Otherwise, the average of the two tests is the maximum specific gravity. The result of the tests of the asphalt cores from runway 4-22 of Double Eagle II airport is presented in Table 3.10. The results for all the airports are presented in Appendix IV.

The percent of air voids is determined according to AASHTO T-269-97. Percent air void is calculated using the formula and reported to the nearest 0.1% :

$$Percent\ Air\ Void = \frac{G_{mm}-G_{mb}}{G_{mm}} \times 100 \tag{3.7}$$

The result of the tests of the asphalt cores from runway 4-22 of Double Eagle II airport is presented in Table 3.11. It can be seen from Table 3.11 that the values for the two samples are 8.2 % and 9.7 %. These values are a bit high as air voids are expected to be within the limits of 6-7 %. It will be interesting if permeability tests are done on the

samples. As these cores have high air voids, they are more likely susceptible to water damage. The results for all the airports are presented in Appendix IV.

3.3.3.4 Asphalt Content

The asphalt content of the mix is determined using the NCAT Asphalt Content Tester according to guidelines of AASHTO T 308. Figure 3.24 shows the NCAT oven. The ignition furnace is preheated to 538 ℃. The basket assembly is weighed empty and the mass is recorded to nearest 0.1 gram. Approximately 2000 grams of the sample is put in the basket, spread out and put in the oven to dry to constant mass. After drying, the assembly with the sample is weighed again and the mass recorded. The initial mass of the sample is calculated by subtracting the mass of the empty basket from the mass of the basket with the sample. The initial mass of the sample is input into the ignition furnace controller. The basket assembly is then put into the NCAT oven. The test automatically stops if the change in mass does not exceed 0.01 % for three consecutive minutes. The furnace controller prints a ticket with the asphalt binder content. The assembly is then taken out of the furnace and weighed. The final mass of the sample is calculated. After cooling, the sample from the basket is collected for gradation analysis. Wire brush is used to make sure that all of the sample is collected. The asphalt content test results for runway 4-22 of Double Eagle II airport is presented in Table 3.12. It can be seen from Table 3.12 that the values for the two samples are 5.94 % and 6.38 %. The optimum asphalt content with a maximum aggregate size of 50 mm may be as low as 3.0 – 3.5 % while for a 9.5 mm maximum aggregate size, the asphalt content may be as high as 7.0 – 7.5 % (Roberts et al. 1996). For our sample with maximum aggregate size of 22.4 mm,

the values seem reasonable. Also, we would see even higher values of air voids if the asphalt content was less. The results for all the airports are presented in Appendix IV.

3.3.3.5 Gradation Analysis

Gradation analysis is carried out on the sample collected after burning the asphalt binder according to AASHTO T 30. Figure 3.25 shows the aggregate collected after burning the asphalt binder. The result of the gradation analysis for runway 4-22 of Double Eagle II airport is presented in Table 3.13. We can see from Table 3.13 that the first sieve size to retain more than 10 % of the sample is 9.5 mm. The nominal maximum size which is one sieve size larger than the first sieve to retain more than 10 % in our case is 19 mm. The maximum aggregate size is one sieve size larger than the nominal maximum size, which in our case is 22.4 mm. Based on the results of the particle size distribution, the coefficient of curvature (C_c) and the coefficient of uniformity (Cu) were calculated using Eq. (3-1) and Eq. (3-2). The results for all the airports are presented in Appendix V.

Table 3.1 PCI of the Runways of Evaluated Airports

Airport No.	Name of Airport	Runway	Date of PCI Inspection	PCI	Remarks
1	Double Eagle II	17-35	04/28/2007	98	X
		4-22		54	Coring
2	Sierra Blanca Regional	6-24	03/10/2007	84	X
		12-30		88	Coring
3	Raton Municipal	2-20	06/23/2007	79	Coring
		7-25		68	Coring
4	Moriarty Municipal	8-26	04/28/2007	60	Coring
5	Las Cruces International	4-22	12/18/2006	28	X
		8-26		66	Coring
		12-30		43	Coring
6	Grant County (Silver City)	8-26	12/19/2006	55	Coring
7	Deming Municipal	4-22	02/24/2007	60	Coring
		8-26		72	Coring
8	Roswell International Air Center	12-30	03/14/2007	61	X
		17-35		87	X
		3-21		65	Coring
9	Belen Municipal	3-21	11/09/2006	51	Coring
10	Clayton Municipal	12-30	06/23/2007	71	Coring
		2-20		73	Coring

Table 3.2 FWD Data of Runway 17-35 at Double Eagle II Airport (5ft. from C/L NBL)

Dist., Ft.	Dynamic Load, kips	Sensor Measurement, mils							Material Temp, °F	Subgrade Modulus
		0"	8"	12"	18"	24"	36"	60"		
0.0	9	21.13	13.74	10.81	7.54	5.48	3.16	1.75	91.9	11,468
0.0	9	21.58	13.77	10.86	7.58	5.55	3.18	1.79	91.9	11,459
0.0	12	26.08	19.09	14.85	10.08	7.57	4.31	2.15	91.9	11,193
0.0	12	25.26	19.17	14.95	10.22	7.70	4.35	2.35	91.9	11,108
0.0	16	33.25	26.32	19.98	13.48	10.18	5.80	2.78	91.9	10,876
0.0	16	34.72	26.96	20.57	14.07	10.65	6.05	4.39	91.9	10,671
200.0	9	19.42	12.61	10.03	7.11	5.11	2.87	1.71	93.8	12,557
200.0	9	17.33	12.63	10.12	7.17	5.16	2.91	1.69	93.8	12,344
200.0	12	24.42	17.25	13.78	9.57	7.06	3.94	2.42	93.8	12,142
200.0	12	27.02	17.47	13.95	9.66	7.21	4.04	1.64	93.8	11,921
200.0	16	31.91	24.10	19.23	13.00	9.86	5.44	2.12	93.8	11,794
200.0	16	29.53	24.53	19.68	13.43	10.01	5.63	3.81	93.8	11,588
402.0	9	17.10	11.18	8.33	5.32	3.54	2.03	1.38	93.8	17,754
402.0	9	18.72	11.27	8.43	5.50	3.61	2.05	1.40	93.8	17,580
402.0	12	23.69	15.92	11.87	7.39	5.02	2.75	1.89	93.8	17,324
402.0	12	24.24	16.02	11.99	7.34	5.04	2.81	1.86	93.8	17,096
402.0	16	31.19	23.07	16.89	10.54	6.98	3.75	3.00	93.8	16,896
402.0	16	32.71	23.11	16.95	10.93	7.18	3.83	3.10	93.8	16,825
600.0	9	24.45	14.49	10.23	6.19	4.02	2.03	1.37	93.4	17,419
600.0	9	24.04	14.51	10.33	6.24	4.07	2.05	1.36	93.4	17,385
600.0	12	32.86	20.71	14.41	8.46	5.51	2.68	1.77	93.4	17,567
600.0	12	32.51	20.73	14.57	8.39	5.63	2.76	1.80	93.4	17,159
600.0	16	46.82	30.18	20.56	11.96	7.51	3.62	2.13	93.4	17,238
600.0	16	47.95	31.27	21.40	12.33	7.88	3.76	2.58	93.4	16,989
805.0	9	22.19	14.05	10.94	7.50	5.21	2.71	1.49	94.1	13,225
805.0	9	21.40	14.04	11.01	7.50	5.29	2.74	1.49	94.1	13,153
805.0	12	27.71	19.35	15.04	10.09	7.22	3.72	1.81	94.1	12,839
805.0	12	27.16	19.45	15.20	10.21	7.41	3.80	1.65	94.1	12,716
805.0	16	36.07	26.58	20.66	13.97	9.74	5.00	2.31	94.1	12,656
805.0	16	37.14	26.97	21.06	14.20	10.06	5.19	2.79	94.1	12,532
1002.0	9	40.75	30.22	23.33	14.85	9.52	3.85	1.95	93.0	8,831
1002.0	9	40.38	30.51	23.60	15.11	9.77	3.95	2.02	93.0	8,729
1002.0	12	52.38	42.70	32.61	20.85	13.44	5.33	2.61	93.0	8,518
1002.0	12	53.79	44.14	33.65	21.70	14.13	5.56	2.68	93.0	8,345
1002.0	16	68.85	58.46	45.16	28.71	18.35	7.13	3.65	93.0	8,275
1002.0	16	71.28	59.65	46.67	29.42	19.19	7.44	3.47	93.0	8,070
1206.0	9	28.26	21.34	17.11	11.96	8.50	4.14	1.93	93.8	8,464
1206.0	9	27.18	21.41	17.28	12.17	8.68	4.22	1.94	93.8	8,427
1206.0	12	39.16	30.79	24.64	16.96	12.22	5.86	3.28	93.8	8,246
1206.0	12	35.32	30.92	24.85	17.03	12.37	6.02	2.55	93.8	8,126
1206.0	16	48.18	41.16	33.03	23.27	15.96	7.82	4.42	93.8	8,128
1206.0	16	48.66	41.87	33.54	23.60	16.37	8.00	3.86	93.8	7,970

Table 3.3 Skid Results for Runway 4-22 at Double Eagle II Airport

Test Section	Average SN	Min. SN	Max. SN	Speed, mph	Offset from C/L, feet	Direction
1	54.1	45	60	41.1	10	North Bound
2	54.1	46	61	40.7		
3	56.6	54	60	41.0		
4	60.1	56	63	40.6		
5	54.3	47	59	40.8	10	South Bound
6	55.2	51	59	41.8		
7	59.3	56	63	40.1		
8	55.0	51	59	41.0		
9	58.9	55	61	40.3		
10	59.3	54	64	40.2		
11	54.4	50	60	40.4		
12	54.2	51	58	40.7		
13	52.7	48	57	40.6		
14	60.6	57	65	40.8	20	North Bound
15	57.7	52	64	40.6		
16	58.4	54	63	40.8		
17	62.5	59	65	40.8		
18	61.3	57	65	40.7		
19	58.5	15	67	40.6		
20	58.7	54	62	41.3		
21	56.8	49	60	41.2		
22	60.7	58	64	40.8	20	South Bound
23	60.2	55	66	40.9		
24	59.8	54	64	40.8		
25	60.4	54	68	41.0		
26	59.0	56	63	41.1		
27	58.2	54	63	41.2		
28	55.2	51	60	41.1		
29	62.9	59	69	40.6	30	North Bound
30	60.9	55	70	41.4		
31	61.7	57	67	41.1		
32	61.2	57	65	40.9		
33	61.4	55	65	40.9		
34	58.9	50	63	40.5		
35	59.5	55	65	40.9		
36	48.7	34	65	41.9	30	South Bound
37	60.8	57	65	41.6		
38	61.9	58	68	42.0		
39	60.5	55	65	41.8		
40	62.3	49	70	42.1		
41	40.9	25	62	42.1		

Table 3.4 Borehole Information of Runway 2-20 at Raton Municipal Airport

☒ Subgrade	☐ Borrow	☐ Surfacing	☐ Filler	☒ Thru Pavement

Source Location:		Runway 2-20					
Lab No.	Sack No.	Hole & Sample Number		Depth From	Depth To	Material Type	Remarks & Material Identification
Mile Post: 1000 ft.	Rt. or Lt. ☐ ☒	C/L 348 in.	Distress ☐None	(1) ☒Transverse (2) ☒Longitudinal (3) ☐ Alligator (4) ☐ Pothole (5) ☐ Bleeding (6)☐ Raveling (7)☐ Polished Aggregate (8) ☐Reflective (9) ☐Blade Path (10) ☐Rutting (11)☐ Pumping			
	N/S	Hole#9	A	0.0	8.0	PMBP	location measured in ft. north of Runway 02 threshold
	G 98		B	8.0	15.0	Base Course	asphalt treated
	N 44		C	15.0	33.0	Subgrade	gravely gray-green sandy clay (plastic clay fraction); angular 1/2□-11/2□ lithic arkose
	G 61		D	33.0	40.0	Subgrade	dark gray-green sandy clay with rust and black sandy mottles
	N 72		E	40.0	53.0	Subgrade	dark tan sandy clay (moist, moderate ribbon)
	G 22		F	53.0	71.0	Subgrade	light tan sandy clay (moist, moderate ribbon, adhesive)
Mile Post: 2000 ft.	Rt. or Lt. ☒ ☐	C/L 348 in.	Distress ☐None	(1) ☒Transverse (2) ☒Longitudinal (3) ☐ Alligator (4) ☐ Pothole (5) ☐ Bleeding (6)☐ Raveling (7)☐ Polished Aggregate (8) ☐Reflective (9) ☐Blade Path (10) ☐Rutting (11)☐ Pumping			
	N/S	Hole#10	A	0.0	8.0	PMBP	location measured in ft. north of Runway 02 threshold
	B 11		B	8.0	14.0	Base Course	
	V 45		C	14.0	28.0	Subgrade	gravely gray-green sandy clay
	G 60		D	28.0	42.0	Subgrade	dark gray-green sandy clay (moist, strong ribbon)
	85 D		E	42.0	51.0	Subgrade	tan sandy clay (slightly moist, moderate ribbon)
	V 41*		F	51.0	71.0	Subgrade	lime stabilization sample (same as above)
Mile Post: 3000 ft.	Rt. or Lt. ☐ ☒	C/L 348 in.	Distress ☐None	(1) ☒Transverse (2) ☒Longitudinal (3) ☐ Alligator (4) ☐ Pothole (5) ☐ Bleeding (6) ☐Raveling (7)☐ Polished Aggregate (8) ☐Reflective (9) ☐Blade Path (10) ☐Rutting (11) ☐ Pumping			
	N/S	Hole#11	A	0.0	5.0	PMBP	location measured in ft. north of Runway 02 threshold
	L 54		B	5.0	11.0	Base Course	asphalt treated
	WT 205		C	11.0	30.0	Subgrade	gravelly black-green sandy clay (moist, plastic clay fraction

Table 3.5 CBR Results - Runway 4-22 at Double Eagle II

Location	Hole No.	Depth, ft.		Layer thickness	Group symbol	CBR
		From	To			
Runway 4-22	1	0	2.5	2.5	PMBP	
		2.5	9	6.5	SW	56
		9	21	12	SW-SM	22
		21	36	15	SP-SM	20
		36	55	19	SP-SM	19
	2	0	2.5	2.5	PMBP	
		2.5	8	5.5	SW	53
		8	16	8	SP-SM	20
		16	21	5	SP-SM	21
		21	55	34	SP-SM	20
	3	0	2.5	2.5	PMBP	
		2.5	8	5.5	GW	64
		8	21	13	SP-SM	20
		21	39	18	SW-SM	26
		39	55	16	SW-SM	20
	4	0	2.25	2.25	PMBP	
		2.25	9	6.75	GW	58
		9	27	18	SW-SM	20
		27	37	10	SW-SM	22
		37	55	18	SW-SM	20
	5	0	2	2	PMBP	
		2	9	7	SW	50
		9	23	14	SP-SM	20
		23	33	10	SW-SM	18
		33	41	8	SP-SM	18
		41	55	14	SP-SM	17
	6	0	2.5	2.5	PMBP	
		2.5	9	6.5	GW	60
		9	29	20	SP-SM	19
		29	37	8	SP-SM	19
		37	55	18	SW-SM	29
	7	0	3	3	PMBP	
		3	10	7	GW	59
		10	29	19	SW-SM	22
		29	55	26	SP-SM	19
	8	0	2.5	2.5	PMBP	
		2.5	9	6.5	SW	53
		9	19	10	SP-SM	20
		19	38	19	SW-SM	22
		38	55	17	SP-SM	18

Table 3.6 Direct Shear Test Results

Airport	Runway	Friction Angle, ϕ
Double Eagle II	4-22	37
Sierra Blanca Regional	12-30	42
Raton Municipal	7-25	39
	2-20	40
Moriarty Municipal	8-26	36
Las Cruces International	12-30	36
	8-26	37
Grant County	8-26	41
Deming Municipal	4-22	39
	8-26	36
Roswell International Air Center	3-21	39
Belen Alexander	3-21	35
Clayton Municipal	12-30	41
	2-20	40

Table 3.7 Resilient Modulus Test Result for Runway 4-22 at Double Eagle II Airport

Project	Location	Bag No.	Core No.	Sitt-ing loadlb (P_o)	Repeated load, lb (P)	Horizontal Deflection 10^{-6} inches (H)	Average Thickness, inches (t)	Resilient Modulus, psi Mr = 0.62[(P-P_o)/Ht]	Average Resilient Modulus, psi
Double Eagle II	RW 4-22	N-82	A	2	41	45	2.03	264696	274635
		N-82	B	4	42	43	2.00	273953	
		N-82	C	3	43	42	2.07	285254	
		S-28	A	4	42	39	2.28	264957	262282
		S-28	B	5	41	42	2.31	230056*	
		S-28	C	4	38	35	2.32	259606	

*Note: Poisson's Ratio assumed to be 0.35, (*)This value not used for averaging*

Table 3.8 Indirect Tensile Test Result for Runway 4-22 at Double Eagle II

Project	Location	Bag No.	Core No.	Diameter inches (D)	Maximum load, lbf (P)	Average Thickness, inches (t)	IDT Strength, psi $S_t = [(2\ P)/(\pi\ D\ t)]$	Average IDT Strength, psi
Double Eagle II	RW 4-22	N-82	A	4.0	3090.3	2.03	242.3	246.2
		N-82	B	4.0	3100.6	2.00	246.7	
		N-82	C	4.0	3249.1	2.07	249.8	
		S-28	A	4.0	3300.7	2.28	230.4	236.0
		S-28	B	4.0	3458.2	2.31	238.2	
		S-28	C	4.0	3490.0	2.32	239.4	

Table 3.9 G_{mb} Test Results for Runway 4-22 at Double Eagle II

Project	Location	Bag No.	Core No.	Weight in air, (g) (A)	Weight in water, (g) (B)	Weight surface dry, (g) (C)	G_{mb} = [A/(C-B)]	Average G_{mb}
Double Eagle II	RW 4-22	N-82	A	853.3	456.5	854.1	2.146	2.138
		N-82	B	842.7	450.9	845.5	2.136	
		N-82	C	860.8	459.4	863.2	2.132	
		S-28	A	980.7	509.8	985	2.064	2.069
		S-28	B	1001.2	529.2	1009.4	2.085	
		S-28	C	1030.1	533.9	1034.2	2.059	

Table 3.10 G_{mm} Test Results for Runway 4-22 at Double Eagle II

Project	Location	Bag No.	Wt. of Sample in air g (A)	Wt. of Flask with water g (B)	Wt. of Flask with Water and Sample g (C)	G_{mm} = A/(A+B-C)
DE II	RW 4-22	N-82	1004.7	2565.1	3138.5	2.329
		S-28	1063.6	2565.1	3164.7	2.292

Table 3.11 Percent Voids for Runway 4-22 at Double Eagle II

Project	Location	Bag No.	G_{mm}	G_{mb}	% Voids = 100* (G_{mm} - G_{mb})/ G_{mm}
DE II	RW 4-22	N-82	2.329	2.138	8.2
		S-28	2.292	2.069	9.7

Table 3.12 Asphalt Content Test Results for Runway 4-22 at Double Eagle II

Project	Location	Bag No.	Sample Weight (g)	Weight Loss (g)	Percent Loss %	Temp Comp %	Bitumen Ratio %	Calibrated Asphalt Content %
DE II	RW 4-22	N-82	2517	152.6	6.06	0.12	6.34	5.94
		S-28	3027	196.0	6.48	0.10	6.82	6.38

Table 3.13 Gradation Results of Sample N 22 of Runway 4-22 at Double Eagle II

Sieve Size, mm	Sieve Wt., g	Sieve Wt. with Soil, g	Soil Wt. g	% Retained	Cumulative % Passing
19	495.3	525.3	30.0	1.3	98.7
9.5	482.3	993.2	510.9	21.6	77.2
4.75	531.4	1052.6	521.2	22.0	55.2
2.00	463.9	796.2	332.3	14.0	41.1
0.425	368.8	709.2	340.4	14.4	26.7
0.150	414.0	832.5	418.5	17.7	9.1
0.075	513.0	658.8	145.8	6.2	2.9
Pan	376.6	445.0	68.4	2.9	
		Total	2367.5		

Note: Sample Weight (g): 2368.3

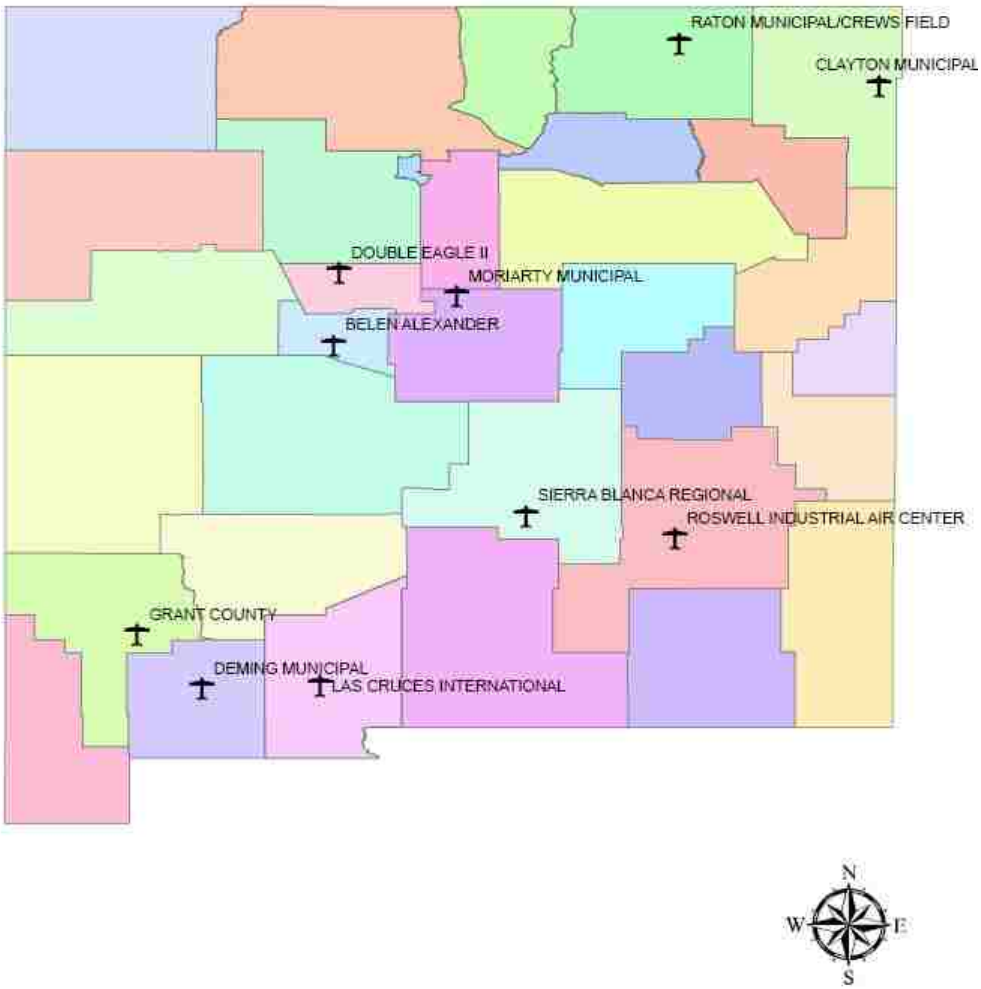

Figure 3.1 Evaluated Airports in New Mexico

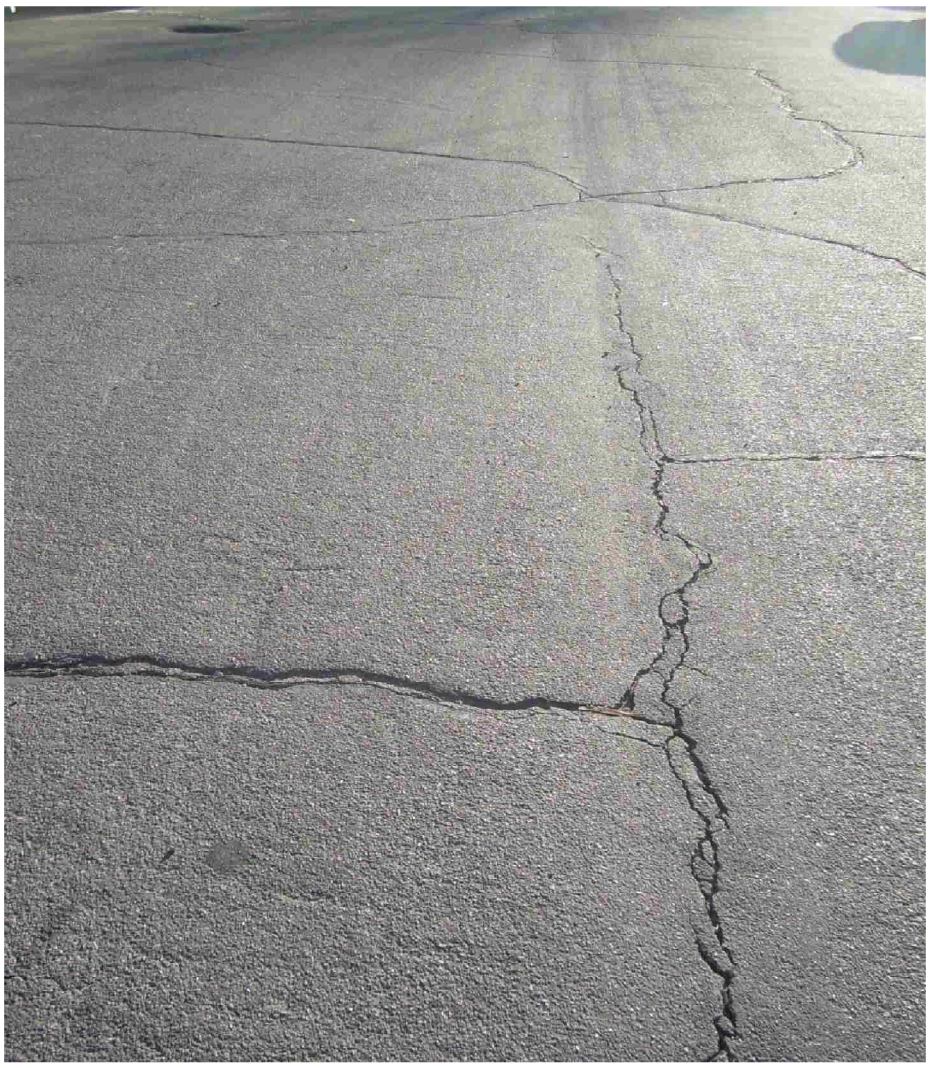

Figure 3.2 Longitudinal and Transverse Cracking on Runway 4-22 of Double Eagle II

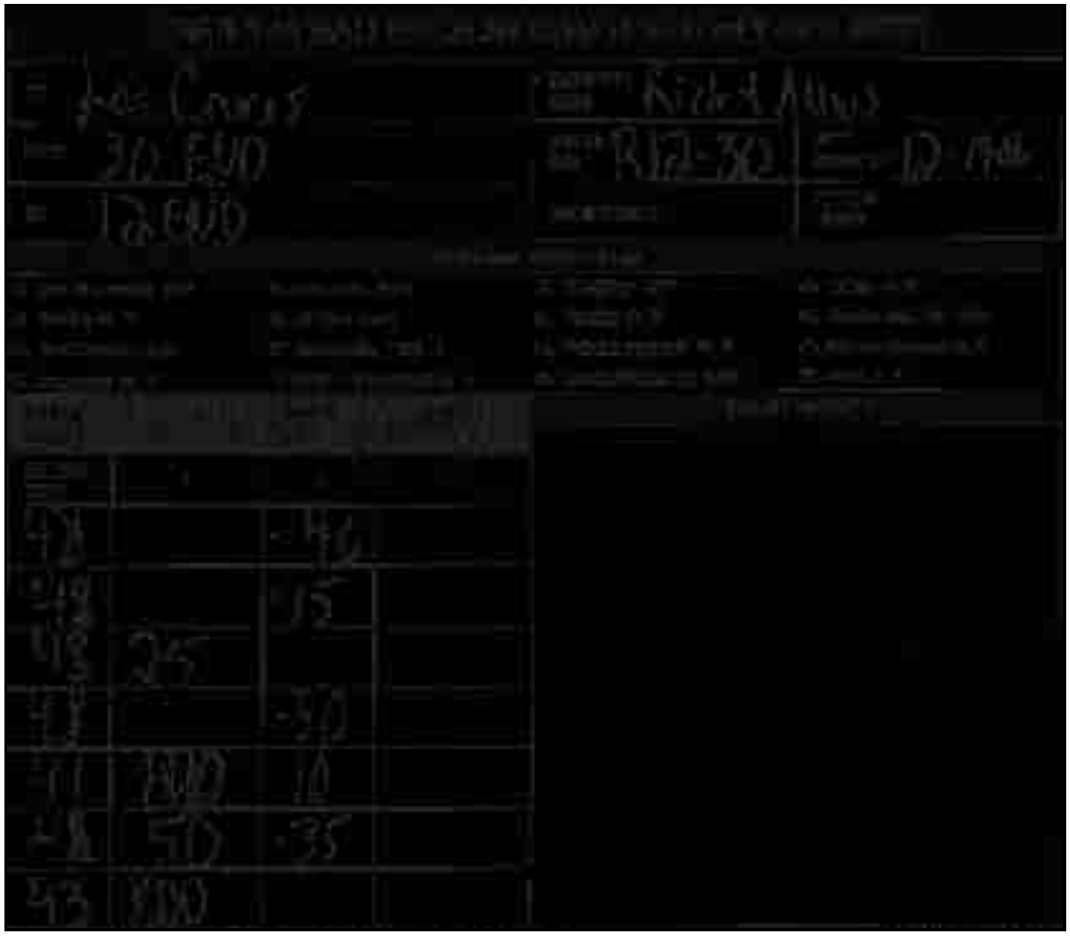

Figure 3.3 Field Distress Data Collection Sheet

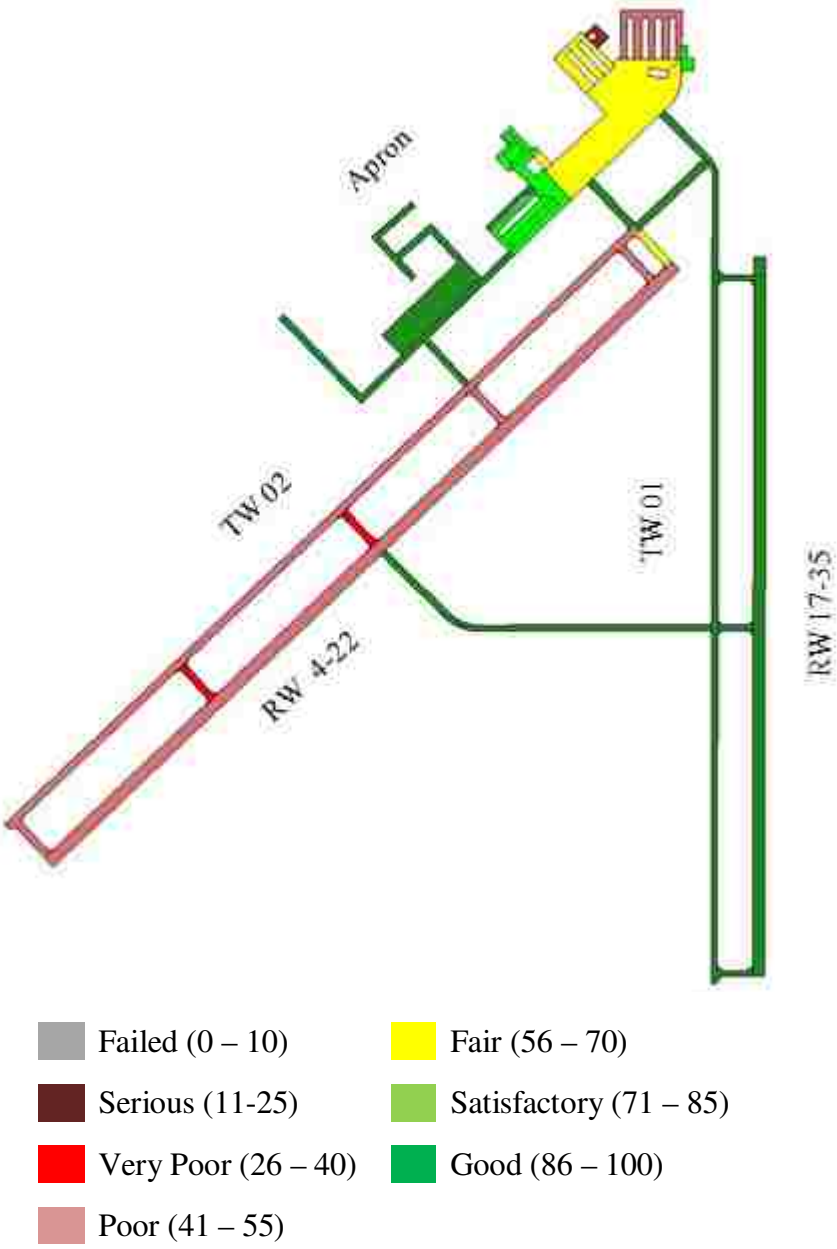

Figure 3.4 PCI of Pavements at Double Eagle II Airport

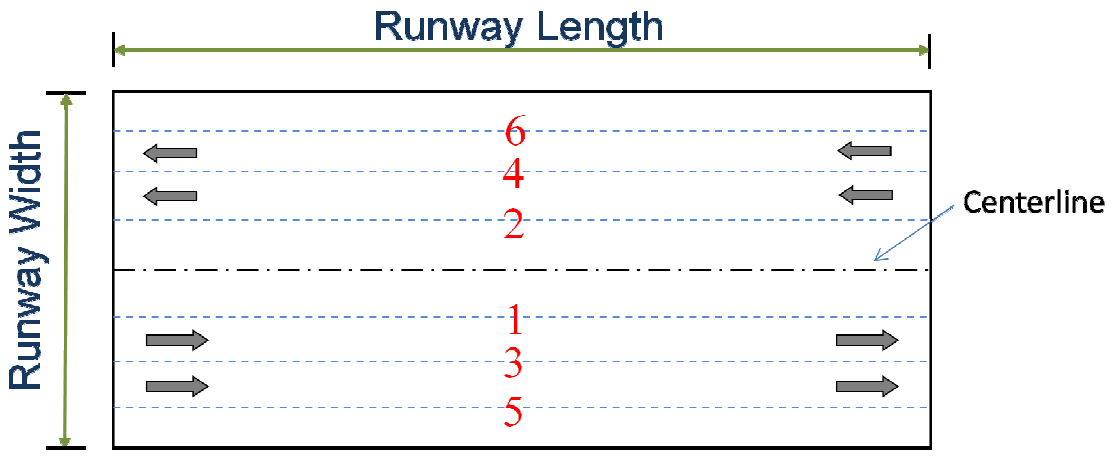

Note:

Runs 1 & 2 - 5 feet from centerline

Runs 3 & 4 - 20 feet from centerline

Runs 5 & 6 - 30 ~ 40 feet from centerline (depending on width of runway)

Figure 3.5 FWD Testing Plan

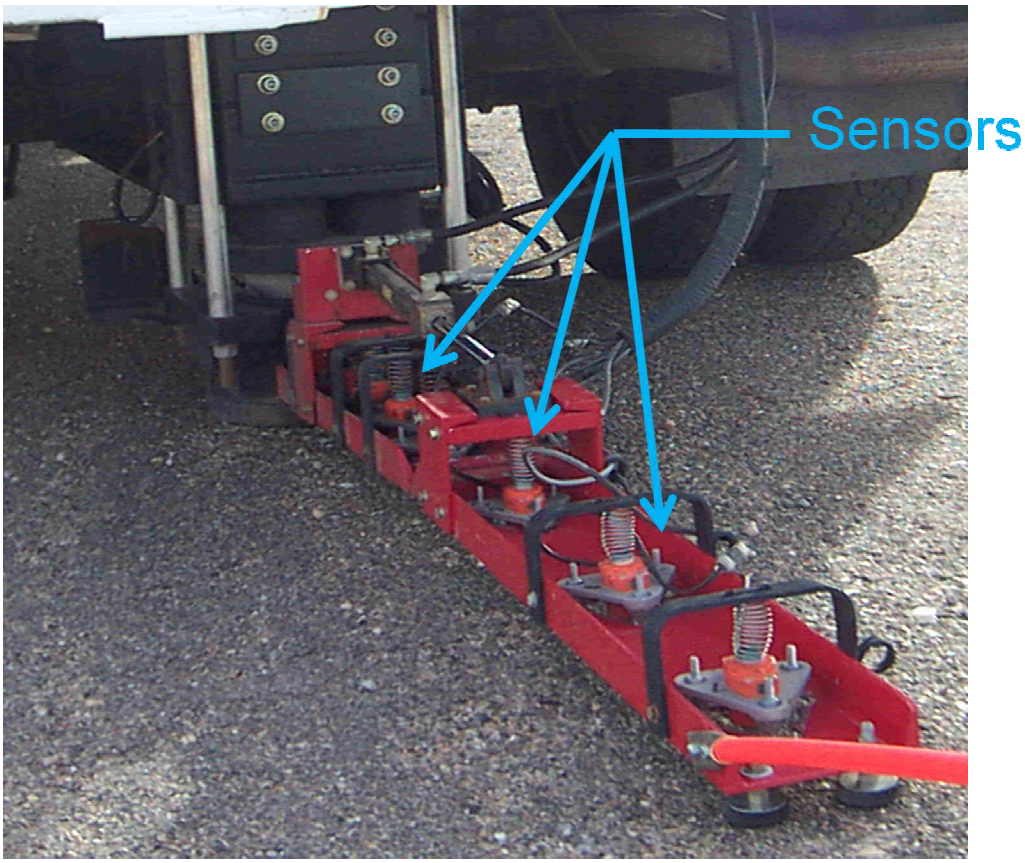

Figure 3.6 Jills FWD Equipment with Seven Sensors

Figure 3.7 Dynatest Skid Resistance Equipment

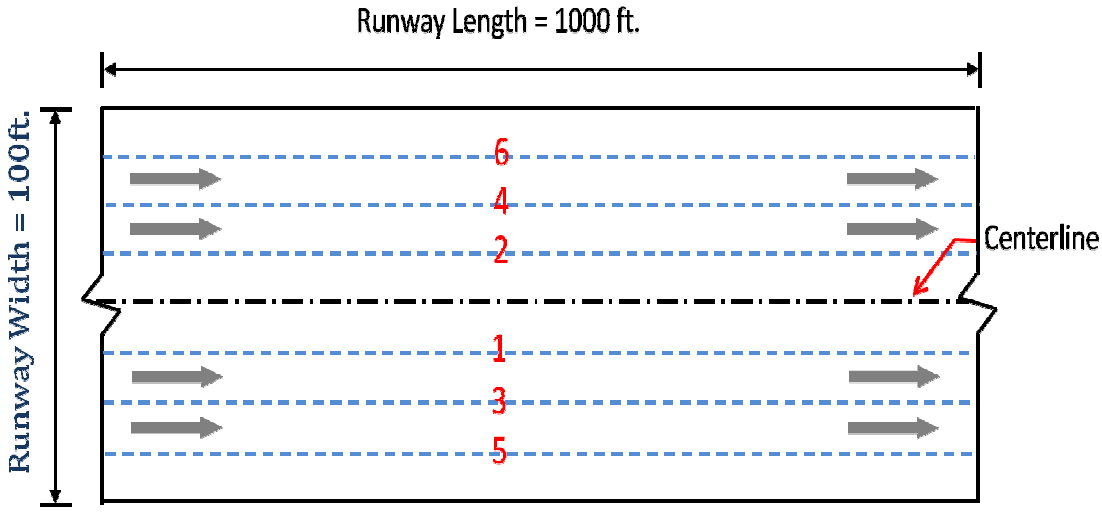

Note:

Runs 1 & 2 - 5 feet from centerline

Runs 3 & 4 - 20 feet from centerline

Runs 5 & 6 - 30 ~ 40 feet from centerline (depending on width of runway)

Figure 3.8 Skid Test Plan

Figure 3.9 Layout of Runway 12-30 with Borehole Locations at Sierra Blanca Airport

Form No. 1154
Rev. 02/06 (Formerly MT-29)

New Mexico Department of Transportation
Materials and Testing Laboratory

Project: 1

Sheet: 1 of 5

LOG OF TEST HOLES

Location: Belen Municipal
District: 3

Control Number: AV-E8001
Operator: Kenny

☐ Subgrade	☐ Borrow	☐ Surfacing	☐ Filler	☒ Thru Pavement

Source Location: Runway 03-21 (Distances measured from 03 Threshold)

Lab No.	Sack No.	Hole & Sample Number		Depth From	Depth To	Station Sample Or Material Types	Remarks & Material Identification
Mile Post: 900'	**Rt or Lt** ☒ ☐	**C/L 120 in**	**Distress** ☐ None	(1) ☐ Transverse (2) ☐ Longitudinal (3) ☐ Alligator (4) ☐ Pothole (5) ☐ Bleeding (6) ☐ Raveling (7) ☐ Polished Aggregate (8) ☐ Reflective (9) ☐ Blade Patch (10) ☐ Rutting (11) ☐ Pumping			
	WT-CX	**Hole #1**	**A**	0.00	2.25"	PMBP/OGFC	CORE A
			B		2.25"		CORE B
			C		2.25"		CORE C
			D		2.25"		CORE D
			E				
			F				
Mile Post: 1900'	**Rt or Lt** ☐ ☒	**C/L 144 in**	**Distress** ☐ None	(1) ☐ Transverse (2) ☐ Longitudinal (3) ☐ Alligator (4) ☐ Pothole (5) ☐ Bleeding (6) ☐ Raveling (7) ☐ Polished Aggregate (8) ☐ Reflective (9) ☐ Blade Patch (10) ☐ Rutting (11) ☐ Pumping			
	WT-HN	**Hole #2**	**A**	0.00	2.25"	PMBP/OGFC	CORE A
			B		2.25"		CORE B
			C		2.25"		CORE C
			D		2.25"		CORE D
			E				
			F				
Mile Post: 2900"	**Rt or Lt** ☒ ☐	**C/L 180 in**	**Distress** ☐ None	(1) ☐ Transverse (2) ☐ Longitudinal (3) ☐ Alligator (4) ☐ Pothole (5) ☐ Bleeding (6) ☐ Raveling (7) ☐ Polished Aggregate (8) ☐ Reflective (9) ☐ Blade Patch (10) ☐ Rutting (11) ☐ Pumping			
	WT-F1	**Hole #3**	**A**	0.00	2.25"	PMBP/OGFC	CORE A
			B		2.25"		CORE B
			C		2.25"		CORE C
			D		2.25		CORE D
			E				
			F				
Mile Post: 3750'	**Rt or Lt** ☐ ☒	**C/L 120 in**	**Distress** ☐ None	(1) ☐ Transverse (2) ☐ Longitudinal (3) ☐ Alligator (4) ☐ Pothole (5) ☐ Bleeding (6) ☐ Raveling (7) ☐ Polished Aggregate (8) ☐ Reflective (9) ☐ Blade Patch (10) ☐ Rutting (11) ☐ Pumping			
	R 99	**Hole #4**	**A**	0.00	2.25"	PMBP/OGFC	CORE A
			B		2.25"		CORE B
			C		2.25"		CORE C
			D		2.25"		CORE D
			E				
			F				

*Lime stabilization

Sampled By: Roger Martinez

Date: 08/11/09

Submitted By: Roger Martinez

Figure 3.10 Field Log with Asphalt Core Details

Figure 3.11 Collection of Soil Samples

Figure 3.12 Soil Samples in Bags

Figure 3.13 Splitting of the Soil Samples

Figure 3.14 Hydrometer Analysis

Figure 3.15 Liquid Limit Test

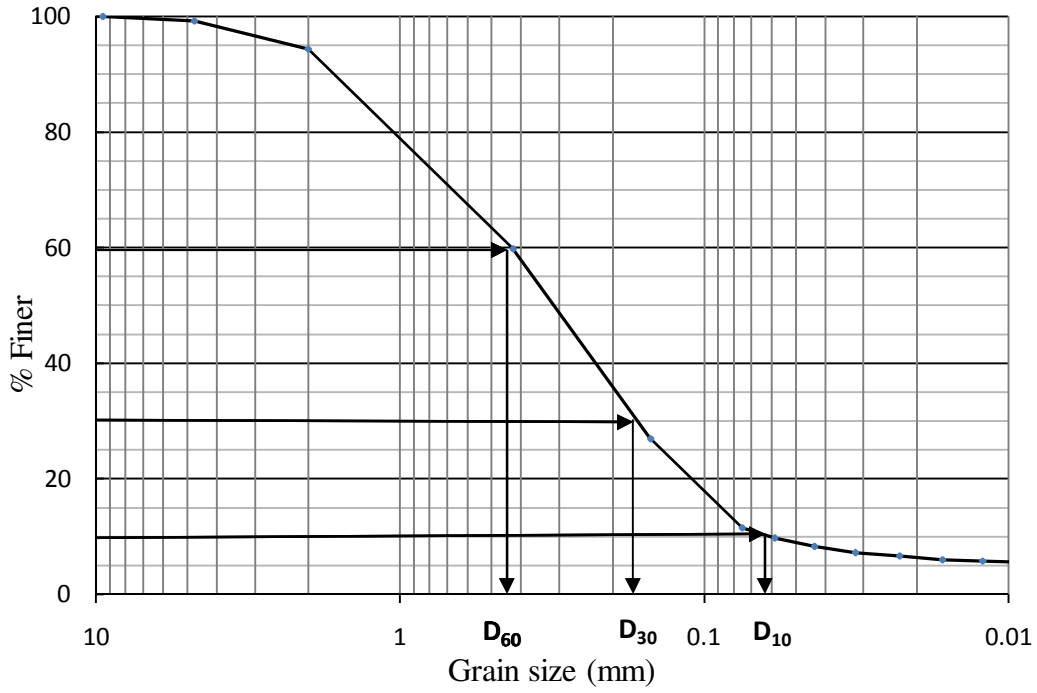

Figure 3.16 Particle-size Distribution Curve

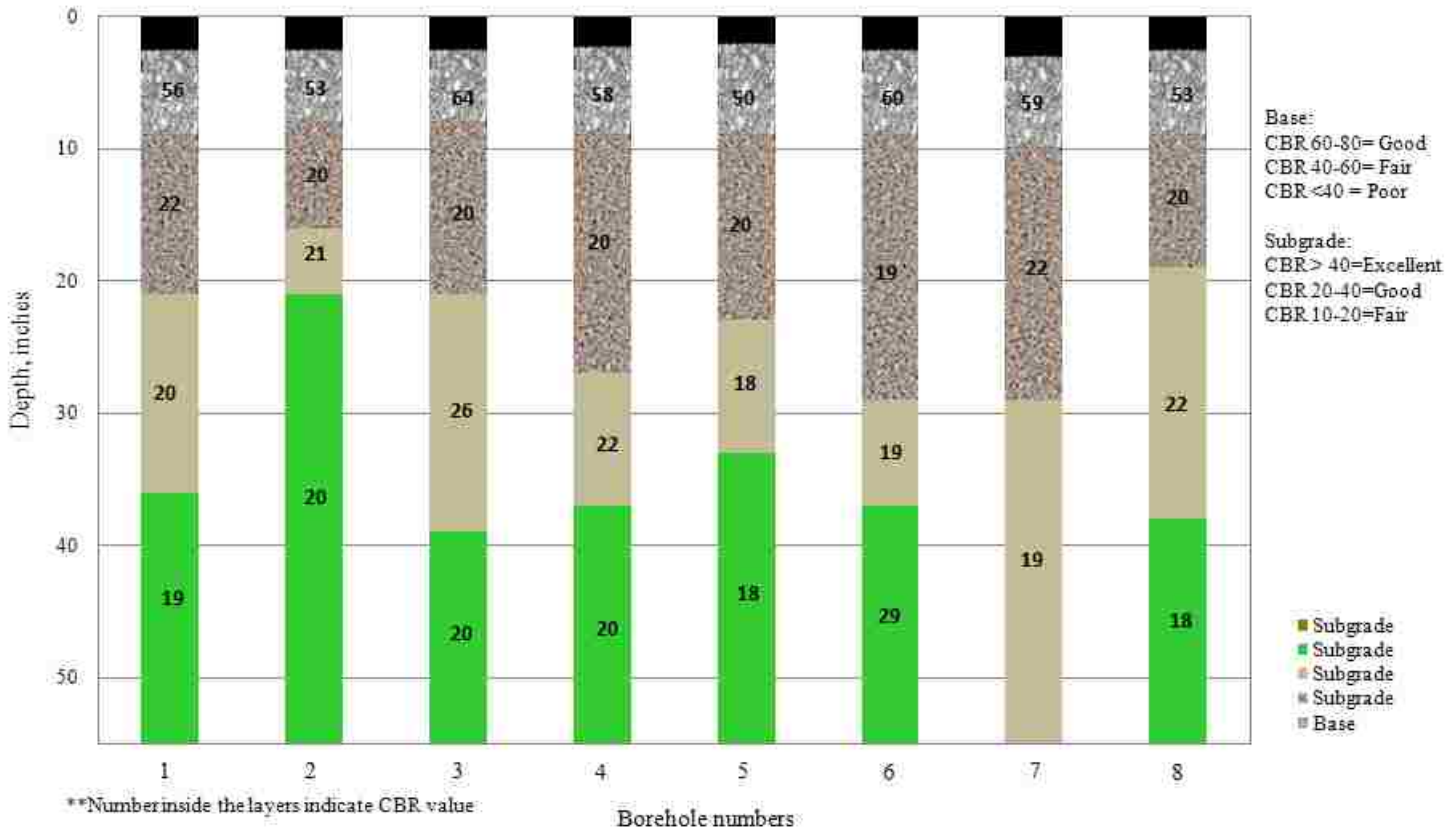

Figure 3.17 Soil Profile of Runway 4-22 at Double Eagle II Airport with CBR Values

Figure 3.18 Shear Box with Sample

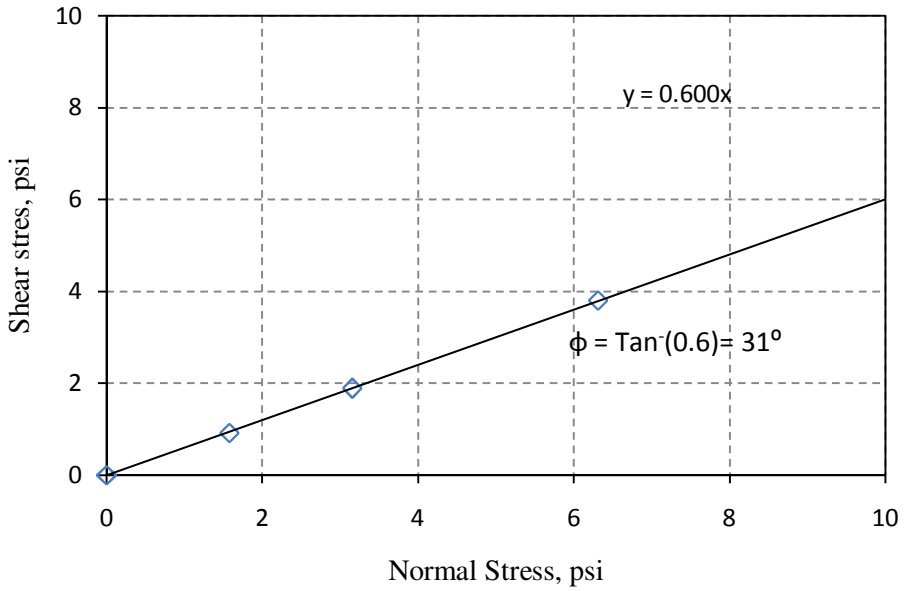

Figure 3.19 Plot of Direct Shear Results for Ottowa Sand

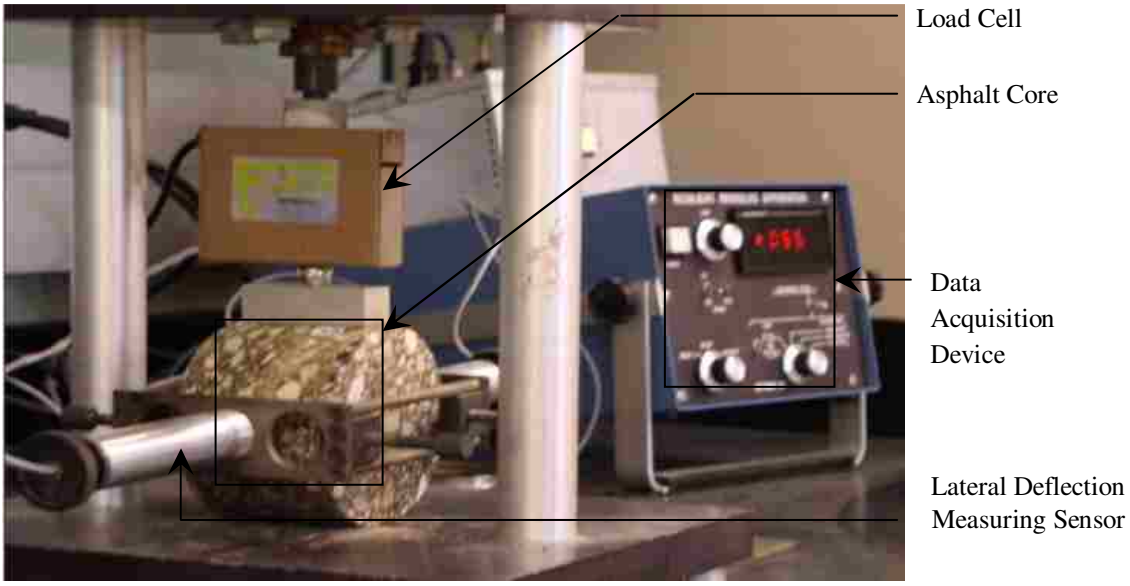

Figure 3.20 Resilient Modulus Test Apparatus

Figure 3.21 Indirect Tensile Strength Test

Figure 3.22 Bulk Specific Gravity Test

Figure 3.23 Theoretical Maximum Specific Gravity Test

Figure 3.24 NCAT Asphalt Content Tester

Figure 3.25 Sample for Gradation Analysis after Determination of Asphalt Content

CHAPTER 4

RANKING OF AIRPORTS

4.1 Criteria Used for Ranking

Pavement Condition Index (PCI) inspection data can be turned into a key tool for planning to maintain and improve airport pavements (Thuma et al. 2008). FAA Advisory Circular 150/5380-6B recommends PCI inspection to be carried out once a year. Pavement sections with PCI values below 55 become candidates for complete reconstruction depending on the type of distresses. Overtime, the skid resistance of runway pavement deteriorates due to mechanical wear and polishing action from aircraft tires. Structural pavement failure such as rutting, raveling, or settling can also contribute to friction losses. FAA Advisory Circular 150/5320-12C recommends skid test to be carried out at least once a year to determine the Skid Number (SN) depending on the number of aircraft landings. A pavement may have the structural soundness to support a load but cannot function as an aircraft operating surface due to poor frictional characteristics (Walrond and Christiansen 1993). Poor frictional characteristics lead to safety hazards for the passengers and foreign object damage potential for aircrafts. Pavement surface texture that contribute to resistance to skidding are the microtexture and macrotexture (Ahammed and Tighe 2008). The PCI and SN values are used for the functional and overall evaluation of the runway pavements.

As outlined in FAA Advisory Circular 150/5320-6E, the CBR value of the subgrade is used for flexible pavement design whereas the resilient modulus of the subgrade is used for rigid pavement design. For gravelly material, the FAA design procedure recommends

a maximum CBR value of 33 for use in design. Also, the relationship to obtain the resilient modulus from CBR is:

$$M_R = 1500\,CBR \tag{4.1}$$

Ward (2008) used the results of the dynamic cone penetrometer (DCP) to determine the CBR value when field expediency was required using the following relationship:

$$CBR = \frac{292}{DCP^{1.12}} \tag{4.2}$$

The subgrade and base course CBR values are used for the structural and overall evaluation of the runway pavements.

Pavement design methods for flexible pavements are based on the assumption that pavement life is inversely related to the magnitude of the traffic-induced pavement strains (Zuo et al. 2007). These strains vary with the stiffness and the stiffness of the asphalt varies with the temperature. The Resilient Modulus (M_R) of the asphalt cores are determined to find the stiffness of the asphalt layer. The Indirect Tensile Strength (ITS) is a measure of the strength of the material. Its of the asphalt cores were determined in the laboratory. Guler (2008) found that the yield stress for fine gradation is larger than for coarse gradation. The use of a linear AC temperature profile significantly affects the calculated critical tensile strains, especially when the AC layer is thin (Zuo et al. 2007). Pavement designs based on monthly average temperatures neglect the significant damage that occurs during brief periods of high temperature. ITS increases as moisture content decreases. The increase is more significant when the moisture content decreases from

1.0% to 0.5% (Lee et al. 2008). MR and ITS values are used for the structural and overall evaluation of the runway pavements.

4.2 Evaluation Based on Pavement Condition Index (PCI)

The 19 runways of the 10 airports were ranked according to the standard PCI rating scale presented in Table 2.2 (Greene 2004). The results of the rating are presented in Table 4.1. It can be seen that the PCI values range from 98 to 28. Based on the PCI values, three runways having PCI value more than 85 are in good condition, five runways having PCI value more than 70 are in satisfactory condition, six runways having PCI value more than 55 are in fair condition, four runways having PCI value less than 55 are in poor condition and one runway having PCI value less than 40 is in very poor condition. Therefore, if rehabilitation design is considered based on PCI, which is a functional index, 5 out of the 19 runway pavements need immediate remedial action.

4.3 Evaluation Based on Skid Number

The maximum likelihood skid number (SN) of the runways for all 10 airports was determined. Maximum likelihood value is the value with the highest frequency in a data set. It is obtained by drawing a histogram and the value corresponding to the peak frequency is the maximum likelihood value. When there is a small data set, maximum likelihood value is better than simple "mean" or "average" value. Figure 4.1 shows the maximum likelihood skid number of Runway 2-20 at Raton Municipal Airport. The maximum likelihood SN is equal to 60 with a frequency of 19. This plot also shows that SN of Runway 2-20 varies from 47 to 62. The results for all the airports are shown in Table 4.2. FAA: AC 150/5320 – 12C specifies that the minimum required SN value is 50.

A runway with a SN value of 60 or less requires maintenance work. The SN value of these runways ranges from 72 to 30. According to the SN criteria, five runways having SN more than 60 are in fair condition, seven runways having SN between 50 and 60 require maintenance planning. Six runways have values which are below the required minimum, therefore they require immediate attention.

Low skid resistance values can be improved by grooving, by surface treatment or thin overlay, or by heater planer (Huang 2004). Grooving is the process of cutting shallow, narrow channels on the surface. However, grooves in asphalt pavements with high asphalt content could flow together in hot weather and lose their effectiveness. Surface treatment and/or thin overlay includes open-graded friction course. Open-graded friction course are specially designed to reduce hydroplaning. Proper selection of aggregate type, gradation, and transverse slope help reduce hydroplaning. Heater planer is used to correct bleeding problems. It is done by heating and cutting and removing the excess binder. Next, stone chips or sand is spread on the surface and compacted.

4.4 Evaluation Based on Subgrade Soils

The soil samples were tested in the laboratory to determine index properties, gradation, moisture, classification, strength, CBR and friction angle.

4.4.1 Evaluation Based on Subgrade CBR

The CBR values are usually calculated for material of each layer. If a single layer constitutes of several different materials, CBR values have to be determined for each layer. Next, the question is how to find a CBR value for an entire runway. Well, it can be

done by using weighted average value of CBR. The weighted average CBR of the subgrade for each runway was calculated using the equation:

$$CBR_{weighted} = \frac{\sum CBR_i \times t_i}{\sum t_i} \quad (4.3)$$

where CBR_i is the CBR of the i th layer, t_i is the thickness of the i th layer and $\sum t_i$ is the total thickness of all the subgrade layers. The results of the calculations are presented in Table 4.3. It can be noted that samples were collected from only 14 runways out of 19. Five runways were not cored as they are relatively new. The weighted CBR values range from 52 to 20. The subgrade CBR values were evaluated according to FAA: AC 150/5320 - 6D Part 1. Five runways have excellent subgrade CBR values (>40) and nine runways have good subgrade CBR values (>20). Based on the subgrade CBR values, no action is required to correct the subgrade at any of the airports. Therefore, it can be concluded that all the New Mexico runways have good subgrade.

4.4.2 Evaluation Based on Friction Angle

The friction angle of soil samples immediately below the base course from boreholes across the runway was determined from the Direct Shear Test. The average friction angle was calculated for each runway. The results for all the ten airports are presented in Table 4.4. The friction angle values range from 42 to 35. The soils were mainly sand with silt and pebbles. Usually, silty sand has a friction angle more than 30°. The soils tested herein had pebbles (engineered soil), therefore, high friction angle values were obtained. Apparently, the top 12 inches of the subgrade looks like engineered soil.

4.5 Evaluation Based on Base course

The base course samples were tested in the laboratory to determine the CBR value.

4.5.1 Evaluation Based on Base Course CBR

The weighted average CBR of the base course was determined for each runway using Eq. 4-3. The base course CBR values are presented in Table 4.6. The results were evaluated using Table 4.5. The CBR values range from 66 to 42. Four runways have good CBR values (>60), nine runways have fair CBR values (>40), and Runway 8-26 at Moriarty Municipal Airport has no base course. Runway 8-26 at Moriarty Municipal Airport is a full depth asphalt concrete pavement. Based on the base course CBR values, no action is required to correct the base course at any of the airports.

4.6 Evaluation Based on Asphalt Cores

In this section, surface course of airport pavements are evaluated using the Resilient Modulus (M_R), Indirect Tensile Strength (ITS), Void Ratio, and Asphalt Content values.

4.6.1 Evaluation Based on M_R

Six asphalt cores from each runway were tested and the M_R values were averaged to come up with a single value for the runway. The results for all the runways of the 10 airports are presented in Table 4.7. The M_R values range from 183,656 to 268,459 psi. The values for new pavements range from 500,000 to 1,000,000 psi (Huang 2004). The obtained values are reasonable considering air voids, damage and micro cracking over the years. One runway has M_R value of less than 200,000 psi and requires attention.

4.6.2 Evaluation Based on ITS

Six asphalt cores from each runway were tested and the ITS values were averaged to come up with a single value for the runway. The results for all the runways of the 10 airports are presented in Table 4.8. The ITS values range from 164.8 to 307.4 psi. These values are comparable to the values in Table 2.1 which were obtained by Bell et al. (2008) in their study of various airport pavements. Any ITS value more than 100 psi is really good to resist low temperature cracking.

4.6.3 Evaluation Based on Void Ratio and Asphalt Content

The bulk specific gravity of the asphalt cores and the theoretical maximum specific gravity of the mix were determined in the laboratory. The percent of voids were calculated using Eq. (3-7). The values were averaged to obtain a single value for a runway. The results are presented in Table 4.9. The percent of voids varies from 2.5 to 10.1 %. The runways that have high air voids are probably relatively new compared to the runways with low air voids. There are runways which have more than 7% air voids, which tells us that poor compaction was done during construction. These runways may show wheel path rut due to compaction under aircraft loading.

The asphalt content of the mix was determined in the laboratory by burning the asphalt. The average value of the asphalt content for each runway was calculated. The results for all the 10 airports are shown in Table 4.9. The asphalt content values range from 5.55 to 7.89 %.

4.7 Overall Rating

The runway pavements are ranked based on six different test results: PCI, SN, Base CBR, Subgrade CBR, Surface M_R, and Surface ITS results. Weights were assigned for different range of values for all the test results in this study as presented in Table 4.10. It can be seen that each runway is assigned 0 if the particular test result is poor and a weight value of 3 if the result is good for PCI, SN, Base CBR, and Subgrade CBR. The assigned weight value range for Surface M_R and Surface ITS are 0 to 6. This was done to account for the change in the stiffness and strength values of the asphalt surface course with time. Also, the surface course is more expensive as compared to the other layers and has the important role of protecting the underlying layers. The CBR values for the base course and subgrade do not really change with time. First, all the 18 runways of ten airports were evaluated and ranked based on PCI and SN results presented in Figure 4.2. It can be seen that the functional condition of Runway 17-35 at Double Eagle II Airport is very good while that of Runway 3-21 at Belen Municipal Airport and Runway 12-30 at Las Cruces International is poor. No skid test was carried out on Runway 12-30 at Roswell International Air Center. No coring was done on Runway 17-35 at Double Eagle II, Runway 17-35 at Roswell International Air Center, and Runway 6-24 at Sierra Blanca Regional Airport.

All 14 runways were evaluated and ranked based on Base CBR, Subgrade CBR, Surface M_R, and Surface ITS test results. It is so called structural strength and the results are presented in Figure 4.3. It can be seen that the structural health of Runways 2-20 and 7-25 Raton Municipal Airport is good while that of Runway 3-21 at Roswell International Airport and Runway 3-21 at Belen Municipal Airport is poor. Finally, the overall rating

of the 14 runways was done based on all the six test results. The results are presented in Figure 4.4. It can be seen that Runways 2-20 and 7-25 Raton Municipal Airport are in the best condition with weight values of 18 each out of 24 maximum possible weight values. Runway 3-21 at Belen Municipal Airport with weight value of 11 is at the bottom of the list. Based on all the results, it is apparent that Runway 3-21 at Belen Municipal Airport, Runway 12-30 at Las Cruces International Airport and Runway 3-21 at Roswell International need attention. No coring was carried out on Runway 4-22 at Las Cruces International Airport as it is not funded and coring was abandoned on Runway 12-30 at Roswell International Air Center upon encountering concrete. The remaining 14 runways were cored to determine the structural health of the pavements.

Table 4.1 PCI Ranking of Runways of Evaluated Airports

Runway No.	Name of Airport	Runway	PCI	Remarks
1	Double Eagle II	17-35	98	Good
2	Sierra Blanca Regional	12-30	88	Good
3	Roswell International Air Center	17-35	87	Good
4	Sierra Blanca Regional	6-24	84	Satisfactory
5	Raton Municipal	2-20	79	Satisfactory
6	Clayton Municipal	2-20	73	Satisfactory
7	Deming Municipal	8-26	72	Satisfactory
8	Clayton Municipal	12-30	71	Satisfactory
9	Raton Municipal	7-25	68	Fair
10	Las Cruces International	8-26	66	Fair
11	Roswell International Air Center	3-21	65	Fair
12	Roswell International Air Center	12-30	61	Fair
13	Moriarty Municipal	8-26	60	Fair
14	Deming Municipal	4-22	60	Fair
15	Grant County (Silver City)	8-26	55	Poor
16	Double Eagle II	4-22	54	Poor
17	Belen Municipal	3-21	51	Poor
18	Las Cruces International	12-30	43	Poor
19	Las Cruces International	4-22	28	Very Poor

Table 4.2 SN Ranking of Runways of Evaluated Airports

Runway No.	Name of Airport	Runway	SN	Remarks
1	Clayton Municipal	2-20	72	Fair
2	Las Cruces International	4-22	67	Fair
3	Double Eagle II	17-35	65	Fair
4	Deming Municipal	8-26	63	Fair
5	Raton Municipal	7-25	61	Fair
6	Raton Municipal	2-20	60	Maintenance Planning
7	Double Eagle II	4-22	59	Maintenance Planning
8	Roswell International Air Center	17-35	58	Maintenance Planning
9	Clayton Municipal	12-30	58	Maintenance Planning
10	Roswell International Air Center	3-21	52	Maintenance Planning
11	Sierra Blanca Regional	6-24	50	Maintenance Planning
12	Grant County (Silver City)	8-26	50	Maintenance Planning
13	Las Cruces International	8-26	46	Below Minimum
14	Sierra Blanca Regional	12-30	45	Below Minimum
15	Deming Municipal	4-22	45	Below Minimum
16	Las Cruces International	12-30	43	Below Minimum
17	Belen Municipal	3-21	35	Below Minimum
18	Moriarty Municipal	8-26	30	Below Minimum

Table 4.3 CBR Ranking of Runway Subgrades of Evaluated Airports

Runway No.	Name of Airport	Runway	CBR	Remarks
1	Sierra Blanca Regional	12-30	52	Excellent
2	Raton Municipal	2-20	50	Excellent
3	Raton Municipal	7-25	44	Excellent
4	Grant County (Silver City)	8-26	41	Excellent
5	Roswell International Air Center	3-21	41	Excellent
6	Las Cruces International	12-30	36	Good
7	Clayton Municipal	2-20	31	Good
8	Las Cruces International	8-26	30	Good
9	Deming Municipal	8-26	25	Good
10	Clayton Municipal	12-30	23	Good
11	Deming Municipal	4-22	21	Good
12	Double Eagle II	4-22	20	Good
13	Moriarty Municipal	8-26	20	Good
14	Belen Municipal	3-21	20	Good

Table 4.4 Friction Angle Values of Runway Soils of Evaluated Airports

Runway No.	Name of Airport	Runway	Average Friction Angle, φ (degrees)
1	Sierra Blanca Regional	12-30	42
2	Grant County (Silver City)	8-26	41
3	Clayton Municipal	12-30	41
4	Raton Municipal	2-20	40
5	Clayton Municipal	2-20	40
6	Raton Municipal	7-25	39
7	Deming Municipal	4-22	39
8	Roswell International Air Center	3-21	39
9	Double Eagle II	4-22	37
10	Las Cruces International	8-26	37
11	Moriarty Municipal	8-26	36
12	Las Cruces International	12-30	36
13	Deming Municipal	8-26	36
14	Belen Municipal	3-21	35

Table 4.5 Typical California Bearing Ratio (CBR) Values of Base Course

Name	CBR	Value as Subgrade	Value as Base Course
Gravel or sandy gravel well graded	60 - 80	Excellent	Good
Gravel or sandy gravel poorly graded	35 - 60	Good to excellent	Poor to fair
Gravel or sandy gravel uniformly graded	25 - 50	Good	Poor
Silty gravel or silty sandy gravel	40 - 80	Good to excellent	Fair to good
Clayey gravel or clayey sandy gravel	20 - 40	Good	Poor
Sand or gravelly sand well graded	20 - 40	Good	Poor
Sand or gravelly sand poorly graded	15 - 25	Fair to good	Poor to not suitable
Sand or gravelly sand uniformly graded	10 - 20	Fair to good	Not suitable
Silty sand or silty gravelly sand	20 - 40	Good	Poor
Clayey sand or clayey gravelly sand	10 - 20	Fair to good	Not suitable

Table 4.6 CBR Ranking of Runway Base Course of Evaluated Airports

Runway No.	Name of Airport	Runway	CBR	Remarks
1	Raton Municipal	2-20	66	Good
2	Raton Municipal	7-25	66	Good
3	Las Cruces International	8-26	62	Good
4	Roswell International Air Center	3-21	61	Good
5	Double Eagle II	4-22	56	Fair
6	Sierra Blanca Regional	12-30	56	Fair
7	Grant County (Silver City)	8-26	54	Fair
8	Deming Municipal	4-22	53	Fair
9	Clayton Municipal	12-30	53	Fair
10	Belen Municipal	3-21	51	Fair
11	Deming Municipal	8-26	46	Fair
12	Clayton Municipal	2-20	46	Fair
13	Las Cruces International	12-30	42	Fair
14	Moriarty Municipal	8-26	NA	No Base

Table 4.7 M_R Ranking of Runways of Evaluated Airports

Runway No.	Name of Airport	Runway	Modulus M_R, psi
1	Clayton Municipal	12-30	296986
2	Clayton Municipal	2-20	286894
3	Double Eagle II	4-22	268459
4	Las Cruces International	12-30	266290
5	Deming Municipal	8-26	263671
6	Raton Municipal	2-20	263218
7	Las Cruces International	8-26	258123
8	Deming Municipal	4-22	255399
9	Raton Municipal	7-25	253255
10	Sierra Blanca Regional	12-30	251804
11	Grant County (Silver City)	8-26	244363
12	Belen Municipal	3-21	240171
13	Moriarty Municipal	8-26	221775
14	Roswell International Air Center	3-21	183656

Table 4.8 ITS Ranking of Runways of Evaluated Airports

Runway No.	Name of Airport	Runway	ITS, psi
1	Roswell International Air Center	3-21	307.4
2	Sierra Blanca Regional	12-30	271.7
3	Las Cruces International	8-26	263.1
4	Clayton Municipal	2-20	261.3
5	Clayton Municipal	12-30	254.0
6	Las Cruces International	12-30	250.5
7	Moriarty Municipal	8-26	244.1
8	Double Eagle II	4-22	241.1
9	Belen Municipal	3-21	240.9
10	Deming Municipal	8-26	239.1
11	Grant County (Silver City)	8-26	214.9
12	Deming Municipal	4-22	190.1
13	Raton Municipal	2-20	181.1
14	Raton Municipal	7-25	164.8

Table 4.9 Asphalt Content and Void Ratio of Runways of Evaluated Airports

Runway No.	Name of Airport	Runway	Void Ratio, %	Fines, %	Asphalt Content, %
1	Raton Municipal	2-20	4.5	4.9	7.89
2	Las Cruces International	8-26	8.2	5.5	7.85
3	Deming Municipal	8-26	6.3	5.4	7.81
4	Grant County (Silver City)	8-26	5.7	4.8	7.52
5	Deming Municipal	4-22	8.0	5.0	7.38
6	Raton Municipal	7-25	10.1	5.0	6.52
7	Sierra Blanca Regional	12-30	4.8	6.1	6.39
8	Roswell International Air Center	3-21	4.9	5.3	6.34
9	Clayton Municipal	12-30	5.3	6.3	6.19
10	Double Eagle II	4-22	9.0	3.2	6.16
11	Las Cruces International	12-30	10.0	4.4	5.98
12	Clayton Municipal	2-20	5.9	6.1	5.88
13	Moriarty Municipal	8-26	2.5	6.5	5.72
14	Belen Municipal	3-21	2.9	3.8	5.55

Table 4.10 Pavement Ranking Guideline

Assigned Weight Value	Evaluating Criteria				Assigned Weight Value	Evaluating Criteria	
	Based on PCI	Based on SN	Based on Base CBR	Based on Subgrade CBR		Based on $M_{R,}$ ksi	Based on ITS, psi
0	Poor	< 50	Poor	Poor	0	< 200	< 50
1	Fair	50 - 60	Fair	Fair	2	200-250	50-75
2	Satisfactory	60 - 70	Good	Good	4	251-300	75-100
3	Good	> 70	Excellent	Excellent	6	>300	>100

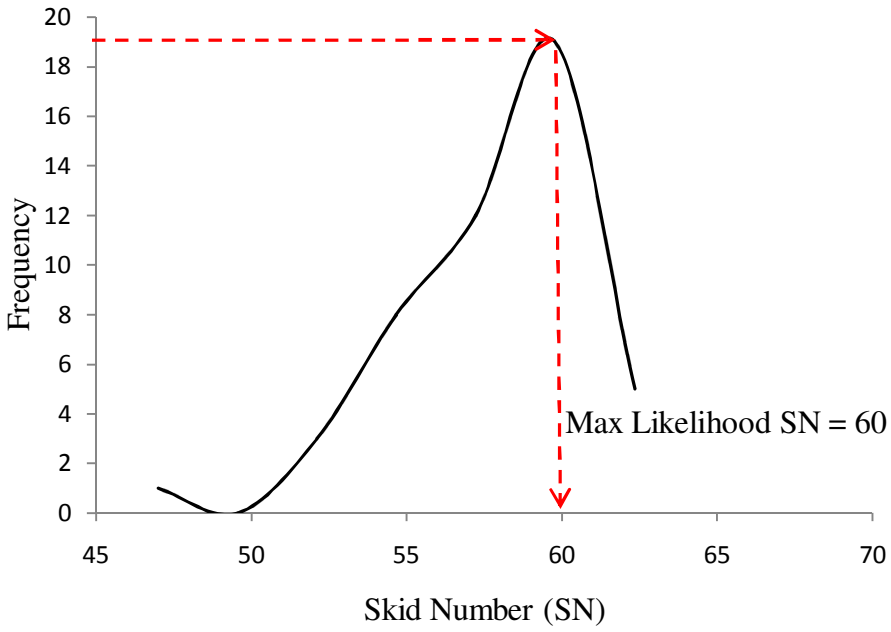

Figure 4.1 Maximum Likelihood SN of Runway 2-20 at Raton Municipal Airport

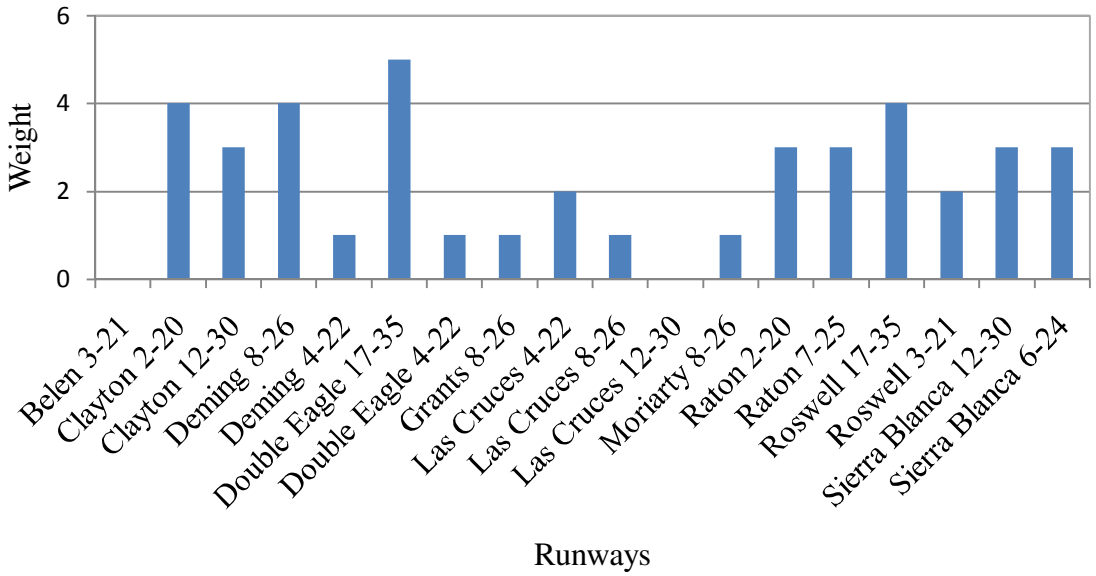

Figure 4.2 Ranking of 19 Runways Based Functional Condition

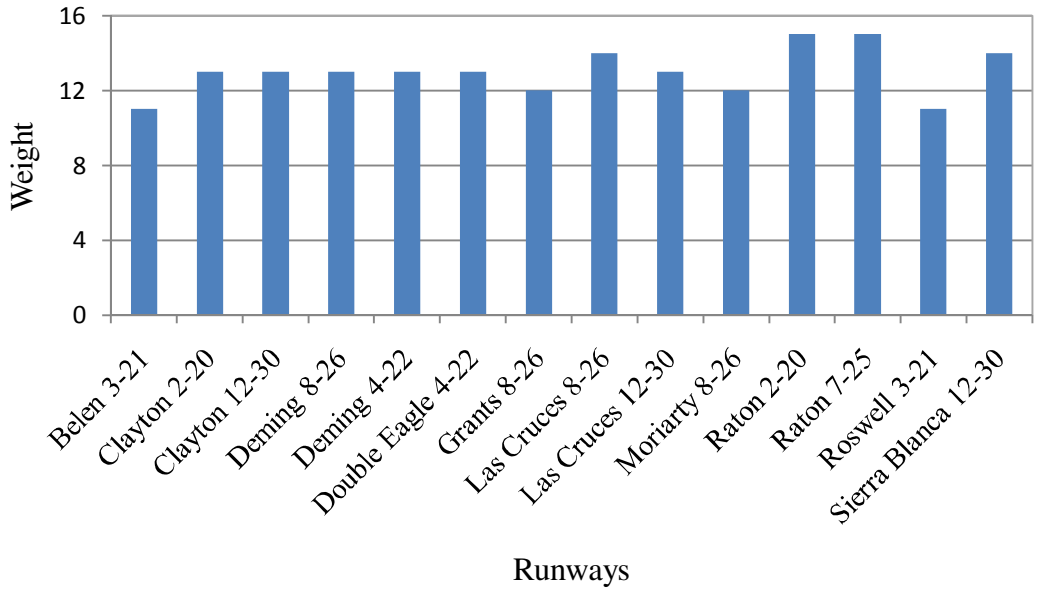

Figure 4.3 Ranking of 14 Runways Based on Structural Strength

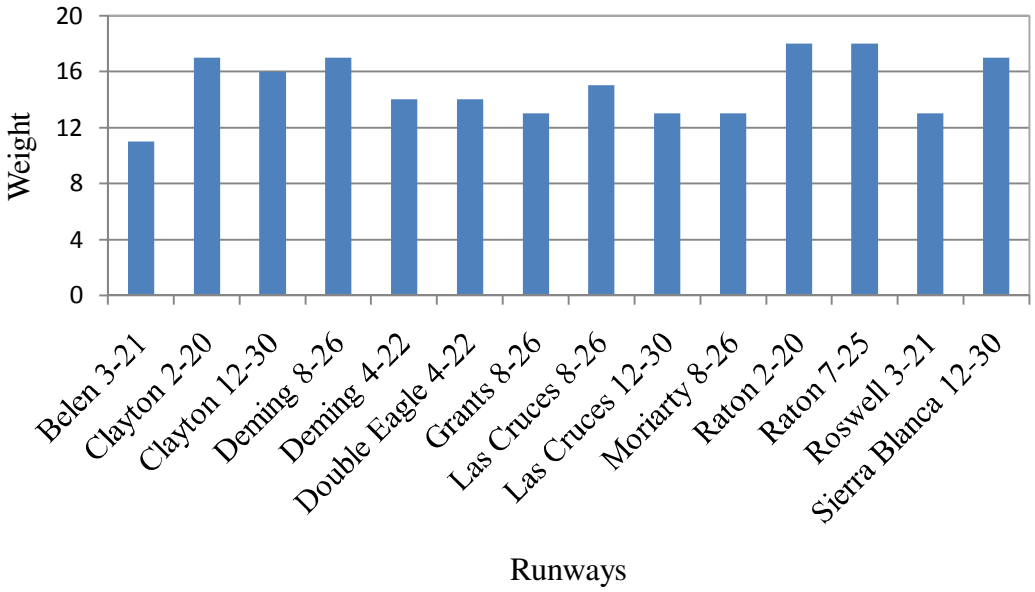

Figure 4.4 Overall Ranking Based on Both Structural Strength and Functional Condition

CHAPTER 5

CONCLUSIONS

In New Mexico, there are about 50 public use airports which include primary, reliever, commercial, and general aviation airports. In this study, the pavements of 10 of these airports have been evaluated for their functional and structural capacity. These airports are: Double Eagle II, Sierra Blanca Regional, Raton Municipal, Moriarty Municipal, Las Cruces International, Grant County, Deming Municipal, Roswell International Air Center, Belen Alexander, and Clayton Municipal Airports. The goal is to rank these airports pavements to make the correct forecasting decisions for NMDOT-AD for repair and rehabilitation of the airport pavements.

Phase I of the study involved collection of distress data of the pavements at these airports (Lucero 2008). These distress data were used in MicroPaver as inputs to determine the Pavement Condition Index (PCI) value for each of the runway, taxiway and apron. Phase

II of the study involved Falling Weight Deflectometer (FWD) test, Skid test, coring for asphalt core samples, and boring for collection of base course and subgrade samples. The FWD and Skid data were analyzed. The cores, aggregate, and soil samples were transferred to the Pavement Materials Laboratory at the University of New Mexico for further testing. Particle size analysis, Atterberg limit tests, Hydrometer analysis, and Direct Shear test was done to classify the subgrade samples. Particle size analysis was done to classify the base material. The soil index properties were used to calculate the CBR values of the base and subgrade materials. Resilient Modulus (M_R) test, Indirect Tensile test (IDT), and Asphalt Content test were carried out on the asphalt cores.

Gradation analysis was done on the aggregate after burning the asphalt. Also, the bulk specific gravity (G_{mb}) and the theoretical maximum specific gravity (G_{mm}) of the asphalt concrete were determined to find out the percent of voids.

The following conclusions are made:

- Based on PCI value, five runways at four airports have poor PCI values of 55 or less requiring immediate attention. The five runways are Runway 8-26 at Grant County Airport, Runway 4-22 at Double Eagle II Airport, Runway 3-21 at Belen Municipal Airport, and Runways 12-30 and 4-22 at Las Cruces International Airport.
- Based on SN value, six runways at five airports have below the required minimum SN value of 50 requiring immediate attention and seven runways of six airports have SN values of 60 or less requiring maintenance planning. The six runways are Runways 12-30 and 8-26 at Las Cruces International Airport, Runway 12-30 at Sierra Blanca Airport, Runway 4-22 at Deming Municipal Airport, Runway 3-21 at Belen Municipal Airport, and Runway 8-26 at Moriarty Municipal Airport.
- Subgrade CBR of all the runways are above 20 and are therefore good. The friction angle values range from 35 to 42 degrees and are good values.
- Base Course CBR values range from 42-66 and are therefore fair to good.
- Based on Surface M_R, Runway 3-21 at Roswell International Air Center has M_R value of less than 200,000 psi and requires attention.
- Based on ITS value, all the runways have values more than 150 psi which are good values.

- Air voids values range from 2.5 – 10.1% and asphalt content values range from 5.55 – 7.89%. High values of air voids can lead to higher permeability and moisture damage problems.
- Based on functional condition, 7 runways are in poor condition, 7 in fair condition, and 4 in good condition.
- Based on structural strength, 2 runways are in poor condition, 8 in satisfactory condition, and 4 in good condition.
- Based on combined ranking, 5 runways are in poor condition, 3 runways in fair condition, 4 runways in satisfactory condition, and 2 runways in good condition.

Recommendations for future studies:

- A mini database of the ten airports was developed in the present study to analyze the functional and structural health of the pavements. The database should be continued to be populated to develop a database of all the airports in New Mexico.
- Overall ranking should be used to prioritize funding to keep the airports safe.
- Structural strength can be used to design rehabilitation timing and type which have not been done. Rehabilitation alternatives can be further analyzed for life cycle assessment and use the findings for taking major decisions of airport pavement work.
- Using the CBR values in this study, one can design the required thickness for carrying the present traffic. It can be noted these pavements were built 20 years ago. It will be interesting to find if the existing thickness is sufficient to carry the predicted traffic.

- Predict future conditions and recommend maintenance and/or rehabilitation strategy for the pavements based on the combined index.

REFERENCES

AASHTO T 30 - 08. "Standard Method of Test for Mechanical Analysis of Extracted Aggregate".

AASHTO T 166 - 05. "Standard Method of Test for Bulk Specific Gravity of Compacted Hot-Mix Asphalt Using Saturated Surface-Dry Specimens".

AASHTO T 209 - 09. "Standard Method of Test for Theoretical Maximum Specific Gravity and Density of Hot-Mix Asphalt (HMA)".

AASHTO T 269 - 97. "Standard Method of Test for Percent Air Voids in Compacted Dense and Open Asphalt Mixtures".

AASHTO T 308 - 09. "Standard Method of Test for Determining the Asphalt Binder Content of Hot-Mix Asphalt (HMA) by the Ignition Method".

Ahammed, M. A. and Tighe, S. L. (2008). "Pavement Surface Mixture, Texture and Skid Resistance: A Factorial Analysis" *Airfield and Highway Pavements Conference, October 15 – 18, 2008, Bellevue, Washington,* ASCE, Reston, Va., pp. 370-384.

Al-Qadi, I. L., Sebaaly, P. E. and Wambold, J. C. (1991). "New and Old Technology Available for Pavement Management System to Determine Pavement Condition." Pavement Management Implementation, ASTM, STP 1121, pp. 437-465.

Asi, I. M. (2007). "Evaluating Skid Resistance of Different Asphalt Concrete Mixes." *Building and Environment*, Vol. 42, No. 1, pp. 325-329.

ASTM D 422 - 63 (1998). "Standard Test Method for Particle-Size Analysis of Soils".

ASTM D 2487 - 00. "Standard Practice for Classification of Soils for Engineering Purposes (Unified Soil Classification System)".

ASTM D 3080 - 04. "Standard Test Method for Direct Shear Test of Soils Under Consolidated Drained Conditions".

ASTM D 4123 - 82 (1995). "Standard Test Method for Indirect Tension Test for Resilient Modulus of Bituminous Mixtures".

ASTM D 4318 - 00. "Standard Test Methods for Liquid Limit, Plastic Limit, and Plasticity Index of Soils".

ASTM D 5340 - 03. "Standard Test Method for Airport Pavement Condition Index Surveys".

ASTM E 274 – 06. "Standard Test Method for Skid Resistance of Paved Surfaces Using a Full-Scale Tire".

Bazlamit, S. M. and Reza, F. (2005). "Changes in Asphalt Pavement Friction Components and Adjustment of Skid Number for Temperature." *Journal of Transportation Engineering*, Vol. 131, No. 6, June 2005, pp. 470-476.

Bell, H. P., Freeman, R. B. and Brown, E. R. (2008). "Evaluation Criteria for Aged Asphalt Concrete Surfaces- Phase II." *US Army Corps of Engineers, ERDC*, Vicksburg, MS 39180.

Buttlar, W. G., Smith, S. M. and Sherman, D. S. (1999). "Rehabilitation Alternatives for Runway 18-36 at Rantoul- Phase 1: Report on Site Investigation, Preliminary

Testing, Instrumentation Plan, and Construction Sampling Plan." *FAA Center of Excellence for Airport Technology*, COE Report No. 19.

Duncan, J. M. (2004). "Friction Angles for Sand, Gravel and Rockfill." *Notes of a Lecture Presented Kenneth L. Lee Memorial Seminar*, Long Beach, California, April 2004.

Federal Aviation Administration (FAA), 2004. Advisory Circular No. 150/5320 – 6D Part 1. "Airport Pavement Design and Evaluation".

Federal Aviation Administration (FAA), 2004. Advisory Circular No. 150/5320 – 6E Part 2. "Airport Pavement Design and Evaluation".

Federal Aviation Administration (FAA), 2004. Advisory Circular No. 150/5320 – 12C. "Measurement, Construction, and Maintenance of Skid-Resistant airport Pavement Surfaces".

Federal Aviation Administration (FAA), 2004. Advisory Circular No. 150/5370-11A, "Use of Non Destructive Testing in the Evaluation of Airport Pavements".

Federal Aviation Administration (FAA), 2004. Advisory Circular No. 150/5380 – 6B. "Guidelines and Procedures for Maintenance of Airport Pavements".

Garg, N., Guo, E., and McQueen R. (2004). "Operational Life of Airport Pavements." *Final report to U.S. Department of Transportation, Federal Aviation Administration*, Washington, D.C. 20591.

Gopalakrishnan, K. and Thompson, M. R. (2006). "Characterization of NAPTF Subgrade Soils for Mechanistic-Based Analysis and Design of Airport Flexible Pavements." *International Journal of Pavement Engineering*, 8(4), pp. 307-321.

Greene, J., Shahin, M. Y. and Alexander, D. R. (2004). "Airfield Pavement Condition Assessment." *Transportation Research Record*, 1889, pp. 63-70.

Guler, M. (2008). "Effects of Mix Design Variables on Mechanical Properties of Hot Mix Asphalt." *Journal of Transportation Engineering*, Vol. 134, No. 3, March 2008, pp. 128-136.

Huang, Y. H. (2004). "Pavement Analysis and Design", 2nd Ed. Pearson Education Inc. Upper Saddle River, NJ.

Lee, H. D., Im, S. and Kim, Y. (2008). "Impacts of Laboratory Curing Condition on Indirect Tensile Strength of Cold In-place Recycling Mixtures using Foamed Asphalt." *Airfield and Highway Pavements Conference, October 15 – 18, 2008, Bellevue, Washington,* ASCE, Reston, Va., pp. 213-221.

Mechanistic-Empirical Pavement Design Guide, Appendix CC-1, p 7.

Muntasir, A. (2006). "Summary and Comparison of Airfield Pavement Inventory, Condition, and Performance Across the United States." *Airfield and Highway Pavement Speciality Conference, April 30 – May 3, 2006, Atlanta, Georgia*, ASCE, Reston, Va., pp. 972-983.

Rahim, A. M. (2005). "Subgrade Soil Index Properties to Estimate Resilient Modulus for Pavement Design." *The International Journal of Pavement Engineering*, Vol. 6, No. 3, September 2005, pp. 163-169.

Roberts, F. L., Kandhal, P. S., Brown, E. R., Lee, D. and Kennedy, T. W. (1996). "Hot Mix Asphalt Materials, Mixture Design and Construction", 2nd Ed. National Asphalt Pavement Association Research and Education Foundation, Lanham, Maryland.

Romanoschi, S. and Metcalf, J. B. (1999). "Simple Approach to Estimation of Pavement Structural Capacity." *Transportation Research Record*, 1652, pp. 198-205.

Shahin, M. Y. (2005). "Pavement Management for Airports, Roads, and Parking Lots." *Springer Science + Bussiness Media, LLC*, 233 Spring Street, New York, NY 10013, pp. 117-139.

Shahin, M. Y., Darter, M. I. and Kohn, H. D. (1978). "Pavement Condition Evaluation of Asphalt Surfaced Airfield Pavements." *Proceedings of the Association of Asphalt Pavement Technologists,* Vol.47, pp. 190-228.

Thuma, R. G., Fuselier, G. K. and Yip, P. K. (2008). "Using PCI Data to Define Major Rehabilitation Projects at Washington Dulles International Airport." *Airfield and Highway Pavements Conference, October 15 – 18, 2008, Bellevue, Washington,* ASCE, Reston, Va., pp. 279-300.

United States General Accounting Office (USGAO). (1998). "Airfield Pavement: Keeping Nation's Runways in Good condition Could Require Substantially Higher Spending." *Report to the Chairman, Committee on Commerce, Science, and Trans., U.S. Senate*.

Walrond, G. and Christiansen, D. (1993). "Airfield Pavement Structural Evaluations, Current Practice and Future Needs." *Airfield Pavement Innovations Theory to Practice Conference, September 8 – 10, 1993, Vicksburg, Mississippi,* ASCE, Reston, Va., pp. 110-125.

Walston, B. and McQueen, R. D. (2000). "Development of a Reliable Methodology for Assessing the Structural Performance of General Aviation Pavements." *Proceedings of the 26th International Air Transportation Conference, June 18-21, 2000,San Francisco, California*, ASCE, Reston, Va., pp. 1-12.

Ward, P. R. (2008). "Semiprepared Airfield Characteristics at Higher Elevations." *Journal of Transportation Engineering*, Vol. 134, No. 4, April 2008, pp. 163-170.

Zuo, G., Drumm, E. C. and Meier, R. W. (2007). "Environmental Effects on the Predicted Service Life of Flexible Pavements." *Journal of Transportation Engineering*, Vol. 133, No. 1, January 2007, pp. 47-56.

APPENDICES

APPENDIX I

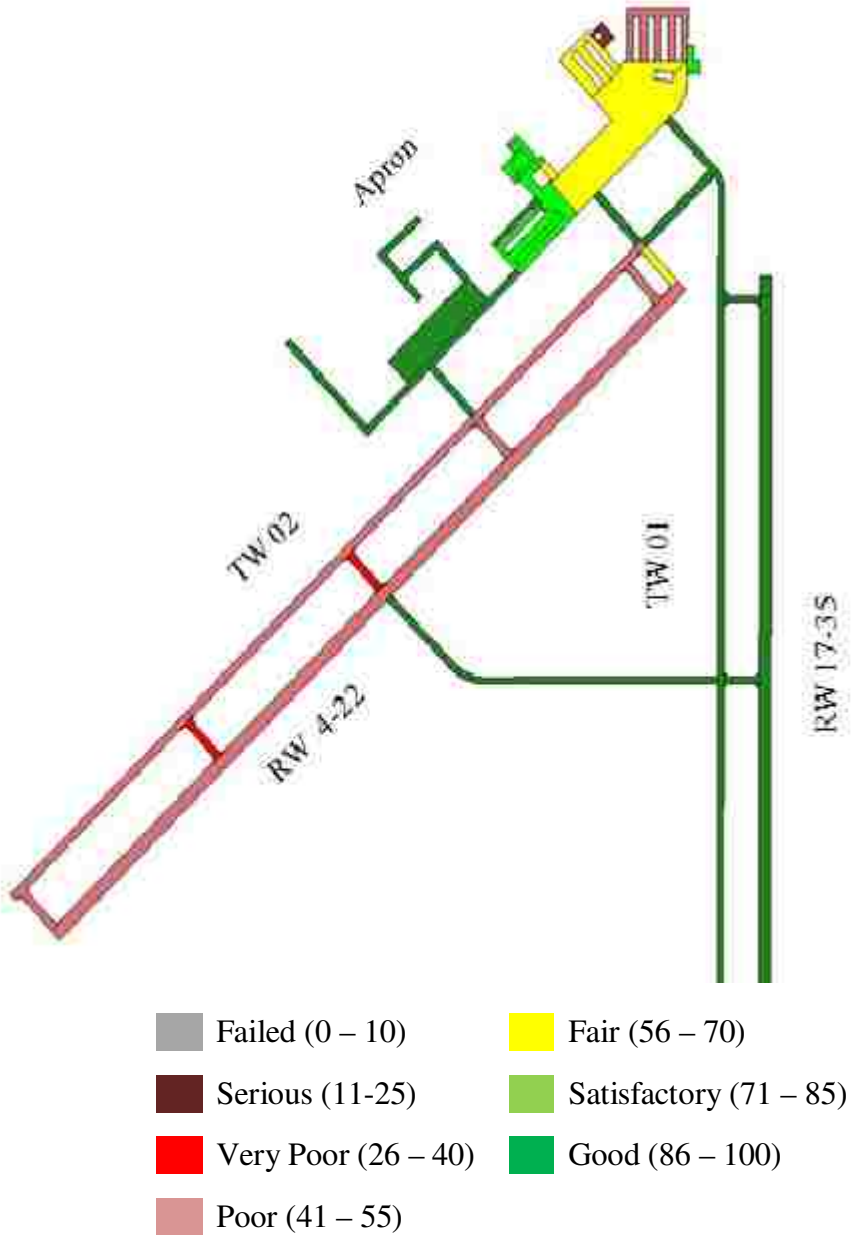

Figure 1. PCI of Pavements at Double Eagle II Airport

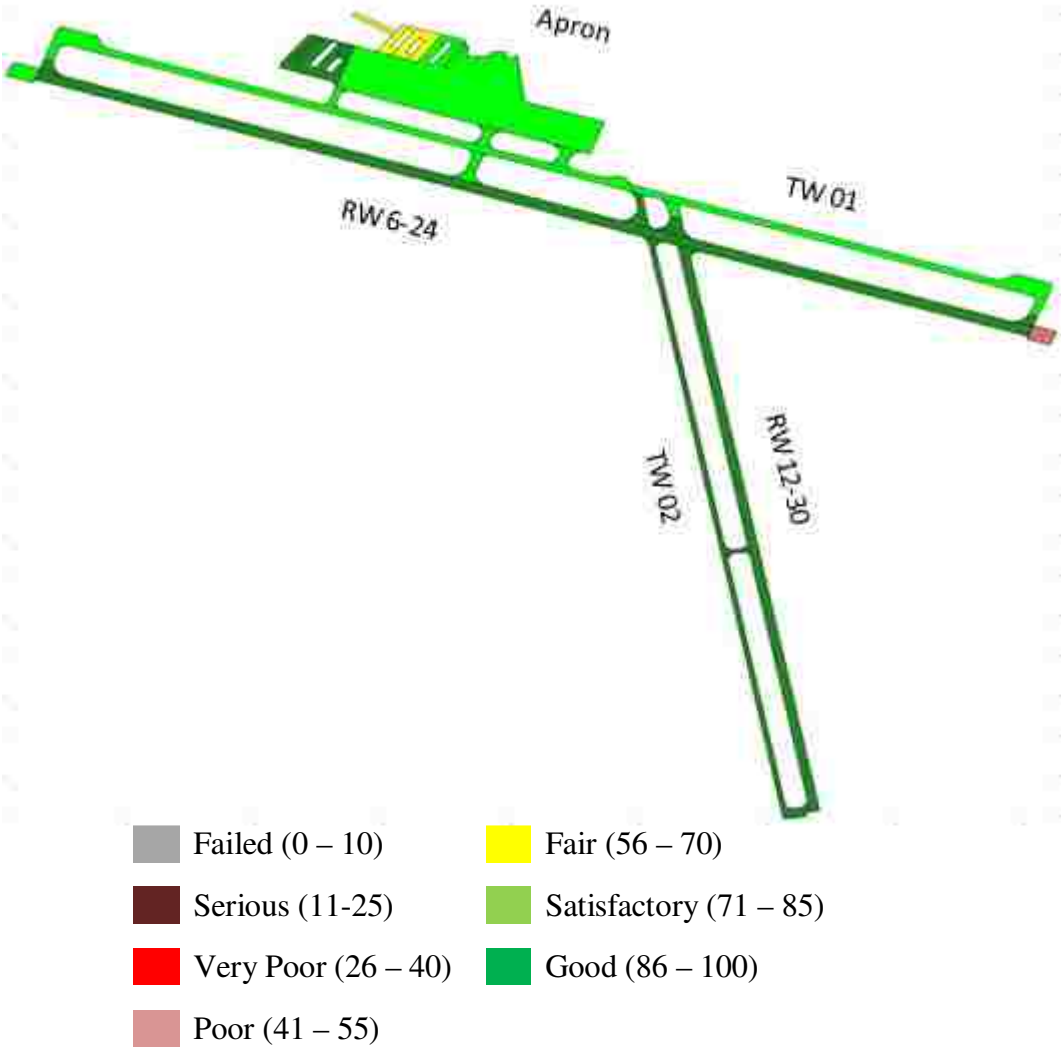

Figure 2. PCI of Pavements at Sierra Blanca Regional Airport

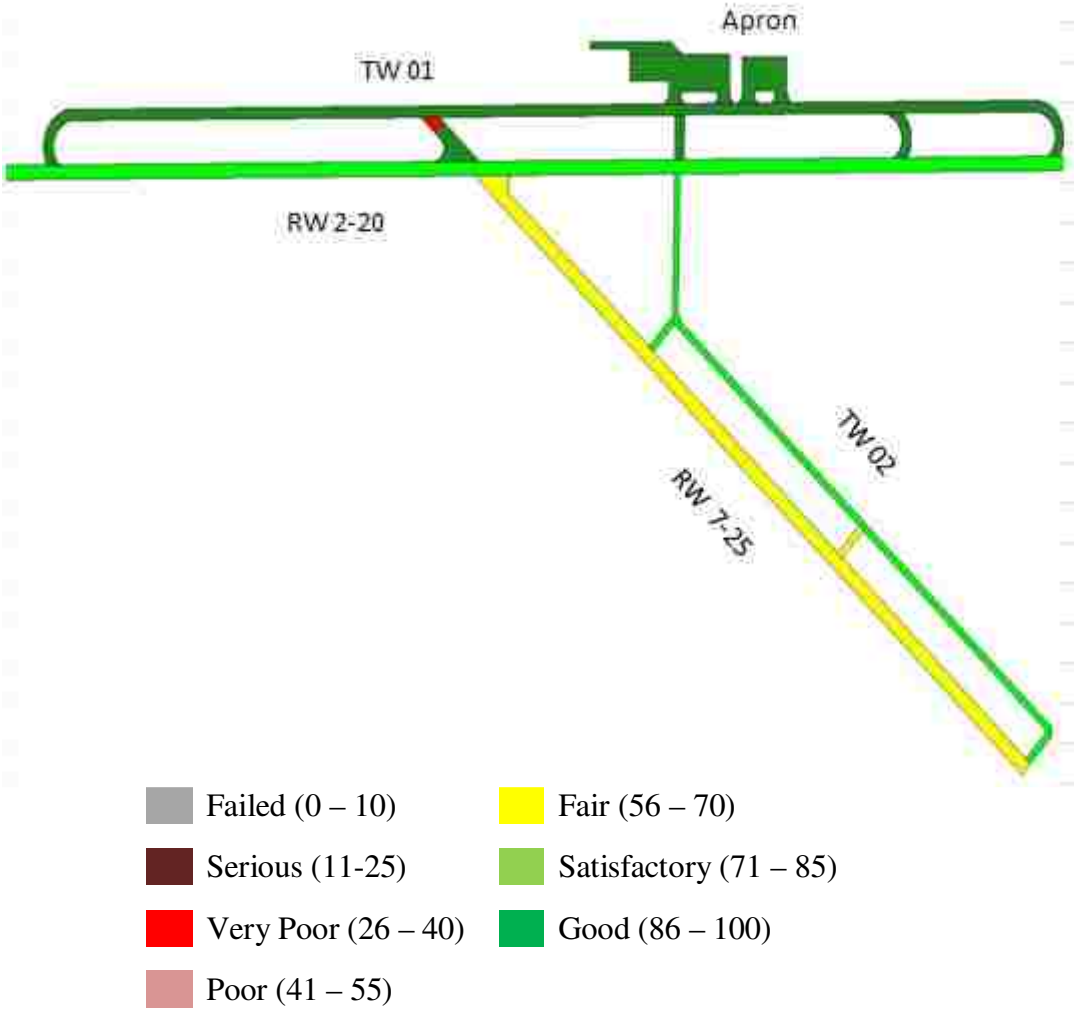

Figure 3. PCI of Pavements at Raton Municipal Airport

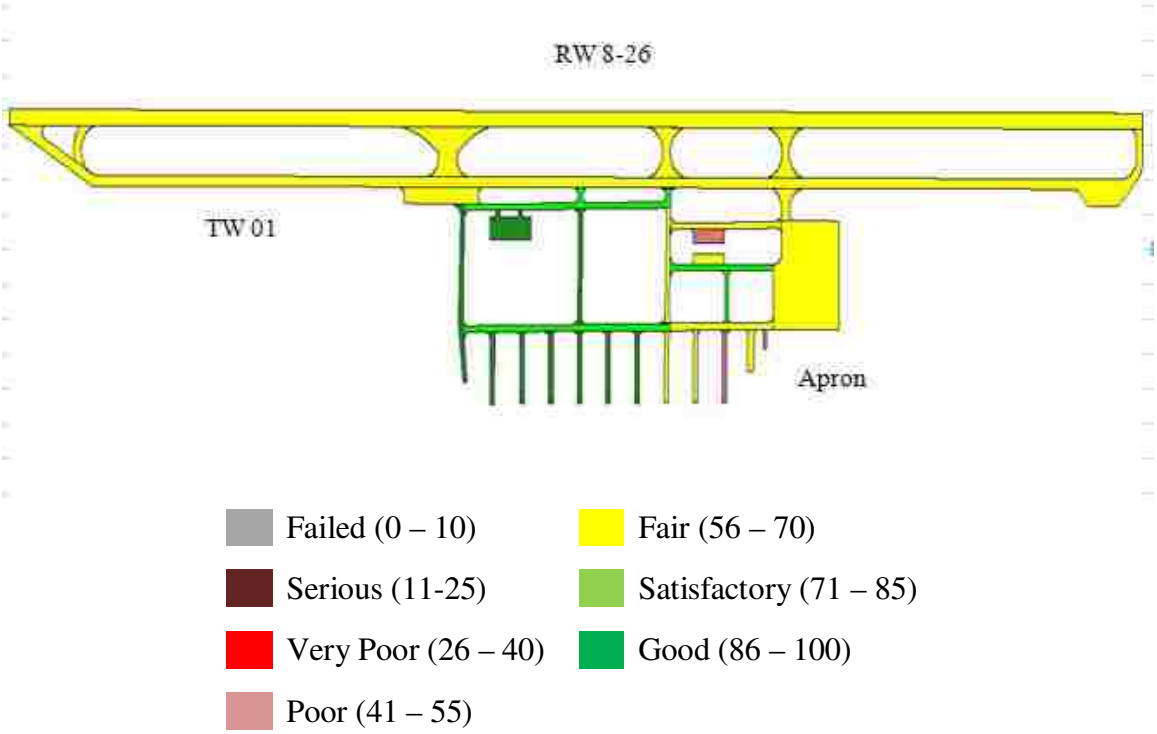

Figure 4. PCI of Pavements at Moriarty Municipal Airport

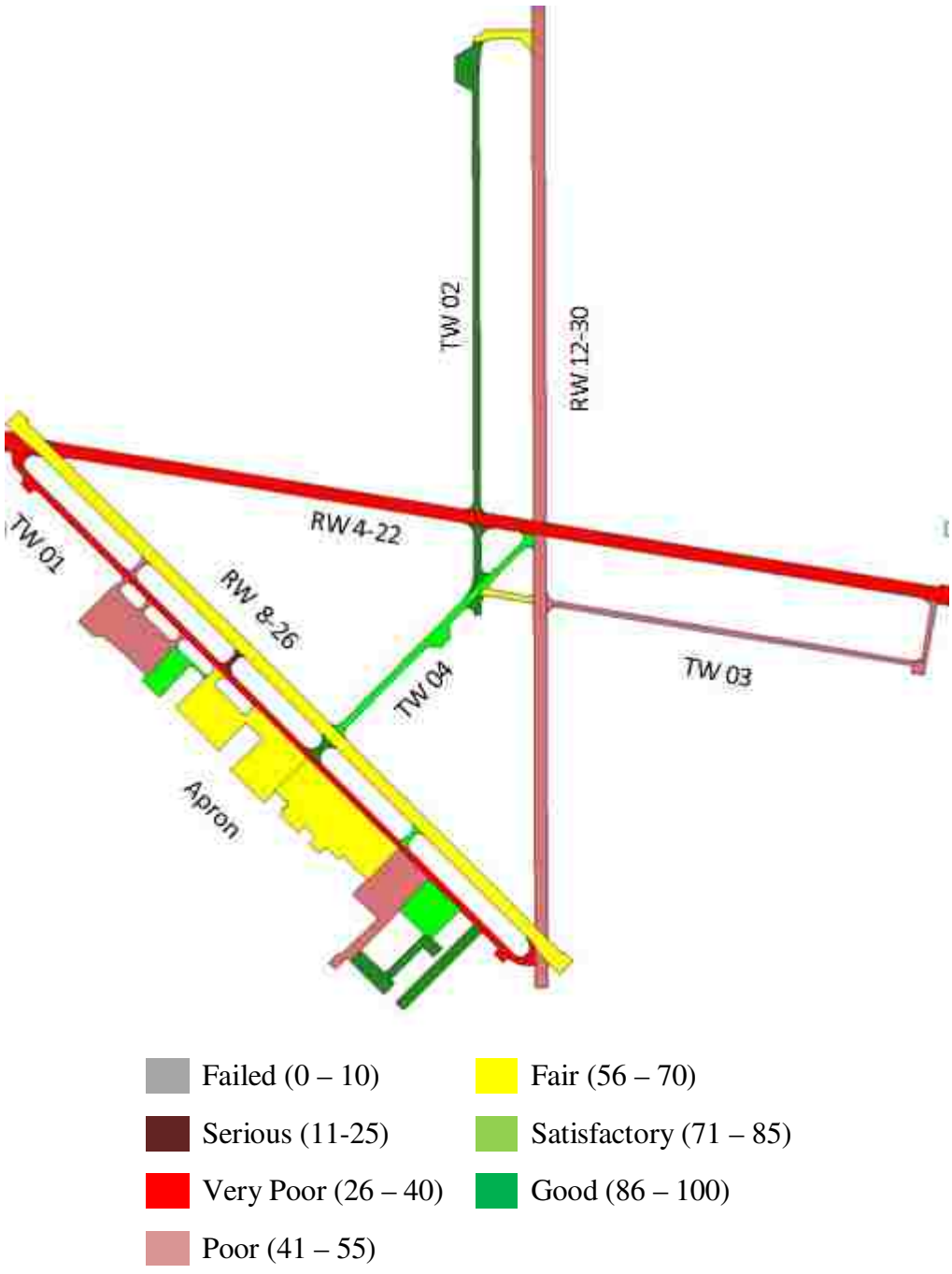

Figure 5. PCI of Pavements at Las Cruces International Airport

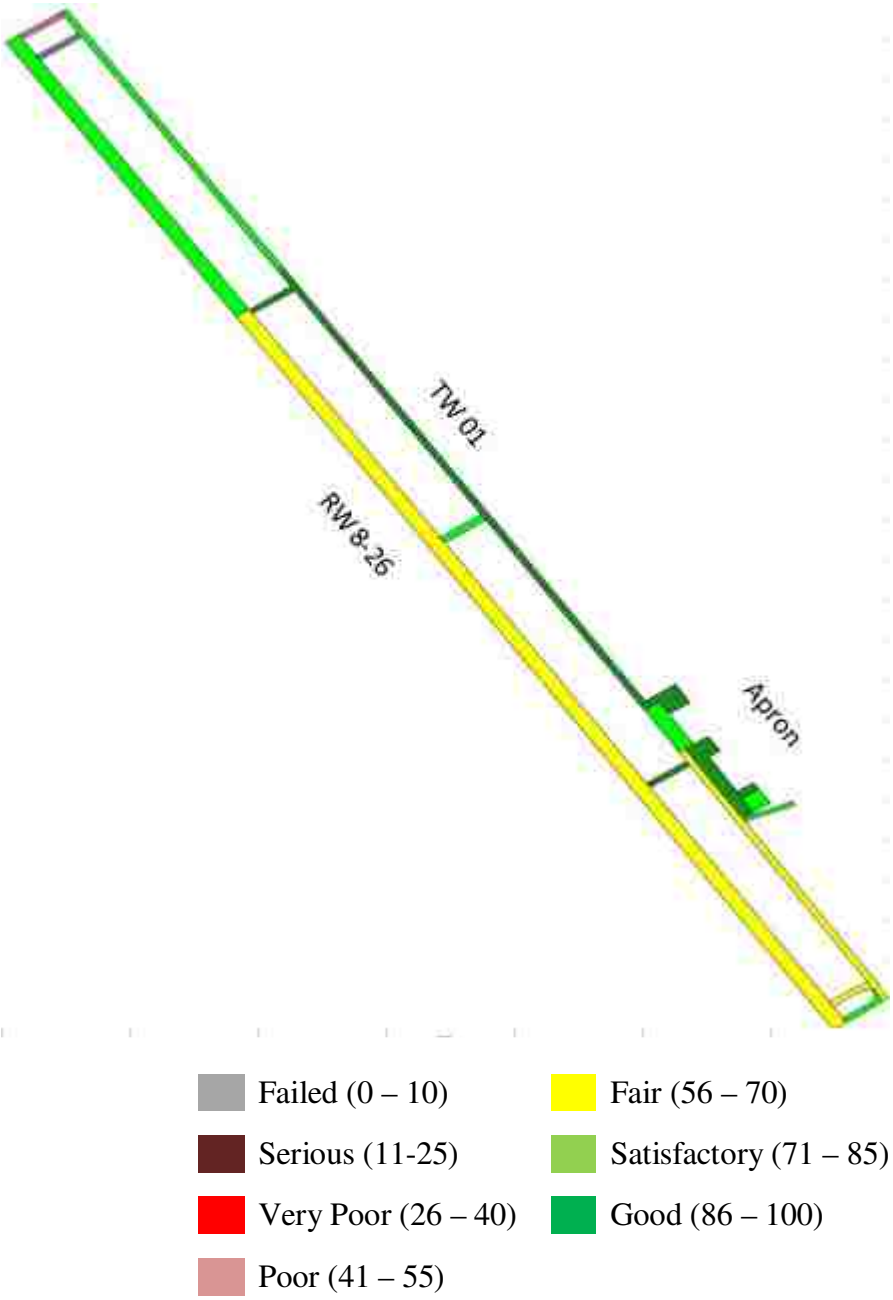

Figure 6. PCI of Pavements at Grant County Airport

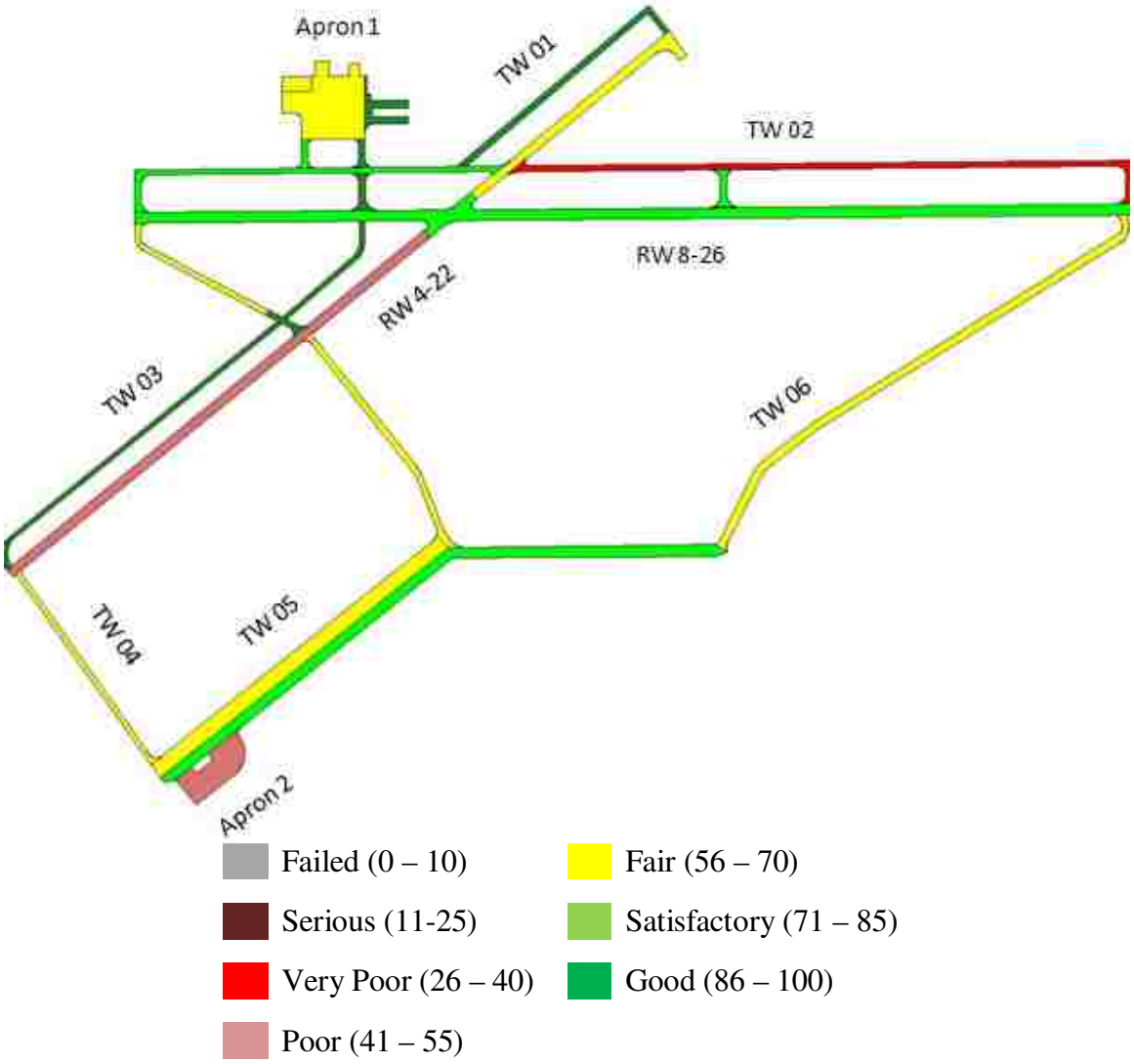

Figure 7. PCI of Pavements at Deming Municipal Airport

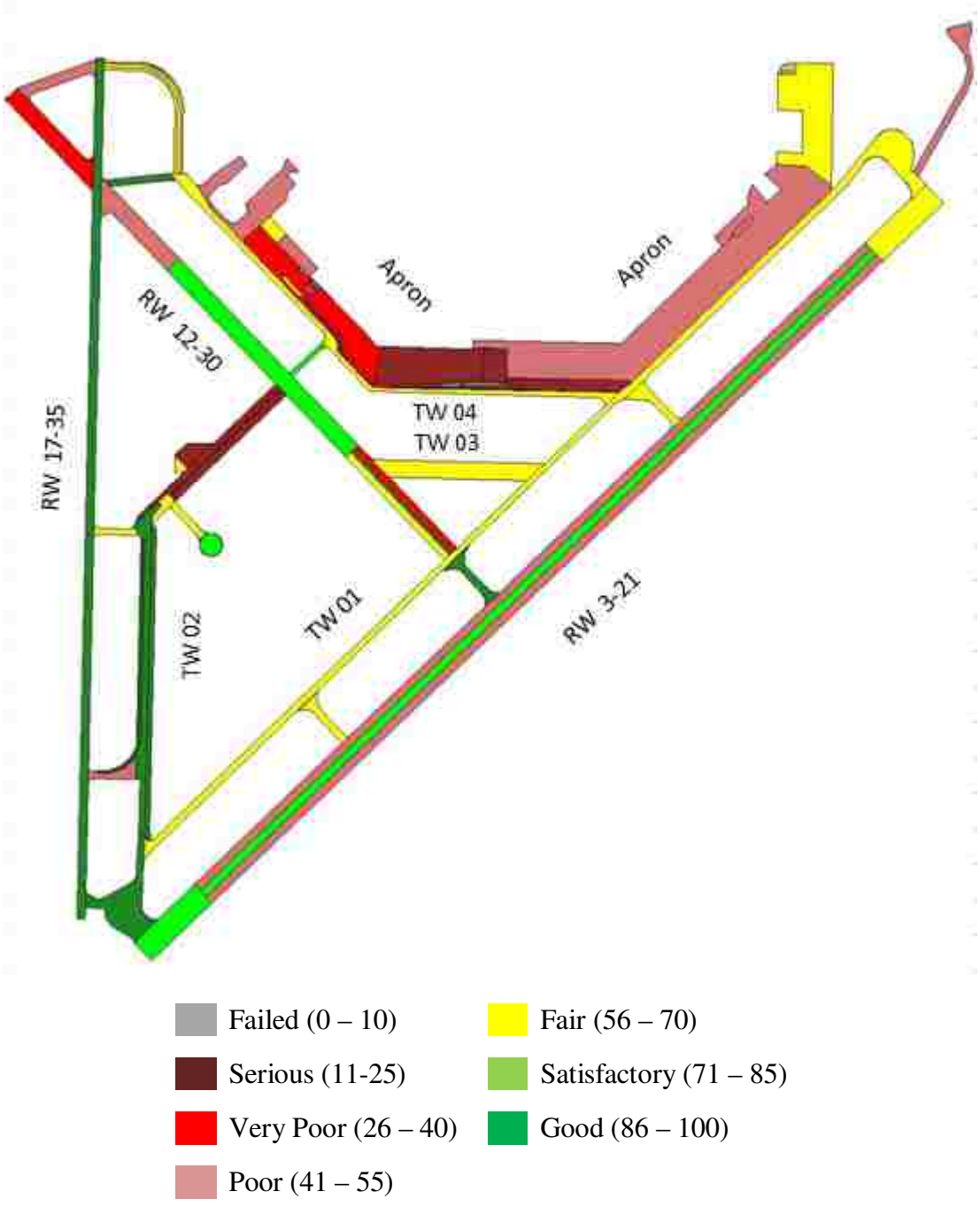

Figure 8. PCI of Pavements at Roswell International Air Center

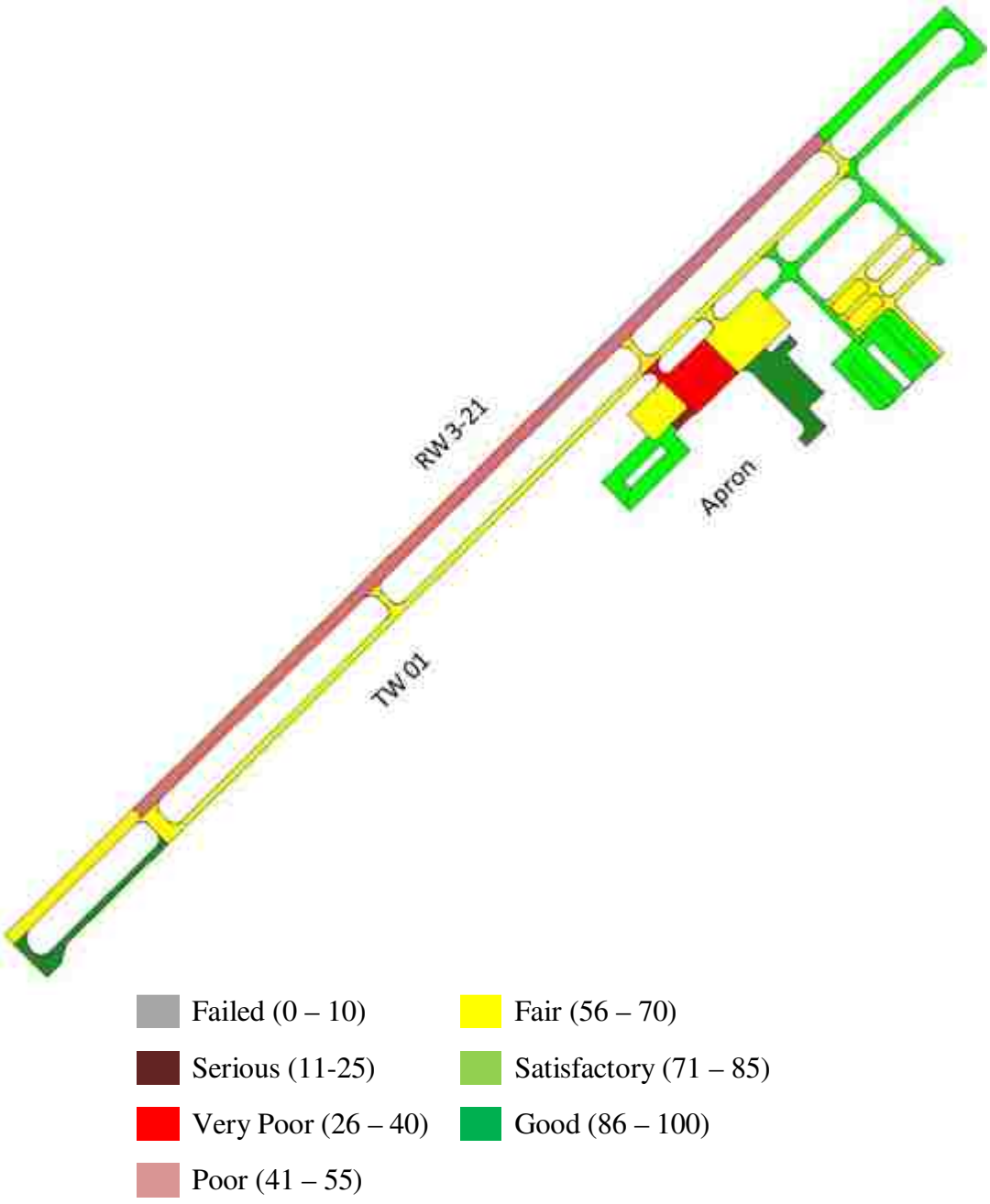

Figure 9. PCI of Pavements at Belen Alexander Airport

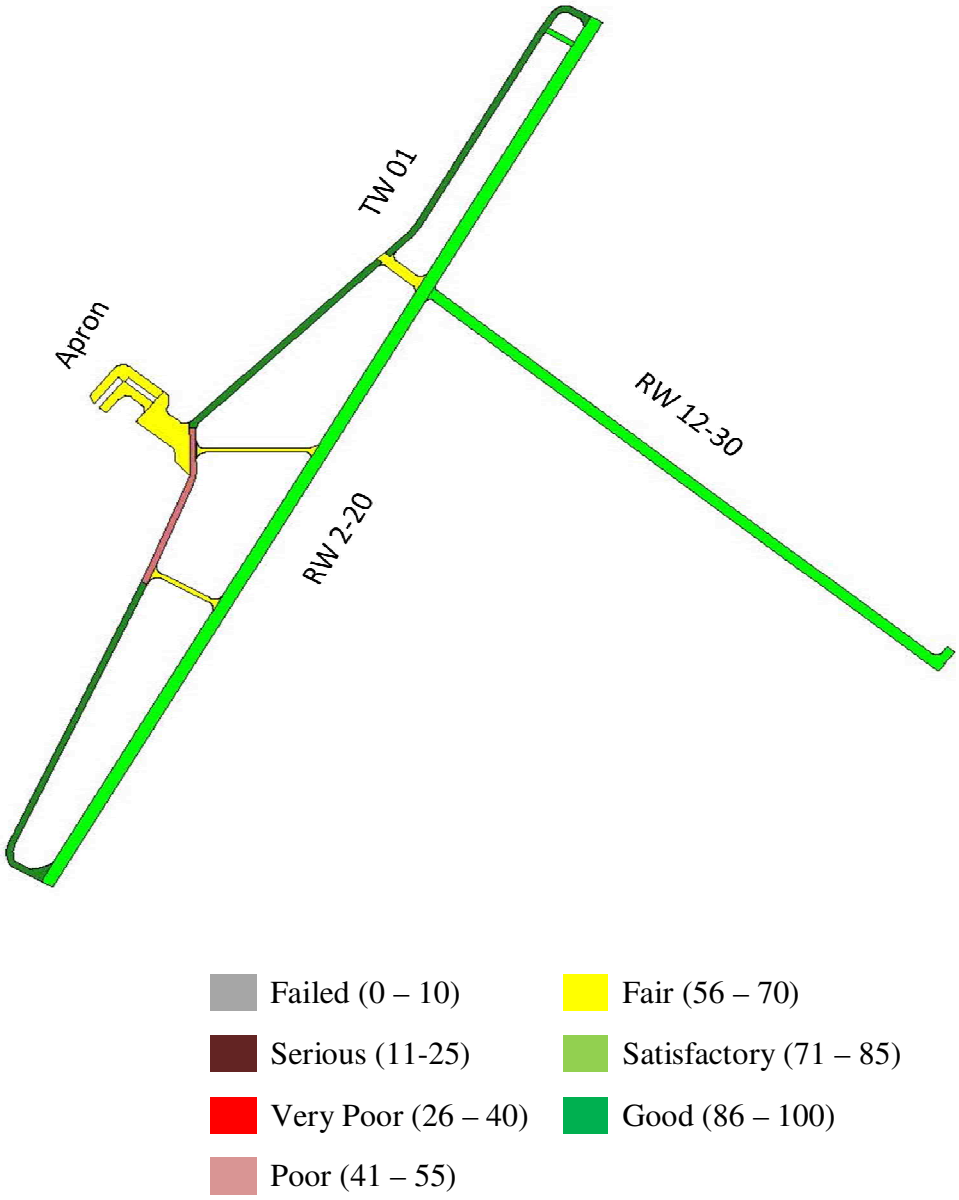

Figure 10. PCI of Pavements at Clayton Municipal Airport

APPENDIX II

Table 1 Skid Results for Runway 4-22 at Double Eagle II Airport

S. No.	Average SN	Min. SN	Max. SN	Speed, mph	Offset from C/L, feet	Direction
1	54.1	45	60	41.1	10	North Bound
2	54.1	46	61	40.7		
3	56.6	54	60	41.0		
4	60.1	56	63	40.6		
5	54.3	47	59	40.8	10	South Bound
6	55.2	51	59	41.8		
7	59.3	56	63	40.1		
8	55.0	51	59	41.0		
9	58.9	55	61	40.3		
10	59.3	54	64	40.2		
11	54.4	50	60	40.4		
12	54.2	51	58	40.7		
13	52.7	48	57	40.6		
14	60.6	57	65	40.8	20	North Bound
15	57.7	52	64	40.6		
16	58.4	54	63	40.8		
17	62.5	59	65	40.8		
18	61.3	57	65	40.7		
19	58.5	15	67	40.6		
20	58.7	54	62	41.3		
21	56.8	49	60	41.2		
22	60.7	58	64	40.8	20	South Bound
23	60.2	55	66	40.9		
24	59.8	54	64	40.8		
25	60.4	54	68	41.0		
26	59.0	56	63	41.1		
27	58.2	54	63	41.2		
28	55.2	51	60	41.1		
29	62.9	59	69	40.6	30	North Bound
30	60.9	55	70	41.4		
31	61.7	57	67	41.1		
32	61.2	57	65	40.9		
33	61.4	55	65	40.9		
34	58.9	50	63	40.5		
35	59.5	55	65	40.9		
36	48.7	34	65	41.9	30	South Bound
37	60.8	57	65	41.6		
38	61.9	58	68	42.0		
39	60.5	55	65	41.8		
40	62.3	49	70	42.1		
41	40.9	25	62	42.1		

Table 2 Skid Results for Runway 17-35 at Double Eagle II Airport

S. No.	Average SN	Min. SN	Max. SN	Speed, mph	Offset from C/L, feet	Direction
1	59.5	57	63	41.4	10	North Bound
2	57.6	55	60	41.2		
3	57.9	56	60	40.9		
4	57.3	54	60	41.7		
5	57.5	55	61	40.6	10	South Bound
6	59.3	56	64	39.9		
7	58.9	56	61	40.7		
8	59.2	58	61	40.6		
9	58.8	57	61	40.5		
10	68.6	66	71	40.8	20	North Bound
11	64.0	62	67	41.0		
12	67.1	64	69	41.1		
13	66.3	64	69	41.1		
14	67.7	66	70	40.8		
15	71.1	69	74	41.0		
16	63.6	61	67	41.0	20	South Bound
17	66.0	64	68	41.2		
18	66.3	63	69	40.8		
19	70.6	68	73	41.2		
20	67.8	65	71	41.0		
21	68.2	65	71	40.7		
22	38.2	37	40	41.5	30	North Bound
23	68.8	66	72	40.4		
24	65.3	61	70	40.5		
25	70.4	67	74	40.7		
26	41.3	39	43	41.2		
27	71.7	69	76	40.6		
28	43.0	40	47	41.3	30	South Bound
29	67.9	65	70	40.7		
30	67.8	65	71	41.1		
31	64.7	55	69	41.3		
32	70.4	68	73	40.6		
33	43.0	40	46	40.8		
34	70.6	68	73	41.7		

Table 3 Skid Results for Runway 6-24 at Sierra Blanca Regional Airport

S. No.	Average SN	Min. SN	Max. SN	Speed, mph	Offset from C/L, feet	Direction
1	48.3	43	53	41.1	5	East Bound
2	49.3	43	57	40.6		
3	52.5	46	57	41.8		
4	47.4	42	53	41.5		
5	46.0	42	51	41.4		
6	42.5	39	45	41.6		
7	44.9	41	56	41.3		
8	43.0	37	51	41.6		
9	44.6	41	49	41.1		
10	45.2	40	50	41.4		
11	48.3	42	59	40.8		
12	46.5	41	53	41.6		
13	56.4	53	59	40.5		
14	49.2	44	54	41.1	5	West Bound
15	50.6	47	54	41.2		
16	49.2	43	56	40.5		
17	55.9	48	62	40.9		
18	54.1	49	59	41.1		
19	48.2	41	54	41.8		
20	47.8	35	58	41.3		
21	47.2	36	56	41.7		
22	46.7	41	53	41.4		
23	44.7	42	48	41.6		
24	42.2	37	46	41.5		
25	48.8	42	52	41.6		
26	45.6	42	50	41.4		
27	48.7	45	52	41.3		
28	44.9	41	48	41.7		
29	47.3	45	52	41.3		
30	46.5	42	58	41.6		
31	48.7	42	56	41.2		
32	55.3	49	61	41.7		

Table 4 Skid Results for Runway 6-24 at Sierra Blanca Regional Airport

S. No.	Average SN	Min. SN	Max. SN	Speed, mph	Offset from C/L, feet	Direction
1	54.3	51	59	42.0	20	East Bound
2	51.5	48	55	42.4		
3	53.8	48	58	41.8		
4	54.1	49	61	41.6		
5	59.0	51	66	41.6		
6	47.9	44	52	41.8		
7	51.1	46	56	41.7		
8	62.6	55	68	41.7		
9	53.9	44	62	41.8		
10	55.2	52	59	41.4		
11	53.5	50	59	41.5		
12	52.5	50	57	41.8		
13	62.7	59	68	38.4	20	West Bound
14	56.8	51	63	41.0		
15	53.1	49	57	40.9		
16	61.5	57	65	40.8		
17	56.9	54	62	40.7		
18	63.7	59	71	40.6		
19	53.8	48	60	40.6		
20	58.9	56	63	40.5		
21	44.9	42	49	40.8		
22	55.0	50	61	40.8		
23	58.2	56	63	40.8		
24	62.5	55	68	40.8		
25	53.4	50	57	40.9		
26	63.5	55	68	40.9		
27	53.8	48	59	41.0	30	East Bound
28	47.6	45	53	41.4		
29	53.8	50	58	41.4		
30	46.8	44	50	41.4		
31	48.2	45	51	41.7		
32	60.1	51	68	41.3		
33	49.4	46	56	41.4		
34	54.3	48	60	41.5		
35	51.2	48	56	41.5		
36	52.4	49	59	41.9	30	West Bound
37	48.7	46	51	41.3		
38	51.6	48	56	41.3		
39	47.8	45	54	41.4		
40	46.8	43	52	41.7		
41	47.0	45	51	41.4		
42	48.3	44	52	41.8		
43	49.0	43	53	41.4		
44	50.1	45	57	41.1		

Table 5 Skid Results for Runway 12-30 at Sierra Blanca Regional Airport

S. No.	Average SN	Min. SN	Max. SN	Speed, mph	Offset from C/L, feet	Direction
1	49.8	43	57	41.4	5	North Bound
2	43.5	37	55	41.3		
3	40.0	35	48	42.7		
4	34.1	31	37	42.2		
5	39.6	28	50	41.3		
6	43.8	40	49	41.3		
7	51.4	49	54	41.3		
8	47.7	43	52	41.7		
9	50.3	38	57	42.6		
10	38.7	32	50	41.6		
11	36.0	29	45	39.5	5	South Bound
12	31.2	26	35	41.5		
13	32.8	28	45	41.7		
14	45.4	40	51	41.5		
15	41.0	35	47	42.2		
16	35.1	29	40	42.5		
17	45.3	42	50	42.0		
18	43.5	39	46	42.0		
19	43.5	39	51	42.4		
20	51.4	41	60	41.7		
21	45.0	39	52	42.6		

Table 6 Skid Results for Runway 12-30 at Sierra Blanca Regional Airport

S. No.	Average SN	Min. SN	Max. SN	Speed, mph	Offset from C/L, feet	Direction
1	43.0	37	46	40.0	20	North Bound
2	49.8	46	54	41.2		
3	42.5	37	47	41.2		
4	40.1	34	46	41.2		
5	46.6	38	54	41.2		
6	45.3	31	56	41.2		
7	54.4	50	59	41.1		
8	53.2	48	56	41.1		
9	31.9	28	38	41.3		
10	22.7	21	25	39.1	20	South Bound
11	37.3	31	45	41.4		
12	52.9	48	57	41.2		
13	51.1	47	55	41.2		
14	48.6	44	53	42.1		
15	50.2	45	59	41.2		
16	52.5	48	57	41.8		
17	37.0	32	49	41.8		
18	38.5	32	46	41.6		
19	46.9	41	56	40.1	30	North Bound
20	45.0	37	54	41.8		
21	51.3	47	55	41.7		
22	43.4	38	50	41.4		
23	41.1	37	46	41.4		
24	39.8	33	49	41.7		
25	32.1	27	35	41.6	30	South Bound
26	35.6	32	41	41.9		
27	37.4	33	42	42.0		
28	38.7	34	43	41.4		
29	42.5	38	50	42.0		
30	42.5	37	47	41.8		
31	29.1	27	33	42.2		
32	29.0	22	37	42.2		

Table 7 Skid Results for Runway 2-20 at Raton Municipal Airport

S. No.	Average SN	Min. SN	Max. SN	Speed, mph	Offset from C/L, feet	Direction
1	57.4	53	62	39.3	5	North Bound
2	56.2	46	61	41.6		
3	52.1	45	61	41.2		
4	54.0	30	62	40.9		
5	56.9	50	64	40.1		
6	59.1	51	63	41.0		
7	58.5	55	61	40.7		
8	57.5	40	63	40.6		
9	59.2	55	63	40.6		
10	58.5	54	62	40.8		
11	57.8	51	61	40.5		
12	50.4	23	62	42.1	5	South Bound
13	57.2	50	63	41.2		
14	56.8	48	63	41.1		
15	56.8	48	61	41.6		
16	54.6	35	60	41.0		

Table 8 Skid Results for Runway 2-20 at Raton Municipal Airport

S. No.	Average SN	Min. SN	Max. SN	Speed, mph	Offset from C/L, feet	Direction
1	62.0	57	66	40.1	20	North Bound
2	53.4	34	68	40.3		
3	59.7	50	69	42.4		
4	63.1	54	69	40.5		
5	59.1	50	65	40.1		
6	59.1	53	67	41.0		
7	58.1	55	62	40.0		
8	58.3	51	62	40.3		
9	57.1	49	64	40.3		
10	53.3	46	58	40.4		
11	52.6	45	61	40.4		
12	55.0	34	60	41.9		
13	59.9	54	67	41.7	20	South Bound
14	57.8	52	67	41.4		
15	59.8	50	67	41.3		
16	56.6	43	72	42.0		
17	60.3	50	68	42.0		
18	64.9	60	70	41.6		
19	58.1	51	68	41.7		
20	59.1	49	66	42.0	30	North Bound
21	53.5	30	65	41.4		
22	58.4	48	64	41.1		
23	54.9	41	65	41.2		
24	52.9	29	69	41.2		
25	58.7	31	67	41.9		
26	53.9	46	59	40.7	30	South Bound
27	51.5	46	62	40.7		
28	47.0	42	54	40.8		
29	55.7	42	65	41.2		
30	59.0	55	63	41.1		
31	56.0	51	61	40.7		
32	56.1	49	67	40.7		
33	57.3	52	64	41.1		
34	60.0	53	67	40.5		

Table 9 Skid Results for Runway 7-25 at Raton Municipal Airport

S. No.	Average SN	Min. SN	Max. SN	Speed, mph	Offset from C/L, feet	Direction
1	56.1	39	64	40.4	5	North Bound
2	54.2	46	61	41.0		
3	61.4	57	66	40.8		
4	61.7	58	65	40.4		
5	57.4	54	61	41.0		
6	60.6	56	65	40.6		
7	57.1	53	63	40.9		
8	61.0	56	65	42.0	5	South Bound
9	61.2	55	66	40.3		
10	58.2	36	66	40.5		
11	59.9	56	64	40.8		
12	60.1	57	63	41.8		
13	60.3	56	64	40.2		
14	61.7	56	66	40.9		
15	60.5	57	65	42.1		
16	65.7	56	70	41.2	20	North Bound
17	60.1	47	70	41.7		
18	64.2	55	69	41.0		
19	65.2	62	68	40.7		
20	64.5	60	68	40.2		
21	63.8	58	69	41.1		
22	64.2	60	68	41.3		
23	58.1	55	63	41.5		
24	65.1	61	69	39.0	20	South Bound
25	62.2	58	66	38.9		
26	63.2	58	67	41.2		
27	66.2	64	69	41.2		
28	58.9	20	67	40.5	30	North Bound
29	64.0	59	68	40.0		
30	64.0	58	70	40.5		
31	59.7	55	65	40.6		
32	60.6	51	66	40.3		
33	58.8	41	68	40.5		
34	62.9	44	69	41.0		
35	57.6	20	69	41.1	30	South Bound

Table 10 Skid Results for Runway 8-26 at Moriarty Municipal Airport

S. No.	Average SN	Min. SN	Max. SN	Speed, mph	Offset from C/L, feet	Direction
1	34.3	29	38	43.3	5	East Bound
2	32.7	30	40	43.1		
3	35.2	30	44	40.0		
4	32.0	30	35	41.0		
5	33.0	26	40	40.6		
6	29.8	28	32	40.6		
7	29.5	27	33	40.6		
8	31.2	29	34	40.7		
9	30.6	28	34	40.6		
10	34.3	29	39	40.6		
11	33.2	27	39	40.1		
12	37.7	33	45	41.0		
13	40.6	37	44	39.8		
14	32.2	22	39	40.0		
15	35.1	31	39	41.1		
16	32.1	28	37	34.1		
17	36.4	29	41	40.4	5	West Bound
18	36.4	33	40	41.3		
19	34.7	31	38	40.4		
20	35.0	30	41	40.8		
21	30.6	26	35	41.0		
22	30.5	27	37	40.7		
23	27.8	25	32	40.7		
24	28.4	25	31	40.7		
25	28.2	26	32	41.0		
26	31.6	28	37	40.5		
27	29.8	27	35	40.7		
28	30.9	29	34	40.9		
29	29.1	25	34	40.7		
30	29.0	24	34	40.8		
31	27.4	25	31	40.8		
32	29.9	27	33	40.7		
33	31.0	28	34	40.8		
34	31.2	29	36	40.8		
35	30.3	28	34	40.7		
36	34.2	29	41	40.3		
37	30.0	28	35	41.1		
38	30.2	28	34	40.7		
39	26.9	24	31	40.6		

Table 11 Skid Results for Runway 8-26 at Moriarty Municipal Airport

S. No.	Average SN	Min. SN	Max. SN	Speed, mph	Offset from C/L, feet	Direction
1	28.7	26	31	41.7	20	East Bound
2	31.6	29	34	40.1		
3	31.4	28	35	40.8		
4	30.5	25	34	41.0		
5	33.9	29	38	40.6		
6	29.3	27	33	40.8		
7	32.1	29	34	40.4		
8	31.9	28	38	40.9		
9	29.8	27	36	40.9		
10	30.2	28	33	40.4		
11	31.2	29	35	40.8		
12	31.6	27	39	40.7		
13	30.9	28	35	40.8		
14	31.3	29	35	40.7		
15	31.1	28	35	40.8		
16	30.2	27	34	40.7		
17	28.5	26	31	40.8		
18	30.4	28	36	40.2	20	West Bound
19	25.5	23	31	41.1		
20	28.1	25	32	40.6		
21	28.4	24	32	40.5		
22	29.5	26	32	40.9		
23	29.4	25	33	40.4		
24	29.0	27	32	40.9		
25	32.4	31	35	40.4		
26	32.9	30	36	40.9		
27	28.9	24	34	40.8		
28	31.7	29	35	40.4		
29	31.2	25	37	41.0		
30	31.8	29	34	40.3		
31	30.1	28	33	41.1		
32	33.3	30	37	40.4		
33	33.4	29	37	40.8		
34	30.4	28	34	40.4		

Table 12 Skid Results for Runway 8-26 at Moriarty Municipal Airport

S. No.	Average SN	Min. SN	Max. SN	Speed, mph	Offset from C/L, feet	Direction
1	36.1	33	40	39.8	30	East Bound
2	30.5	28	34	40.1		
3	29.6	27	32	40.2		
4	32.8	30	35	40.0		
5	29.3	26	32	40.1		
6	29.9	26	32	40.1		
7	31.4	27	35	40.0		
8	32.1	29	37	40.0		
9	30.7	28	34	40.0		
10	34.1	31	38	39.9		
11	30.1	24	35	40.0		
12	32.6	29	35	39.4	30	West Bound
13	33.8	31	37	40.4		
14	31.6	26	35	39.9		
15	30.0	26	34	39.8		
16	32.4	30	35	39.8		
17	34.0	29	38	39.9		
18	33.7	29	39	39.8		
19	34.0	28	38	39.8		
20	33.1	28	36	39.8		
21	36.2	32	41	39.7		
22	32.7	29	36	39.8		

Table 13 Skid Results for Runway 12-30 at Las Cruces International Airport

S. No.	Average SN	Min. SN	Max. SN	Speed, mph	Offset from C/L, feet	Direction
1	43.1	38	47	40.6	20	West Bound
2	44.4	39	50	40.8		
3	41.6	36	46	41.1		
4	41.5	37	46	42.5		
5	39.6	35	45	41.5		
6	37.5	34	42	42.2		
7	46.3	42	53	41.9		
8	39.1	36	42	42.0		
9	44.5	42	48	41.9		
10	42.6	38	47	42.0		
11	38.4	36	42	41.9		
12	40.4	36	44	42.0		
13	44.9	41	49	41.9		
14	45.8	42	50	41.9		
15	42.0	38	47	39.0	20	East Bound
16	41.9	39	47	41.1		
17	40.1	38	42	42.1		
18	40.0	38	43	41.8		
19	40.7	37	44	41.7		
20	40.3	37	45	42.1		
21	39.4	35	44	41.3		
22	40.5	33	48	40.9		
23	41.7	21	47	42.3		
24	40.3	38	43	41.8		
25	41.0	37	45	42.2		
26	42.8	39	48	41.6		
27	40.0	34	45	42.1		
28	43.1	40	47	41.9		
29	37.6	35	41	41.1		

Table 14 Skid Results for Runway 12-30 at Las Cruces International Airport

S. No.	Average SN	Min. SN	Max. SN	Speed, mph	Offset from C/L, feet	Direction
1	40.9	35	47	42.1	30	West Bound
2	44.4	41	48	40.0		
3	49.8	44	59	40.8		
4	47.0	39	53	40.8		
5	50.2	46	54	41.4		
6	44.3	40	48	40.9		
7	45.9	43	50	42.4		
8	44.1	32	52	41.1		
9	47.7	43	53	40.7		
10	52.3	45	59	40.6		
11	47.3	44	52	40.7		
12	44.9	42	51	42.4	30	East Bound
13	44.7	41	50	41.0		
14	42.4	40	45	41.2		
15	44.0	42	46	41.1		
16	40.5	37	44	41.1		
17	39.5	37	42	41.0		
18	40.1	35	47	41.1		
19	41.5	38	44	41.1		
20	43.8	39	47	41.3		
21	41.1	37	45	41.0		
22	24.7	19	30	41.2		
23	40.2	38	43	42.0		

Table 15 Skid Results for Runway 4-22 at Las Cruces International Airport

S. No.	Average SN	Min. SN	Max. SN	Speed, mph	Offset from C/L, feet	Direction
1	69.7	59	82	39.7	5	North Bound
2	69.0	66	72	40.1		
3	65.6	62	68	41.6		
4	63.4	60	69	40.5		
5	67.0	63	71	40.7		
6	66.3	63	69	41.5		
7	62.9	22	72	41.7		
8	65.0	61	70	42.5		
9	62.5	53	67	42.2		
10	64.9	61	69	42.2		
11	63.8	60	67	41.9		
12	64.5	60	69	42.4		
13	65.4	61	69	41.6		
14	66.4	63	70	41.4		
15	68.1	65	72	40.2	5	South Bound
16	65.3	61	68	42.4		
17	64.7	61	68	42.0		
18	64.8	61	69	42.5		
19	65.6	62	68	42.2		
20	63.2	58	67	42.3		
21	63.9	61	67	42.5		
22	67.2	60	78	42.1		
23	68.5	64	73	42.3		
24	67.3	64	71	42.6		
25	69.6	66	73	41.9		
26	67.6	63	73	42.6		
27	67.0	64	70	42.4		
28	66.1	62	69	42.4		
29	65.7	62	69	42.5		
30	64.0	58	68	42.2		
31	61.2	57	66	42.4		
32	65.3	60	69	42.3		
33	66.0	62	70	42.5		
34	67.0	56	75	42.2		
35	38.6	23	68	42.4		
36	69.8	62	83	42.1		

Table 16 Skid Results for Runway 4-22 at Las Cruces International Airport

S. No.	Average SN	Min. SN	Max. SN	Speed, mph	Offset from C/L, feet	Direction
1	70.4	65	74	42.2	20	North Bound
2	67.5	61	77	41.1		
3	65.5	61	71	41.1		
4	66.2	62	69	42.3		
5	65.9	62	69	42.6		
6	65.6	63	69	42.2		
7	63.4	55	72	42.6		
8	64.9	57	69	42.2		
9	59.8	20	74	42.7		
10	47.8	28	71	41.8		
11	60.5	56	67	42.5		
12	65.4	62	69	42.3		
13	65.5	62	68	42.0		
14	65.1	59	69	42.5		
15	66.1	61	72	41.9		
16	64.9	58	69	42.5	20	South Bound
17	65.0	60	68	41.0		
18	65.0	62	68	41.5		
19	62.7	57	68	42.1		
20	63.6	59	67	42.5		
21	64.2	55	70	42.5		
22	61.2	28	72	42.3		
23	64.2	49	69	42.3		
24	62.4	59	66	41.6		
25	64.2	61	67	42.8		
26	63.4	57	67	42.1		
27	63.5	60	68	42.2		
28	61.2	58	64	42.5		
29	64.1	61	67	42.0		
30	64.7	61	68	42.3		

Table 17 Skid Results for Runway 4-22 at Las Cruces International Airport

S. No.	Average SN	Min. SN	Max. SN	Speed, mph	Offset from C/L, feet	Direction
1	65.8	59	72	42.4	30	North Bound
2	66.8	58	74	40.9		
3	61.1	55	67	40.9		
4	57.8	51	66	41.0		
5	60.5	56	68	41.0		
6	62.0	58	68	41.1		
7	63.1	56	68	41.3		
8	65.1	58	71	40.9		
9	68.3	63	74	40.9		
10	67.7	63	73	41.2		
11	75.3	73	78	40.0	30	South Bound
12	60.3	50	69	41.4		
13	69.2	62	75	41.0		
14	68.5	63	80	40.7		
15	66.5	59	78	40.9		
16	66.1	54	75	40.8		
17	66.9	60	75	41.0		
18	59.9	51	68	41.0		
19	69.8	56	80	48.3		
20	73.7	69	83	54.8		

Table 18 Skid Results for Runway 8-26 at Las Cruces International Airport

S. No.	Average SN	Min. SN	Max. SN	Speed, mph	Offset from C/L, feet	Direction
1	39.5	36	43	41.5	5	West Bound
2	39.3	37	43	41.2		
3	41.5	39	46	41.4		
4	52.0	48	58	36.7		
5	42.5	39	46	40.6		
6	42.1	39	44	41.7		
7	40.3	38	43	39.2		
8	39.4	38	41	40.6		
9	38.5	34	42	42.2		
10	41.8	40	44	40.8		
11	44.4	42	46	41.3		
12	44.7	43	46	41.3		
13	45.3	39	48	41.2		
14	46.1	44	51	41.2		
15	43.0	40	48	40.3		
16	46.1	42	50	42.7	5	East Bound
17	45.7	42	49	42.2		
18	43.3	17	47	41.3		
19	45.0	43	48	41.2		
20	41.8	39	46	41.2		
21	40.7	22	45	41.5		
22	40.6	37	43	41.2		
23	39.4	37	41	41.4		
24	39.5	32	44	41.3		
25	43.9	41	46	41.2		
26	41.6	40	43	41.3		
27	44.0	27	47	41.1		
28	45.6	44	48	41.3		
29	44.8	42	48	41.2		
30	52.9	50	56	41.0		

Table 19 Skid Results for Runway 8-26 at Las Cruces International Airport

S. No.	Average SN	Min. SN	Max. SN	Speed, mph	Offset from C/L, feet	Direction
1	52.1	42	63	43.1	20	West Bound
2	43.6	41	46	44.5		
3	44.8	41	48	40.3		
4	42.3	39	48	41.6		
5	40.3	33	45	41.1		
6	40.7	38	43	41.4		
7	44.5	40	48	41.1		
8	45.4	41	53	41.4		
9	45.8	43	49	41.2		
10	47.2	44	50	41.5		
11	46.7	42	51	41.1		
12	45.5	40	49	41.4		
13	46.2	42	49	39.3		
14	44.5	38	52	40.8	20	East Bound
15	43.9	28	49	39.8		
16	47.9	44	54	40.3		
17	47.7	44	50	42.1		
18	42.3	32	47	40.6		
19	47.6	44	51	41.6		
20	42.7	40	45	41.2		
21	43.9	42	46	41.3		
22	43.3	41	46	41.0		
23	42.4	40	45	41.5		
24	45.7	43	48	41.0		
25	57.9	53	68	41.0		

Table 20 Skid Results for Runway 8-26 at Las Cruces International Airport

S. No.	Average SN	Min. SN	Max. SN	Speed, mph	Offset from C/L, feet	Direction
1	53.4	47	66	42.9	30	West Bound
2	51.9	47	58	42.1		
3	50.9	47	55	40.8		
4	44.6	41	49	40.2		
5	47.2	44	52	40.2		
6	54.7	43	60	40.2		
7	50.4	46	56	40.3		
8	53.1	49	63	40.4		
9	50.3	46	54	40.0		
10	50.6	27	57	39.6	30	East Bound
11	50.8	49	53	41.0		
12	49.2	46	53	40.4		
13	44.3	42	47	40.4		
14	43.7	41	48	41.1		
15	45.3	43	48	40.4		
16	48.6	37	64	40.4		
17	38.8	34	42	40.6		
18	55.8	53	60	40.0		

Table 21 Skid Results for Runway 8-26 at Grant County Airport

S. No.	Average SN	Min. SN	Max. SN	Speed, mph	Offset from C/L, feet	Direction
1	44.0	39	50	42.0	5	East Bound
2	45.9	42	52	42.8		
3	44.8	39	52	42.1		
4	45.8	39	52	42.7		
5	48.9	42	55	42.4		
6	49.0	41	55	42.5		
7	42.0	35	48	42.4		
8	41.7	38	45	42.3		
9	42.3	38	47	42.5		
10	44.2	39	49	42.4		
11	46.6	41	52	42.3		
12	47.8	40	53	42.4		
13	48.6	40	53	42.5		
14	45.7	42	51	42.4		
15	41.5	36	46	42.4		
16	47.5	42	54	37.7	5	West Bound
17	46.8	38	54	42.0		
18	47.9	43	57	42.5		
19	46.2	40	53	42.4		
20	46.5	42	51	42.2		
21	45.2	40	51	42.4		
22	44.7	41	48	42.3		
23	41.8	35	45	42.3		
24	45.8	34	52	42.3		
25	43.7	39	50	42.5		
26	49.6	44	60	42.2		
27	50.2	43	56	42.6		
28	48.2	41	56	42.2		
29	48.8	44	54	42.3		
30	49.5	43	55	42.3		
31	44.2	39	49	42.5		

Table 22 Skid Results for Runway 8-26 at Grant County Airport

S. No.	Average SN	Min. SN	Max. SN	Speed, mph	Offset from C/L, feet	Direction
1	52.6	48	62	39.2	20	East Bound
2	47.4	44	51	40.7		
3	46.1	41	51	42.0		
4	47.3	42	55	41.7		
5	46.5	41	58	41.8		
6	48.5	45	51	41.7		
7	50.3	47	53	41.7		
8	46.7	38	53	41.8		
9	53.0	49	57	41.5		
10	49.5	44	56	41.8		
11	52.5	36	60	41.6		
12	50.3	45	55	40.8	20	West Bound
13	54.4	49	61	41.5		
14	51.1	44	57	41.4		
15	38.6	35	43	41.6		
16	49.4	44	55	42.4		
17	53.1	48	59	42.1		
18	50.0	47	55	42.0		
19	49.5	47	52	41.6		
20	52.6	49	56	41.4		
21	50.8	40	56	41.5		
22	48.4	42	54	47.9	30	East Bound
23	47.9	45	55	41.4		
24	46.0	35	51	41.6		
25	51.8	47	58	41.8		
26	42.4	35	54	41.8		
27	39.0	30	53	41.8		
28	47.3	36	62	41.6		
29	48.4	37	55	41.6		
30	48.7	41	56	41.8		
31	46.7	42	51	41.6		
32	50.9	47	59	40.6	30	West Bound
33	47.2	41	54	41.4		
34	51.7	47	57	41.2		
35	49.2	46	53	41.3		
36	47.8	43	51	41.6		
37	53.1	51	56	41.6		
38	49.3	47	52	41.3		
39	49.8	47	52	41.4		
40	48.4	39	54	41.8		
41	51.2	49	57	41.3		

Table 23 Skid Results for Runway 4-22 at Deming Municipal Airport

S. No.	Average SN	Min. SN	Max. SN	Speed, mph	Offset from C/L, feet	Direction
1	42.1	37	57	38.3	5	East Bound
2	34.7	29	43	43.1		
3	38.4	31	44	44.4		
4	47.7	36	55	45.3		
5	41.3	36	46	43.9		
6	40.2	33	47	43.4		
7	40.8	36	46	43.6		
8	42.6	39	45	43.2		
9	34.8	31	41	43.0		
10	57.8	43	67	42.1		
11	48.2	44	53	42.8		
12	45.1	39	51	42.2		
13	40.8	36	47	42.6		
14	41.6	36	47	42.3		
15	46.8	43	52	39.7	5	West Bound
16	47.0	43	50	38.5		
17	41.0	34	51	42.7		
18	57.2	42	75	43.8		
19	51.2	31	71	43.1		
20	40.7	35	48	43.6		
21	47.0	41	52	43.3		
22	46.8	41	54	43.5		
23	41.9	37	49	43.3		
24	48.3	42	57	43.2		
25	43.9	37	54	43.4		
26	44.0	33	50	43.5		

Table 24 Skid Results for Runway 4-22 at Deming Municipal Airport

S. No.	Average SN	Min. SN	Max. SN	Speed, mph	Offset from C/L, feet	Direction
1	37.3	32	43	42.6	15	East Bound
2	44.6	39	50	43.7		
3	40.1	34	47	43.4		
4	31.6	29	36	43.6		
5	34.3	29	44	43.3		
6	32.0	24	40	43.6		
7	32.3	29	35	43.4		
8	35.0	30	40	43.6		
9	56.0	34	65	42.9		
10	40.4	32	47	43.9		
11	39.3	36	46	43.1		
12	29.5	25	34	43.6		
13	30.4	27	36	43.4		
14	47.8	43	53	42.2	15	West Bound
15	56.1	51	65	42.7		
16	49.1	42	57	42.4		
17	37.1	31	45	41.5		
18	38.6	33	46	42.3		
19	45.4	39	57	40.5		
20	48.0	42	58	41.4		
21	55.8	52	59	42.7		
22	55.1	47	63	41.7		
23	44.3	25	54	42.6		
24	41.8	36	47	43.1	25	East Bound
25	45.5	40	55	41.0		
26	43.7	40	48	41.0		
27	37.0	28	48	41.1		
28	41.1	35	48	41.1		
29	59.9	35	68	40.7		
30	42.3	35	51	41.1		
31	40.7	36	45	41.0		
32	32.7	28	41	41.9		
33	56.2	50	68	32.5	25	West Bound
34	51.0	45	62	40.6		
35	42.1	29	62	41.2		
36	56.7	39	67	40.6		
37	41.1	35	51	41.0		
38	49.3	45	53	41.0		
39	42.6	37	48	41.2		
40	46.4	33	54	40.9		
41	46.5	38	57	40.8		

Table 25 Skid Results for Runway 8-26 at Deming Municipal Airport

S. No.	Average SN	Min. SN	Max. SN	Speed, mph	Offset from C/L, feet	Direction
1	58.3	53	64	41.4	5	West Bound
2	24.3	22	29	41.7		
3	56.3	40	64	42.0		
4	57.8	54	65	42.3		
5	55.9	52	60	42.2		
6	55.6	48	61	42.2		
7	54.8	52	58	42.2		
8	56.4	53	62	42.1		
9	54.8	33	60	42.3		
10	55.7	53	58	42.1		
11	58.7	55	61	41.9		
12	58.1	55	60	42.4		
13	55.1	52	58	42.0		
14	55.4	53	59	42.4		
15	56.4	28	63	41.7		
16	55.0	61	95	42.0		
17	55.0	61	96	42.0		
18	54.0	62	91	42.0	5	East Bound
19	52.0	64	85	42.0		
20	56.0	61	87	42.0		
21	52.0	60	82	42.0		
22	52.0	59	91	42.0		
23	53.0	58	89	42.0		
24	52.0	59	90	42.0		
25	55.0	59	85	42.0		
26	54.0	58	84	42.0		
27	54.0	61	89	42.0		
28	53.0	58	85	42.0		
29	50.0	58	83	42.0		
30	51.0	72	90	42.0		
31	50.0	76	81	42.0		
32	39.0	67	52	42.0		
33	56.0	63	72	42.0		
34	54.0	61	74	42.0		
35	49.0	55	68	42.0		

Table 26 Skid Results for Runway 8-26 at Deming Municipal Airport

S. No.	Average SN	Min. SN	Max. SN	Speed, mph	Offset from C/L, feet	Direction
1	59.4	54	65	45.7	20	West Bound
2	56.6	52	61	41.8		
3	59.8	53	64	41.2		
4	60.8	51	71	41.1		
5	61.1	56	66	41.0		
6	57.7	52	61	40.3		
7	58.9	34	66	40.1		
8	64.9	58	69	40.1		
9	64.7	62	69	40.1		
10	61.1	56	65	40.1		
11	60.7	42	65	40.1		
12	65.6	63	68	40.2		
13	60.9	54	72	40.1		
14	64.0	61	68	40.6	20	East Bound
15	62.8	56	69	40.2		
16	61.1	57	65	40.2		
17	61.4	58	64	40.3		
18	60.5	57	63	40.3		
19	60.6	57	64	40.4		
20	59.4	56	62	40.4		
21	58.5	55	63	40.4		
22	62.7	57	74	40.3		
23	60.3	56	65	40.7		
24	58.6	54	63	40.4		
25	57.7	54	62	40.4		

Table 27 Skid Results for Runway 8-26 at Deming Municipal Airport

S. No.	Average SN	Min. SN	Max. SN	Speed, mph	Offset from C/L, feet	Direction
1	55.8	50	61	40.4	30	West Bound
2	56.2	51	62	40.2		
3	63.0	56	74	40.0		
4	60.1	48	69	40.0		
5	62.3	56	67	40.0		
6	63.2	55	67	39.9		
7	64.4	60	69	40.2		
8	62.8	57	67	40.0		
9	62.8	57	67	40.0		
10	61.5	57	65	40.0		
11	64.8	42	70	40.1		
12	68.0	61	72	40.1		
13	66.5	61	72	39.7	30	East Bound
14	65.3	57	69	40.3		
15	62.8	57	70	40.4		
16	61.6	58	65	40.4		
17	63.3	59	67	40.5		
18	63.4	61	66	40.3		
19	61.1	56	67	40.5		
20	59.7	53	66	40.4		
21	56.1	50	59	40.4		
22	61.1	55	66	40.4		
23	52.2	48	59	40.5		
24	56.0	51	61	40.5		

Table 28 Skid Results for Runway 3-21 at Roswell International Airport

S. No.	Average SN	Min. SN	Max. SN	Speed, mph	Offset from C/L, feet	Direction
1	81.4	70	89	44.4	5	East Bound
2	86.9	80	97	42.1		
3	75.0	56	87	42.9		
4	67.3	29	81	43.2		
5	74.0	67	81	42.3		
6	71.6	65	79	41.0		
7	75.6	69	85	41.0		
8	69.3	63	81	42.1		
9	76.0	66	82	41.9		
10	76.6	70	83	41.7		
11	71.3	62	76	41.5		
12	75.7	66	83	42.2		
13	73.0	68	80	40.8		
14	72.9	61	85	41.5		
15	72.5	64	81	40.9		
16	74.8	66	82	42.0		
17	74.3	65	82	41.9		
18	70.2	63	77	41.9		
19	72.8	61	85	41.6		
20	69.3	65	77	42.2		
21	70.7	61	77	41.6		
22	73.4	65	83	41.9		
23	67.7	60	77	41.6		
24	66.2	60	72	41.4		
25	67.0	53	77	42.3		
26	63.1	55	75	41.6		
27	51.0	36	68	42.1		
28	64.1	45	77	41.6		
29	68.6	59	81	41.7		

Table 29 Skid Results for Runway 3-21 at Roswell International Airport

S. No.	Average SN	Min. SN	Max. SN	Speed, mph	Offset from C/L, feet	Direction
1	69.4	58	85	43.0	5	West Bound
2	68.8	61	78	41.6		
3	48.7	34	63	42.2		
4	36.8	28	47	41.8		
5	38.3	32	53	41.8		
6	39.3	31	48	41.9		
7	59.0	48	71	41.8		
8	66.4	57	79	41.7		
9	60.7	53	70	41.8		
10	66.3	56	76	42.1		
11	62.6	54	72	41.8		
12	58.2	45	73	42.0		
13	65.8	57	74	41.7		
14	65.9	57	75	42.1		
15	71.1	61	81	41.9		
16	67.2	55	78	41.9		
17	63.8	52	72	41.5		
18	62.0	51	67	41.9		
19	60.7	50	74	42.0		
20	61.9	52	72	41.6		
21	65.3	58	71	41.7		
22	63.8	53	75	42.0		
23	70.5	64	78	41.8		
24	68.7	63	75	41.7		
25	70.3	58	78	40.7		
26	60.6	49	72	41.3		
27	69.6	61	78	42.0		
28	50.0	36	58	42.1		
29	59.2	49	67	41.4		
30	58.1	45	69	42.2		
31	70.9	61	79	41.4		

Table 30 Skid Results for Runway 3-21 at Roswell International Airport

S. No.	Average SN	Min. SN	Max. SN	Speed, mph	Offset from C/L, feet	Direction
1	38.7	31	46	42.3	20	East Bound
2	51.5	47	58	42.4		
3	41.8	36	50	42.5		
4	47.2	43	54	41.6		
5	51.7	43	60	41.0		
6	51.5	43	58	42.1		
7	49.9	44	57	40.4		
8	60.1	53	68	40.2		
9	51.1	46	57	41.4		
10	53.9	49	59	40.0		
11	53.8	46	60	41.1		
12	55.0	45	64	40.0		
13	51.9	42	61	40.4		
14	59.0	48	64	40.6		
15	52.8	48	58	41.0		
16	52.7	45	58	40.3		
17	46.0	33	57	41.4		
18	55.6	50	61	40.1		
19	53.2	46	59	40.9		
20	46.2	40	55	40.8		
21	51.9	42	57	40.7		
22	54.9	43	62	40.6		
23	47.9	41	57	41.0		

Table 31 Skid Results for Runway 3-21 at Roswell International Airport

S. No.	Average SN	Min. SN	Max. SN	Speed, mph	Offset from C/L, feet	Direction
1	57.9	49	65	37.6	20	West Bound
2	48.4	40	58	41.4		
3	49.2	41	58	38.6		
4	47.9	40	55	41.6		
5	53.0	42	64	40.3		
6	48.6	41	62	41.2		
7	55.0	49	60	40.3		
8	61.4	59	64	41.1		
9	49.6	43	56	39.7		
10	51.9	45	57	41.0		
11	55.6	52	61	41.0		
12	62.1	47	71	40.7		
13	58.9	50	68	40.9		
14	29.8	21	40	41.2		
15	56.8	48	64	40.2		
16	60.1	50	68	40.6		
17	56.0	47	65	41.0		
18	53.1	50	57	40.1		
19	50.5	39	60	41.6		
20	39.1	28	62	40.4		
21	57.1	54	62	40.8		
22	48.1	43	55	40.6		
23	52.5	49	57	40.8		
24	59.5	49	64	40.6		
25	63.3	58	71	41.1		
26	52.9	44	68	40.7		

Table 32 Skid Results for Runway 17-35 at Roswell International Airport

S. No.	Average SN	Min. SN	Max. SN	Speed, mph	Offset from C/L, feet	Direction
1	60.2	56	64	44.5	5	South Bound
2	55.3	51	60	50.4		
3	55.9	53	60	48.6		
4	56.1	53	59	50.7		
5	56.3	54	59	50.3		
6	55.2	52	58	50.9		
7	56.2	53	59	51.6		
8	55.5	53	58	51.1		
9	55.4	52	58	51.3		
10	57.0	53	60	50.2		
11	56.6	54	59	50.5		
12	56.1	53	59	50.2		
13	55.3	53	58	50.1		
14	56.5	54	59	50.1		
15	54.7	49	60	50.7		
16	55.2	50	60	50.2		
17	58.5	52	62	50.0	5	North Bound
18	49.2	43	58	48.9		
19	59.7	55	65	44.3		
20	59.5	57	62	41.6		
21	61.6	59	65	40.4		
22	60.5	57	64	40.3		
23	59.7	57	62	40.4		
24	59.0	57	64	39.5		
25	58.7	55	62	39.3		
26	59.0	56	62	39.5		
27	57.4	56	60	40.8		
28	59.2	56	62	39.8		
29	59.9	57	64	40.6		
30	59.3	56	63	40.5		
31	61.0	56	69	39.6		
32	58.6	55	63	41.1		

Table 33 Skid Results for Runway 17-35 at Roswell International Airport

S. No.	Average SN	Min. SN	Max. SN	Speed, mph	Offset from C/L, feet	Direction
1	66.7	63	74	40.8	30	South Bound
2	62.8	59	66	39.4		
3	67.1	63	70	39.7		
4	64.4	61	68	40.8		
5	66.9	63	71	40.6		
6	65.1	62	69	40.5		
7	64.9	60	69	39.4	30	North Bound
8	63.1	60	68	40.6		
9	63.1	61	66	40.7		
10	63.0	59	68	40.5		
11	62.3	59	66	40.5		
12	64.6	61	68	40.7		
13	64.5	60	69	40.3		

Table 34 Skid Results for Runway 3-21 at Belen Municipal Airport

S. No.	Average SN	Min. SN	Max. SN	Speed, mph	Offset from C/L, feet	Direction
1	34.9	29	40	40.7	5	West Bound
2	36.0	28	47	41.0		
3	37.0	31	42	41.6		
4	36.5	26	44	41.4		
5	35.8	27	41	40.4		
6	32.4	28	37	40.4		
7	31.1	28	35	40.5		
8	31.2	24	35	41.3		
9	30.2	24	35	40.7		
10	33.2	30	37	40.6		
11	32.8	30	36	40.8		
12	31.2	27	34	41.3		
13	32.4	29	37	41.6		
14	32.8	27	35	40.6		
15	34.9	23	41	40.2		
16	32.2	28	38	40.5		
17	34.3	30	38	40.6		
18	30.2	28	32	40.2		
19	35.7	33	40	28.3		
20	30.1	27	37	42.5	5	East Bound
21	33.8	29	40	41.9		
22	34.9	31	40	40.9		
23	34.0	30	38	40.1		
24	35.0	31	39	42.0		
25	34.3	26	39	41.0		
26	35.2	31	40	39.7		
27	35.3	32	38	40.3		
28	32.7	29	35	40.1		
29	33.5	23	41	42.4		
30	34.2	28	40	39.7		
31	35.5	32	40	39.8		
32	37.9	32	46	40.3		
33	34.6	31	39	40.8		
34	35.6	32	40	41.3		
35	37.0	29	43	40.2		
36	34.4	32	37	39.3		

Table 35 Skid Results for Runway 3-21 at Belen Municipal Airport

S. No.	Average SN	Min. SN	Max. SN	Speed, mph	Offset from C/L, feet	Direction
1	26.3	23	29	40.3	20	West Bound
2	33.1	28	39	41.0		
3	36.6	33	42	40.2		
4	36.6	33	40	40.4		
5	34.0	30	39	40.5		
6	33.9	29	37	41.4		
7	36.5	33	42	42.0		
8	37.0	32	41	39.6		
9	36.3	27	41	39.7		
10	35.3	32	38	39.4		
11	32.9	30	36	40.8		
12	31.4	27	34	40.9	20	East Bound
13	33.2	29	38	40.5		
14	35.7	32	41	40.7		
15	33.2	30	37	39.4		
16	36.3	30	43	39.3		
17	35.0	32	38	39.9		
18	33.3	23	39	39.9		
19	33.8	30	39	39.9		
20	38.6	34	44	40.0		
21	34.1	29	43	40.1		
22	34.0	30	38	40.9		

Table 36 Skid Results for Runway 2-20 at Clayton Municipal Airport

S. No.	Average SN	Min. SN	Max. SN	Speed, mph	Offset from C/L, feet	Direction
1	71.7	64	81	51.4	5	West Bound
2	68.2	59	81	51.1		
3	67.9	62	75	52.2		
4	64.7	38	72	50.4		
5	69.8	66	76	51.3		
6	63.8	53	72	50.4		
7	67.5	62	74	51.7		
8	60.9	52	69	50.9		
9	61.1	49	71	51.3		
10	76.4	70	82	48.1	5	East Bound
11	74.1	69	80	50.6		
12	72.4	66	82	51.6		
13	71.2	65	75	52.0		
14	71.1	66	75	51.7		
15	70.4	61	80	50.9		
16	75.5	66	86	51.4		
17	74.9	69	80	52.5		
18	75.7	71	79	51.7		
19	67.5	64	71	52.6	20	West Bound
20	69.7	66	76	51.6		
21	67.9	51	87	50.4		
22	68.9	62	76	50.4		
23	66.1	59	73	50.4		
24	69.6	65	77	50.1		
25	65.9	52	75	51.2		
26	38.4	32	50	50.8		
27	71.8	63	80	50.4		
28	70.4	65	79	51.1		
29	72.2	66	78	51.1	20	East Bound
30	59.5	44	82	52.8		
31	71.5	65	76	51.3		
32	72.2	65	80	52.1		
33	70.5	64	76	51.7		
34	71.7	63	79	50.5		
35	72.3	52	90	49.1		
36	73.0	66	80	50.5		
37	69.6	65	74	49.4		
38	70.1	62	78	50.4		

Table 37 Skid Results for Runway 12-30 at Clayton Municipal Airport

S. No.	Average SN	Min. SN	Max. SN	Speed, mph	Offset from C/L, feet	Direction
1	63.0	51	72	52.0	5	South Bound
2	58.0	36	65	51.4		
3	58.0	49	66	51.6		
4	58.5	55	63	49.8		
5	57.9	53	64	50.7		
6	57.1	50	65	50.0		
7	56.8	53	61	50.1		
8	54.9	48	62	51.8	5	North Bound
9	58.0	53	67	51.9		
10	58.0	53	63	50.6		
11	57.4	53	63	50.5		
12	57.1	52	66	51.4		
13	67.3	59	80	50.6		
14	55.6	51	66	51.2		
15	65.3	56	71	50.2	20	South Bound
16	63.0	38	79	51.5		
17	65.3	57	74	50.8		
18	57.0	49	68	51.4		
19	60.2	50	74	51.3		
20	61.2	55	69	50.0		
21	62.0	38	70	53.2	20	North Bound
22	66.2	60	74	49.7		
23	65.4	58	70	50.4		
24	65.2	57	73	50.1		
25	63.7	58	73	50.6		
26	59.2	51	71	49.7		
27	58.8	42	70	50.9		

APPENDIX III

Table 1 Summary Sheet – Runway 4-22 at Double Eagle II Airport

Location	Hole No.	Depth, ft.		Layer thickness	Group symbol	CBR
		From	To			
Runway 4-22	1	0	2.5	2.5	PMBP	
		2.5	9	6.5	SW	56
		9	21	12	SW-SM	22
		21	36	15	SP-SM	20
		36	55	19	SP-SM	19
	2	0	2.5	2.5	PMBP	
		2.5	8	5.5	SW	53
		8	16	8	SP-SM	20
		16	21	5	SP-SM	21
		21	55	34	SP-SM	20
	3	0	2.5	2.5	PMBP	
		2.5	8	5.5	GW	64
		8	21	13	SP-SM	20
		21	39	18	SW-SM	26
		39	55	16	SW-SM	20
	4	0	2.25	2.25	PMBP	
		2.25	9	6.75	GW	58
		9	27	18	SW-SM	20
		27	37	10	SW-SM	22
		37	55	18	SW-SM	20
	5	0	2	2	PMBP	
		2	9	7	SW	50
		9	23	14	SP-SM	20
		23	33	10	SW-SM	18
		33	41	8	SP-SM	18
		41	55	14	SP-SM	17
	6	0	2.5	2.5	PMBP	
		2.5	9	6.5	GW	60
		9	29	20	SP-SM	19
		29	37	8	SP-SM	19
		37	55	18	SW-SM	29
	7	0	3	3	PMBP	
		3	10	7	GW	59
		10	29	19	SW-SM	22
		29	55	26	SP-SM	19
	8	0	2.5	2.5	PMBP	
		2.5	9	6.5	SW	53
		9	19	10	SP-SM	20
		19	38	19	SW-SM	22
		38	55	17	SP-SM	18

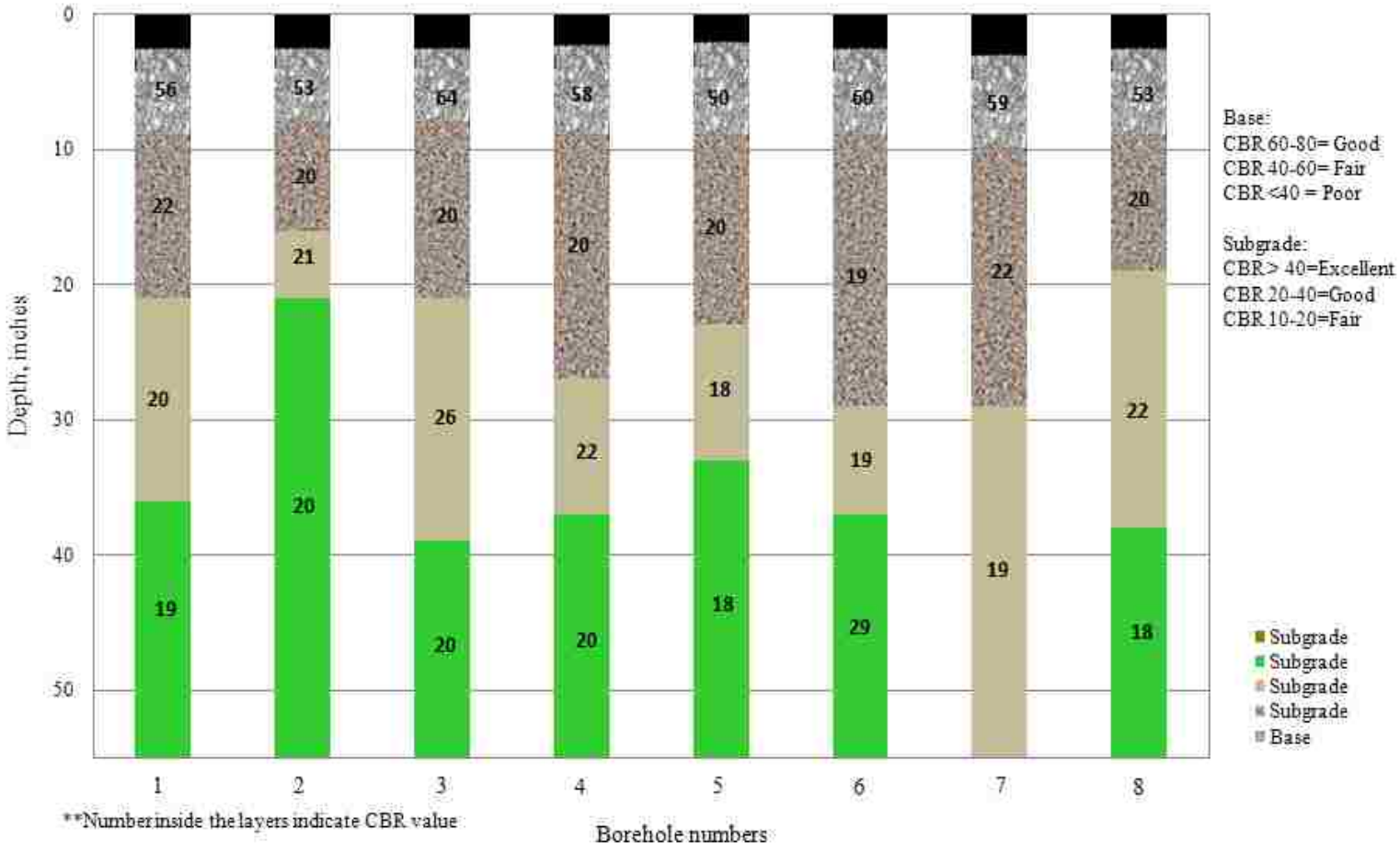

Figure 1 Soil Profile of Runway 4-22 at Double Eagle II Airport with CBR Values

Table 2 Summary Sheet – Runway 12-30 at Sierra Blanca Regional Airport

Location	Hole No.	Depth, ft.		Layer thickness, inches	Group symbol	CBR
		From	To			
Runway 12-30	1	0	5	5	PMBP	
		5	18	13	SW	54
		18	30	12	GW	55
		30	39	9	GW	63
		39	53	14	GW	48
	1A	0	5	5	PMBP	
		5	18	13	GW	64
		18	39	21	SW-SC	49
		39	46	7	GW	48
		46	58	12	SW	48
	2	0	5	5	PMBP	
		5	18	13	GW	56
		18	37	19	GW	53
		37	41	4	GW	63
		41	48	7	SW-SC	36
	3	0	5	5	PMBP	
		5	18	13	GW	55
		18	25	7	GW	47
		25	52	27	GP-GM	61
	4	0	5	5	PMBP	
		5	18	13	SW	53
		18	36	18	GP	67
		36	51	15	SW	53
	5	0	5	5	PMBP	
		5	19	14	SW	54
		19	35	16	SW	55
		35	44	9	GW	56
		44	53	9	SW	39
	6	0	4	4	PMBP	
		4	17	13	GW	56
		17	32	15	GW	48
		32	38	6	GW	55
		38	54	16	SW	42

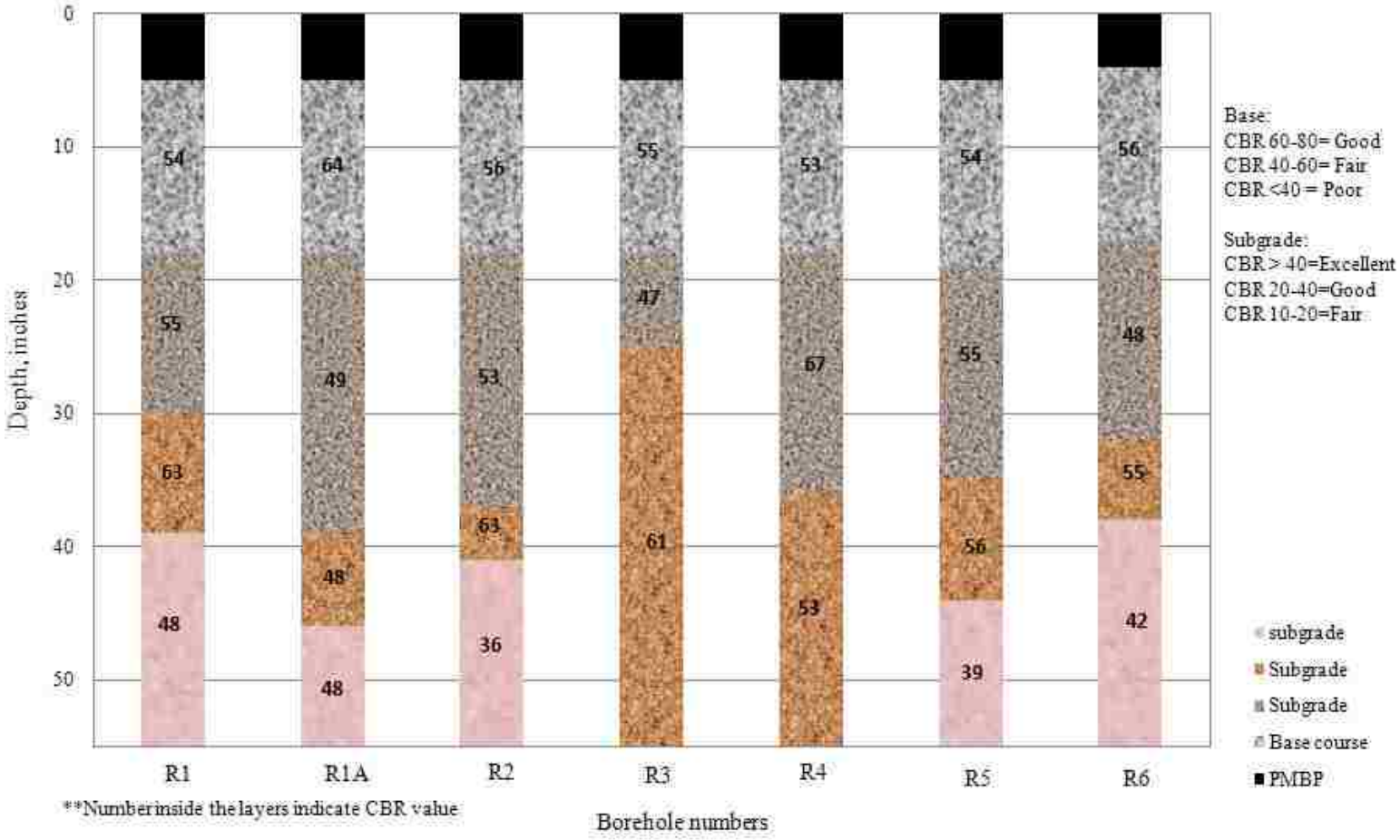

Figure 2 Soil Profile of Runway 12-30 at Sierra Blanca Regional Airport with CBR Values

Table 3 Summary Sheet - Runway 7-25 at Raton Municipal Airport

Location	Hole No.	Depth, inches		Layer Thickness	Group Symbol	CBR
		From	To			
Runway 7-25	1	0	9	9	PMBP	
		9	21	12	GW	77
		21	26	5	GP-GM	56
		26	42	16	SC	32
		42	60	18	SM	42
	2	0	6	6	PMBP	
		6	20	14	GW	68
		20	28	8	SC	30
		28	44	16	SC	29
		44	64	20	SC	36
	3	0	7	7	PMBP	
		7	22	15	GW	72
		22	47	25	SP-SM	37
		47	70	23	GW	72
	4	0	8	8	PMBP	
		8	22	14	SW	54
		22	30	8	SP-SM	35
		30	45	15	GP-GM	61
		45	64	19	GP-GM	60
	5	0	7	7	PMBP	
		7	13	6	SW	56
		13	24	11	SP-SC	37
		24	30	6	SW-SM	43
		30	46	16	SM	26
		46	64	18	SW-SM	46

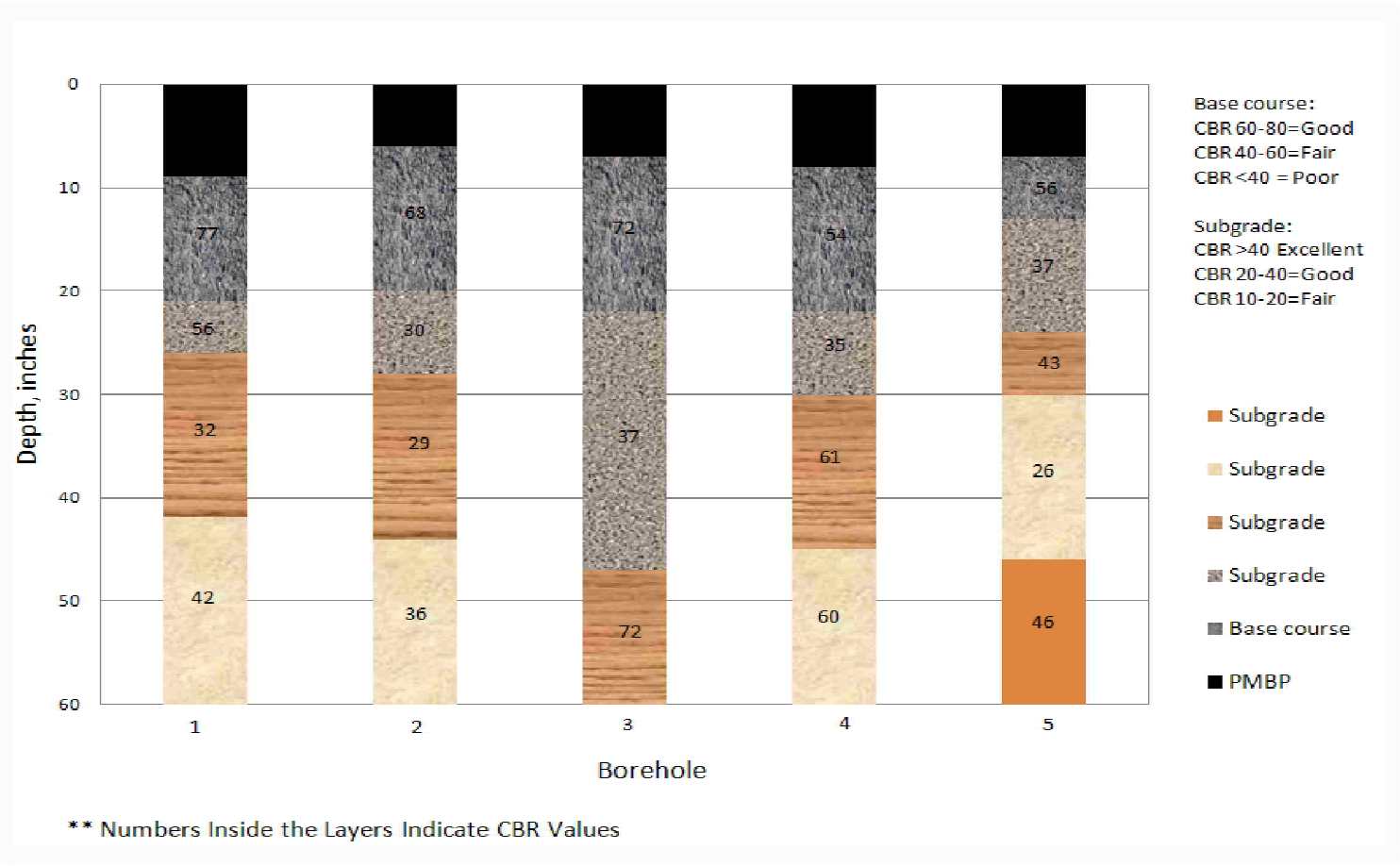

Figure 3 Soil Profile of Runway 7-25 at Raton Municipal Airport with CBR Values

Table 4 Summary Sheet - Runway 2-20 at Raton Municipal Airport

Location	Hole No.	Depth, inches		Layer Thickness	Group Symbol	CBR
		From	To			
Runway 2-20	9	0	8	8	PMBP	
		8	15	7	GW	72
		15	33	18	GP	61
		33	40	7	GP-GC	58
		40	53	13	GP	61
		53	71	18	GP-GC	56
	10	0	8	8	PMBP	
		8	14	6	GW	68
		14	28	14	GW-GC	54
		28	42	14	GW-GC	55
		42	51	9	GW-GC	58
		51	60	9	GP	70
	11	0	5	5	PMBP	
		5	11	6	GW	64
		11	30	19	SP-SC	32
		30	43	13	SC	17
		43	68	25	SC	20
	12	0	7	7	PMBP	
		7	15	8	GW	66
		15	32	17	GP	77
		32	62	30	SP-SC	53
	13	0	6	6	PMBP	
		6	15	9	GW	63
		15	36	21	GP	50
		36	56	20	GP-GC	33
		56	67	11	GP-GC	66
	14	0	7	7	PMBP	
		7	12	5	GW	66
		12	18	6	GW	65
		18	33	15	GP	52
		33	48	15	GP	68
		48	55	7	GW-GC	41

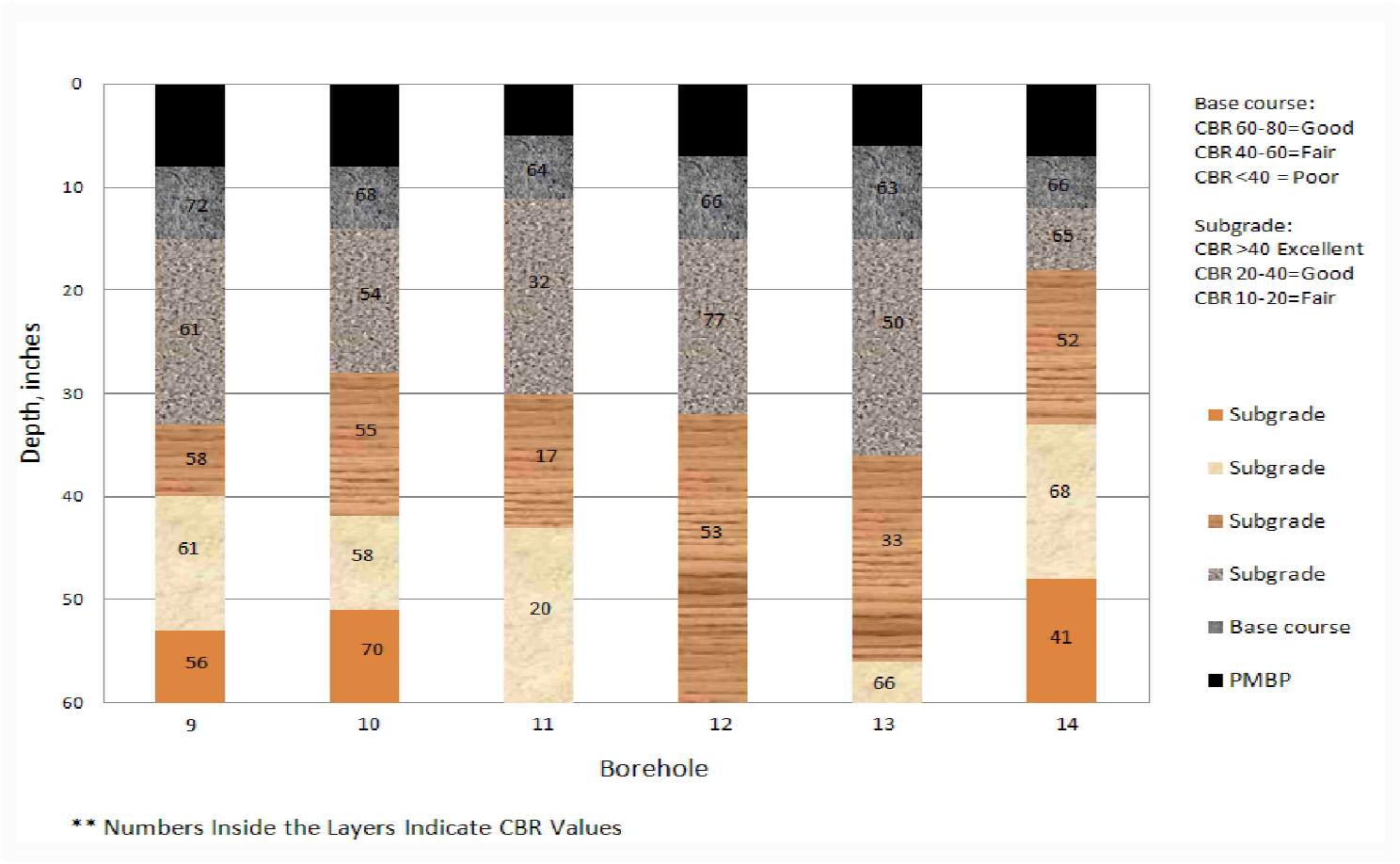

Figure 4 Soil Profile of Runway 2-20 at Raton Municipal Airport with CBR Values

Table 5 Summary Sheet - Runway 08-26 at Moriarty Municipal Airport

Location	Hole No.	Depth, inches		Layer Thickness	Group Symbol	CBR
		From	To			
Runway 08-26	1	0	6.5	6.5	PMBP	
		6.5	20	13.5	SP-SM	24
		20	39	19	SP-SM	20
		39	64	25	SP-SM	20
	2	0	6.5	6.5	PMBP	
		6.5	20	13.5	SM	18
		20	33	13	SP-SM	29
		33	66	33	SP-SM	26
	3	0	6.5	6.5	PMBP	
		6.5	18	11.5	SM	17
		18	41	23	SP-SM	22
		41	59	18	SM	17
	4	0	6	6	PMBP	
		6	38	32	SM	17
		38	57	19	SM	16
		57	68	11	SM	17
	5	0	6	6	PMBP	
		6	10	4	SM	15
		10	19	9	SP-SM	17
		19	34	15	SM	14
		34	45	11	SM	26
	6	0	6	6	PMBP	
		6	17	11	SM	45
		17	57	40	SM	14
		57	63	6	SM	31
	7	0	6	6	PMBP	
		6	22	16	SM	14
		22	42	20	SM	23
		42	64	22	SM	28

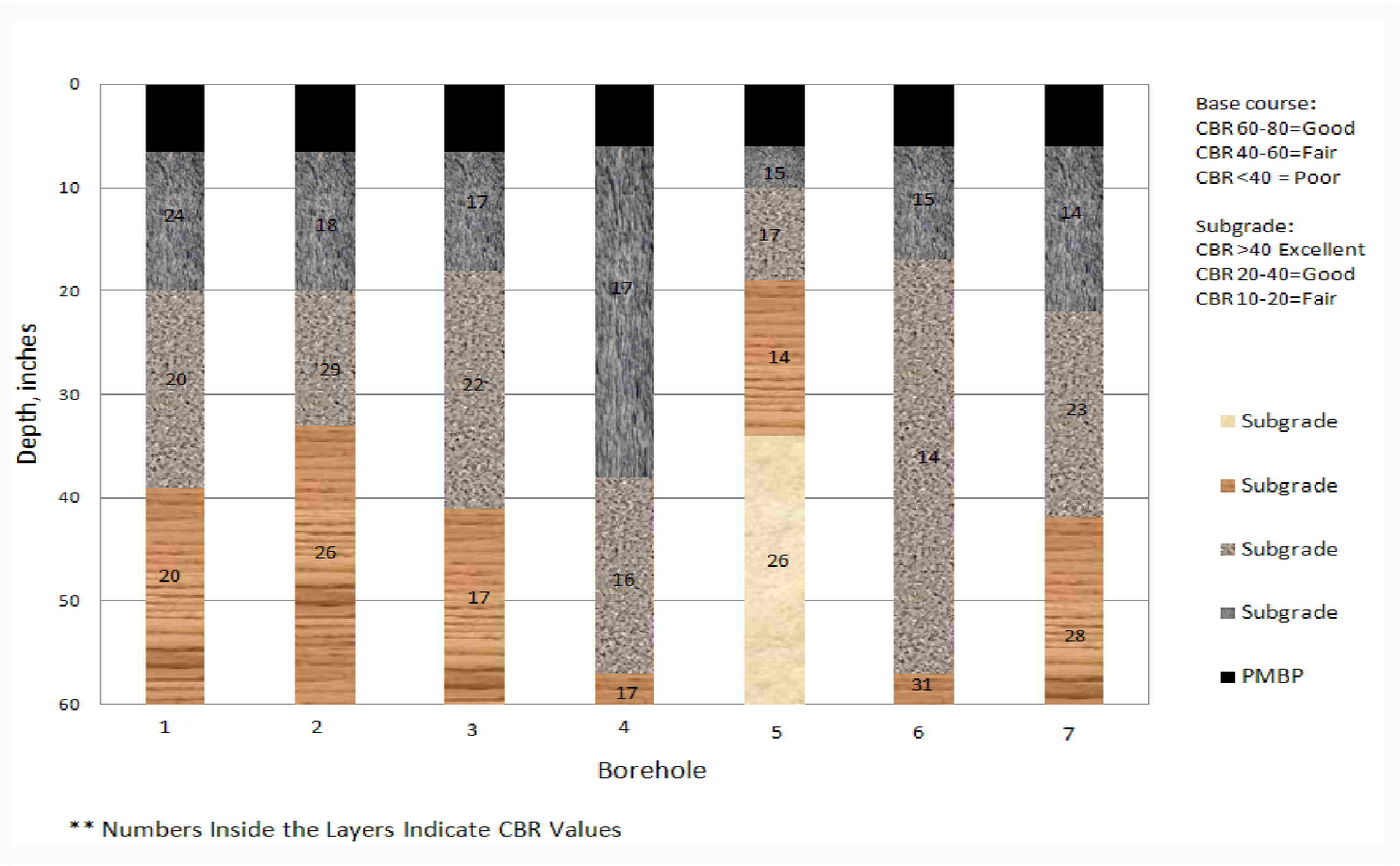

Figure 5 Soil Profile of Runway 08-26 at Moriarty Municipal Airport with CBR Values

Table 6 Summary Sheet - Runway 12-30 at Las Cruces International Airport

Location	Hole No.	Depth, inches		Layer Thickness	Group Symbol	CBR
		From	To			
Runway 12-30	1	0	4	4	PMBP	
		4	13	9	SP	46
		13	32	19	SP-SM	19
		32	63	31	GW	59
	2	0	4	4	PMBP	
		4	14	10	SP	37
		14	26	12	SP-SC	20
		26	33	7	SP	46
	3	0	3	3	PMBP	
		3	13	10	SP	46
		13	33	20	SP-SM	19
		33	37	4	SP	60
	4	0	4	4	PMBP	
		4	14	10	SP	37
		14	23	9	SP	20
		23	33	10	GP	82
	5	0	3.75	3.75	PMBP	
		3.75	14	10.25	SP	37
		14	20	6	SP	18
		20	29	9	GP	68
	6	0	3.25	3.25	PMBP	
		3.25	11	7.75	SP	37
		11	31	20	SP	21
		31	37	6	SP	46
	7	0	4.5	4.5	PMBP	
		4.5	14	9.5	SP	55
		14	22	8	SP	19
		22	34	12	SP-SM	21
		34	50	16	SP	46

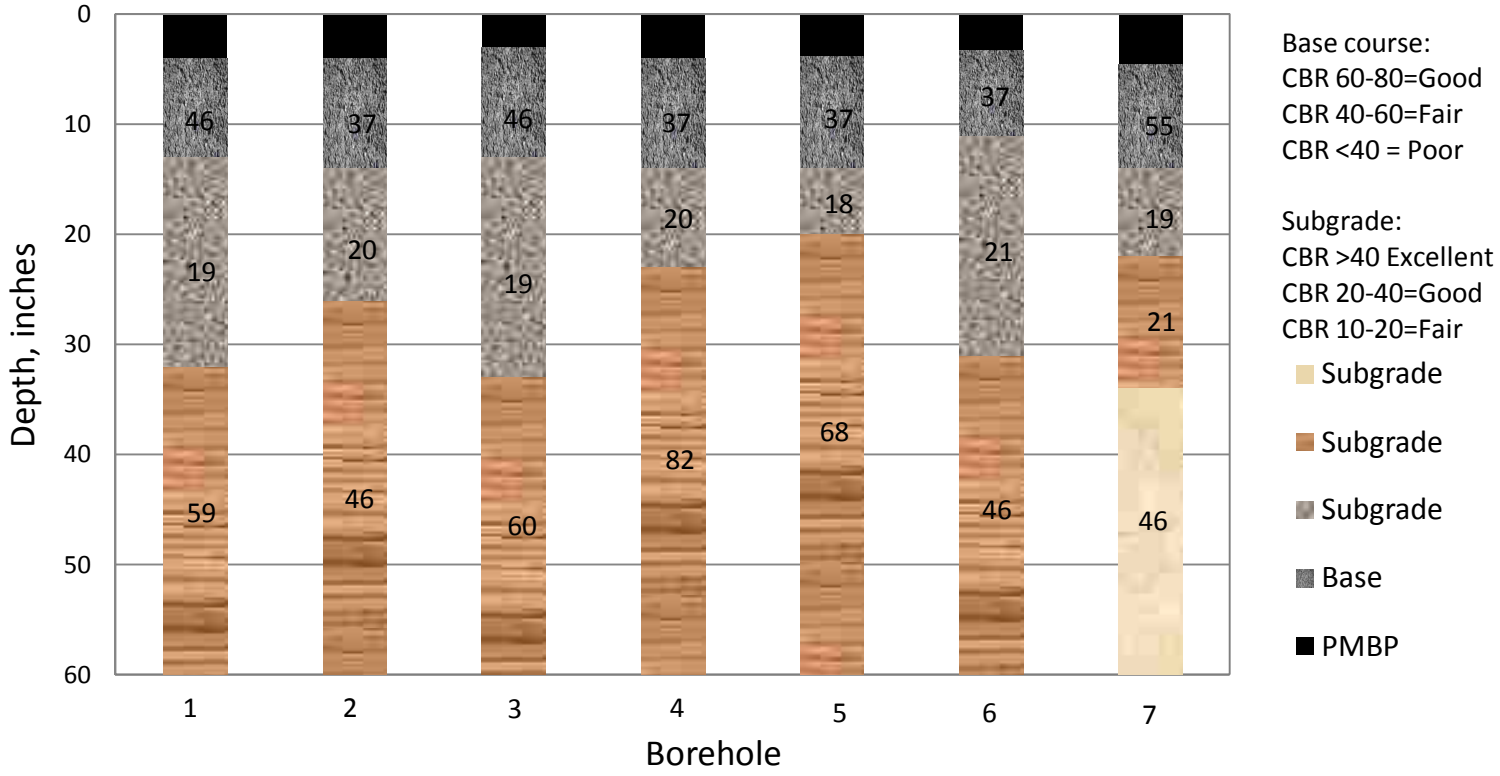

Figure 7 Soil Profile of Runway 12-30 at Las Cruces International Airport with CBR Values

Table 8 Summary Sheet - Runway 08-26 at Las Cruces International Airport

Location	Hole No.	Depth, inches		Layer Thickness	Group Symbol	CBR
		From	To			
Runway 08-26	8	0	5	5	PMBP	
		5	16	11	GP-GM	57
		16	36	20	SP-SM	18
		36	40	4	SP-SM	63
	9	0	4.5	4.5	PMBP	
		4	14	10	GW-GM	59
		14	66	52	SP-SM	44
	10	0	4.5	4.5	PMBP	
		4.5	14	9.5	GP-GM	64
		14	34	20	SP-SM	19
		34	65	31	SP-SM	30
	11	0	6	6	PMBP	
		6	14	8	GW-GM	61
		14	40	26	SP	20
		40	58	18	SP-SM	20
		58	64	6	SP-SM	19
	12	0	5	5	PMBP	
		5	13	8	GW	70
		13	23	10	SP-SM	19
		23	36	13	SP-SM	28
		36	58	22	SP-SM	36

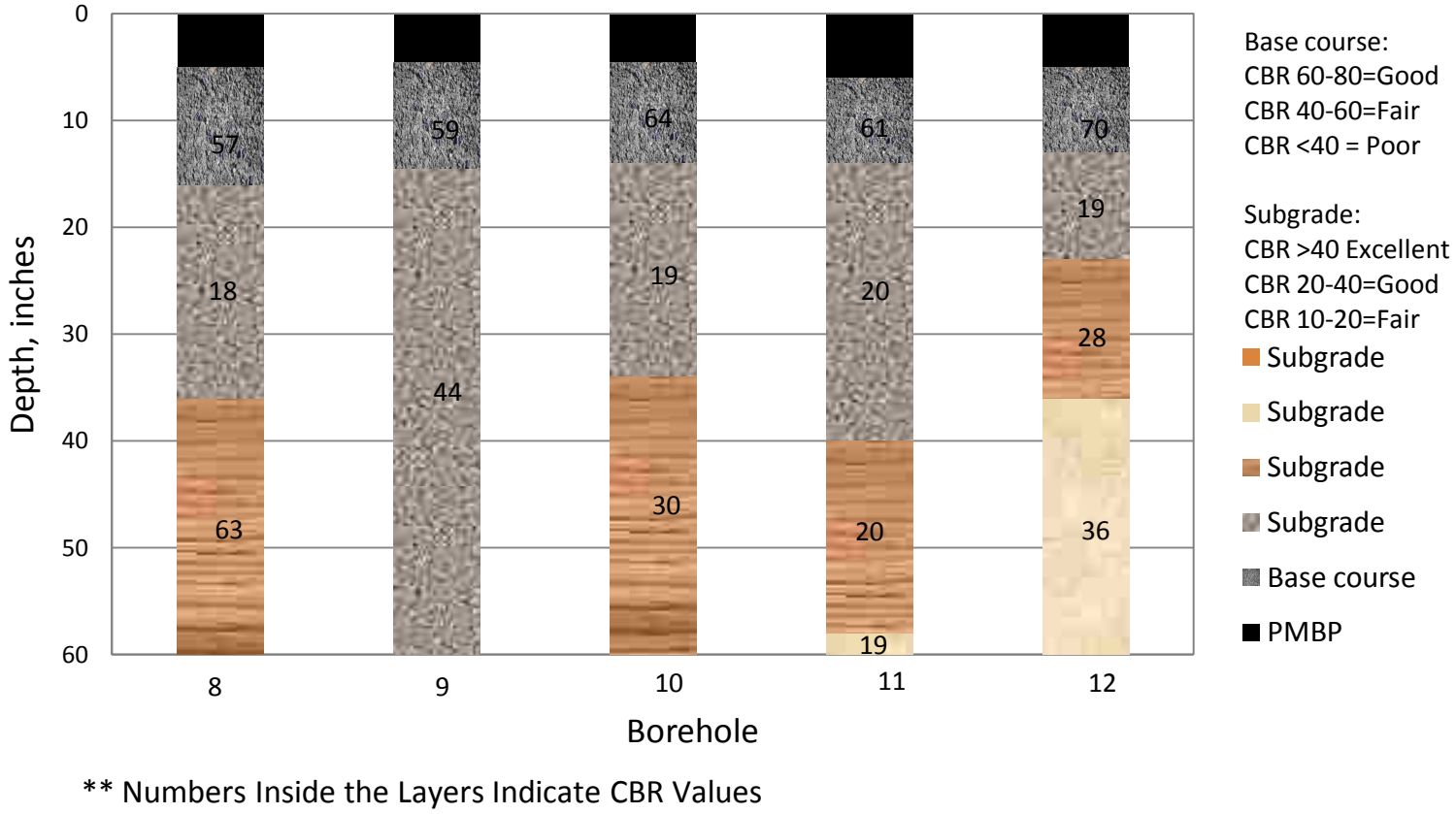

Figure 8 Soil Profile of Runway 8-26 at Las Cruces International Airport with CBR Values

Table 9 Summary Sheet - Runway 08-26 at Grant county Airport

Location	Hole No.	Depth, inches		Layer Thickness	Group Symbol	CBR
		From	To			
Runway 08-26	1a	0	6	6	PMBP	
		6	17	11	SP	50
		17	26	9	SW	50
		26	56	30	SW	51
		56	64	8	SP-SC	27
	1	0	7	7	PMBP	
		7	15	8	GW	59
		15	31	16	SW-SC	40
		31	42	11	SW-SC	28
		42	60	18	SW	28
	2	0	6	6	PMBP	
		6	15	9	SW	51
		15	30	15	SP-SM	35
		30	42	12	SP-SM	45
	3	0	7.5	7.5	PMBP	
		7.5	16	8.5	GW	58
		16	32	16	SP	45
		32	44	12	SP	54
	4	0	8	8	PMBP	
		8	20	12	SW	54
		20	36	16	SW-SC	39
		36	46	10	SP-SM	42
	5	0	6.5	6.5	PMBP	
		6.5	17	10.5	SW	51
		17	26	9	SP	46
		26	33	7	SW-SC	27
		33	57	24	SW	52
	6	0	9.75	9.75	PMBP	
		9.75	23	13.25	GW	58
		23	45	22	SP-SM	39

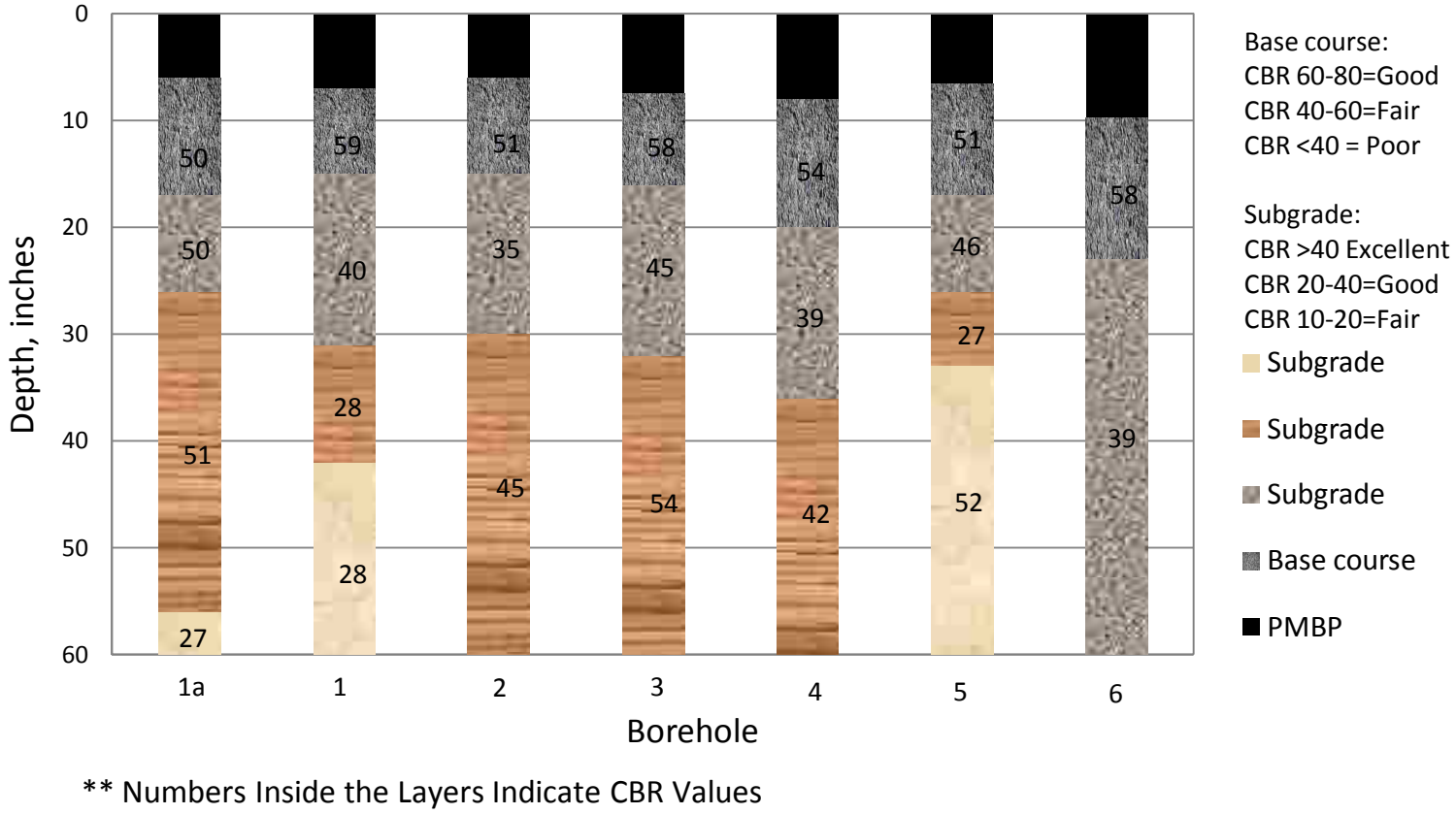

Figure 9 Soil Profile of Runway 8-26 at Grant County Airport with CBR Values

Table 10 Summary Sheet - Runway 08-26 at Deming Airport

Location	Hole No.	Depth, inches		Layer Thickness	Group Symbol	CBR
		From	To			
Runway 08-26	1	0	6	6	PMBP	
		6	16	10	SP	38
		16	34	18	SP-SM	19
		34	47	13	SM	22
		47	59	12	SM	21
	2	0	6	6	PMBP	
		6	16	10	SP	35
		16	28	12	SP-SC	18
		28	47	19	SM	20
		47	58	11	SM	21
	3	0	4.5	4.5	PMBP	
		4.5	11	6.5	SW	51
		11	42	31	GW	56
		42	62	20	SM	26
	4	0	5	5	PMBP	
		5	15	10	SP	57
		15	37	22	SP-SM	18
		37	51	14	SM	26
		51	61	10	SM	28
	5	0	5.5	5.5	PMBP	
		5.5	16	10.5	SP	49
		16	39	23	SP	19
		39	57	18	SM	18
		57	65	8	SM	18
	6	0	5	5	PMBP	
		5	12	7	SP	51
		12	44	32	SC	22
		44	60	16	SP-SM	22

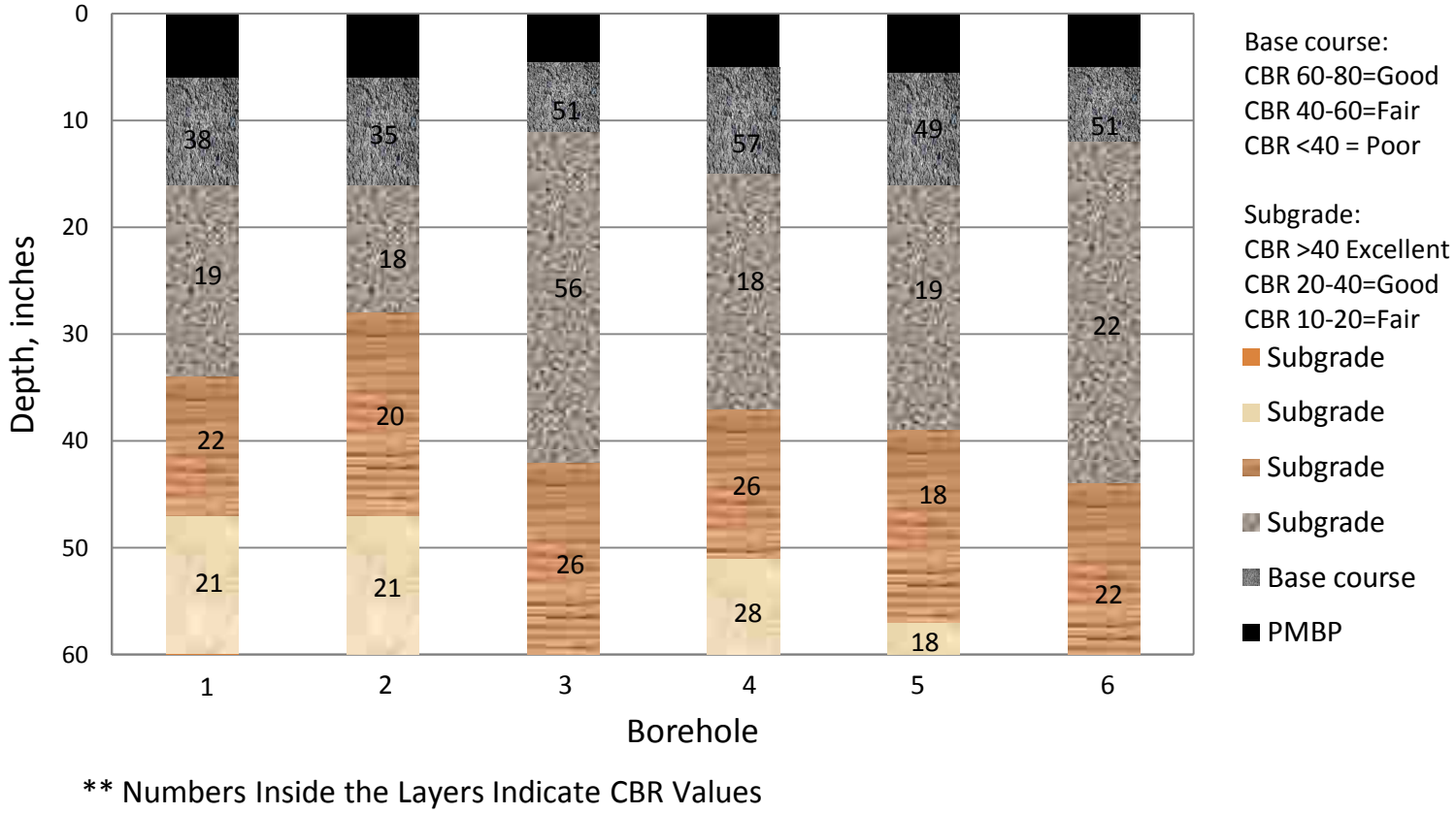

Figure 10 Soil Profile of Runway 8-26 at Deming Municipal Airport with CBR Values

Table 11 Summary Sheet – Runway 04-22 at Deming Airport

Location	Hole No.	Depth, inches		Layer Thickness	Group Symbol	CBR
		From	To			
Runway 04-22	7	0	6	6	PMBP	
		6	16	10	SP	50
		16	38	22	SP	24
		38	63	25	SC	22
	8	0	5	5	PMBP	
		5	11	6	SP	57
		11	55	44	SP-SM	27
		55	70	15	SM	19
	9	0	4	4	PMBP	
		4	27	23	SP	55
		27	60	33	SM	19
	10	0	5	5	PMBP	
		5	13	8	SP	48
		13	40	27	SP-SM	18
		40	58	18	SM	21
	11	0	5.5	5.5	PMBP	
		5.5	12	6.5	GW	57
		12	50	38	SP-SM	19
		50	62	12	SM	19

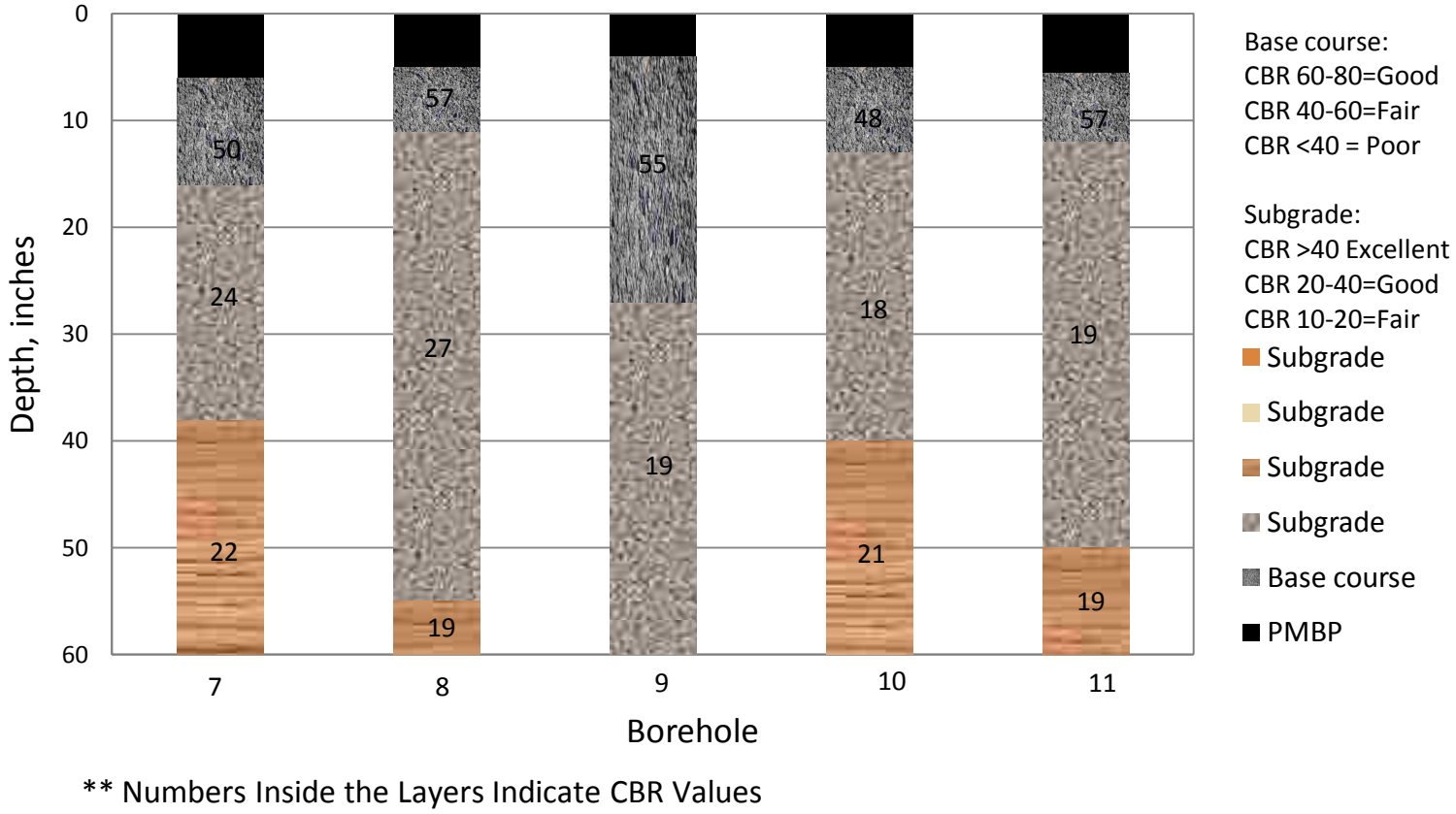

Figure 11 Soil Profile of Runway 4-22 at Deming Municipal Airport with CBR Values

Table 12 Summary Sheet - Runway 03-21 at Roswell International Airport

Location	Hole No.	Depth, inches		Layer Thickness	Group Symbol	CBR
		From	To			
Runway 03-21	11 B	0	6	6	PMBP	
		6	24	18	GP	70
		24	36	12	SW-SM	51
		36	50	14	SC	37
		50	62	12	SC	23
	12	0	3	3	PMBP	
		3	21	18	GP-GM	61
		21	32	11	SW-SM	45
		32	65	33	GW	63
	13	0	4	4	PMBP	
		4	21	17	GP	55
		21	39	18	GW	85
		39	60	21	SP-SC	32
	14	0	4	4	PMBP	
		4	13	9	GP	56
		13	43	30	SP-SC	27
		43	57	14	GP	61
	18	0	6	6	PMBP	
		6	18	12	GP-GM	64
		18	29	11	SW-SM	37
		29	45	16	SC	30
		45	65	20	SP-SC	33
	19	0	7	7	PMBP	
		7	21	14	SP	55
		21	53	32	SM	20
		53	60	7	GW	62
	23	0	7	7	PMBP	
		7	21	14	GP	63
		21	37	16	SP	55
		37	86	49	SP-SC	35

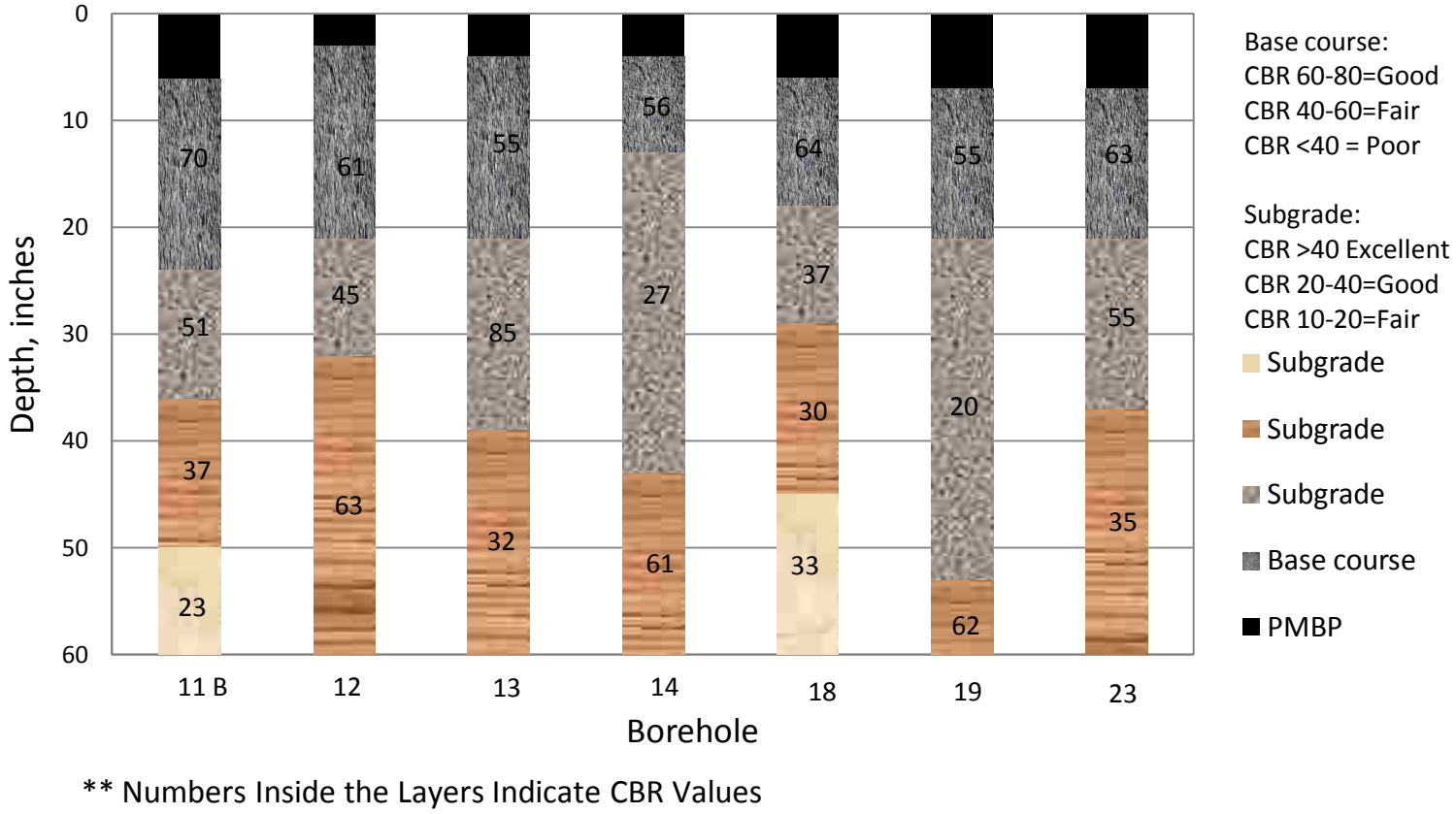

Figure 12 Soil Profile of Runway 03-21 at Roswell International Airport with CBR Values

Table 13 Summary Sheet - Runway 03-21 at Belen Municipal Airport

Location	Hole No.	Depth, inches		Layer Thickness	Group Symbol	CBR
		From	To			
Runway 03-21	1	0	3	3	PMBP	
		3	7	4	GW	56
		7	49	42	SP-SM	19
		49	59	10	SP-SM	21
	2	0	2.5	2.5	PMBP	
		2.5	8	5.5	SP	46
		8	37	29	SP-SM	19
		37	60	23	SP-SM	22
	3	0	2.5	2.5	PMBP	
		2.5	8	5.5	SP	52
		8	48	40	SP-SM	20
		48	61	13	SP-SM	17
	4	0	2.5	2.5	PMBP	
		2.5	9	6.5	SP	41
		9	36	27	SM	19
		36	54	18	SP-SM	18
		54	62	8	SP-SM	20
	5	0	2.5	2.5	PMBP	
		2.5	8	5.5	SP	53
		8	23	15	SW-SM	21
		23	54	31	SP-SM	18
		54	62	8	SP-SM	18
	6	0	2	2	PMBP	
		2	7	5	GP	59
		7	41	34	SP-SM	20
		41	55	14	SC	28
		55	65	10	SW-SC	28
	7	0	2	2	PMBP	
		2	8	6	GW	62
		8	35	27	SP-SM	19
		35	56	21	SP-SM	20
		56	68	21	SP-SC	28
	8	0	2.25	2.25	PMBP	
		2.25	11	8.75	GP	72
		11	29	18	SP-SM	23
		29	50	21	SP	18
		50	65	15	SP-SM	23

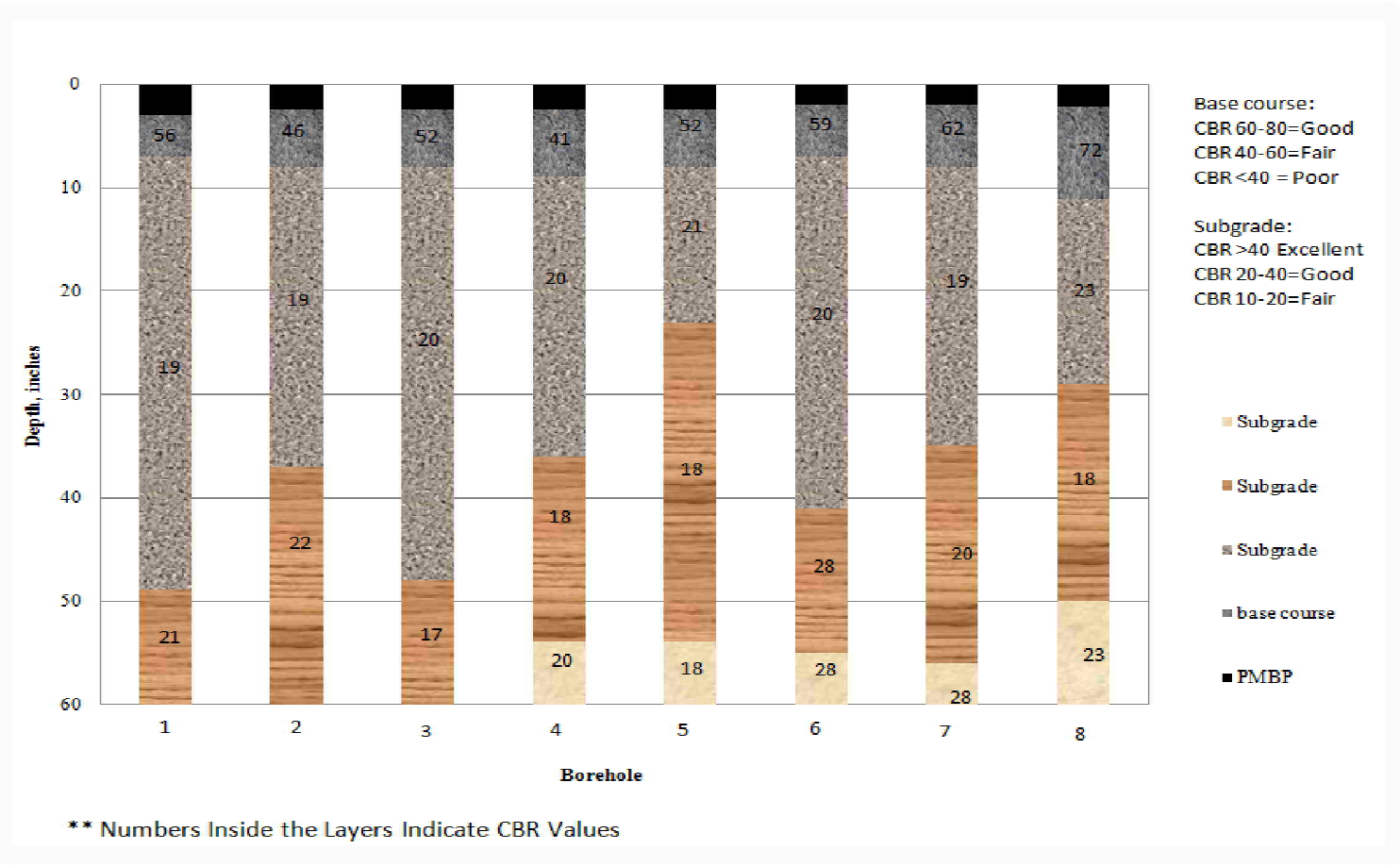

Figure 13 Soil Profile of Runway 03-21 at Belen Municipal Airport with CBR Values

Table 14 Summary Sheet - Runway 2-20 at Clayton Municipal Airport

Location	Hole No.	Depth, inches		Layer Thickness	Group Symbol	CBR
		From	To			
Runway 2-20	1	0	2	2	PMBP	
		2	18	16	SW	42
		18	60	42	SC	24
	2	0	3	3	PMBP	
		3	18	15	GW-GM	53
		18	42	24	SC	22
		42	53	11	SC-SM	23
		53	65	12	SM	22
	3	0	2.5	2.5	PMBP	
		2.5	14	11.5	SP-SM	50
		14	39	25	SP	59
		39	59	20	SC	23
	4	0	2.5	2.5	PMBP	
		2.5	17	14.5	GW-GM	54
		17	39	22	SC	25
		39	61	22	SM	21
	5	0	3.25	3.25	PMBP	
		3.25	20	16.75	GP-GM	56
		20	27	7	SC	27
		27	59	32	SC	25
	6A	0	2	2	PMBP	
		2	21	19	SP-SM	22
		21	42	21	SC	22
		42	61	19	SP	42
	6B	0	3	3	PMBP	
		3	15	12	SP	50
		15	29	14	SC	42
		29	44	15	SC	55
		44	64	20	SP	50

Table 15 Summary Sheet - Runway 12-30 at Clayton Municipal Airport

Location	Hole No.	Depth, inches		Layer Thickness	Group Symbol	CBR
		From	To			
Runway 03-21	7	0	2.5	2.5	PMBP	
		2.5	13	10.5	SP	47
		13	49	36	SM	22
		49	59	10	SM	22
	8	0	2.5	2.5	PMBP	
		2.5	14	11.5	SP	64
		14	54	40	SC	23
		54	63	9	SM	20
	9	0	2.5	2.5	PMBP	
		2.5	15	12.5	SW	48
		15	62	47	SC	25
	10	0	2	2	PMBP	
		2	15	13	GW	55
		15	54	39	SC	23
		54	63	9	SM	23

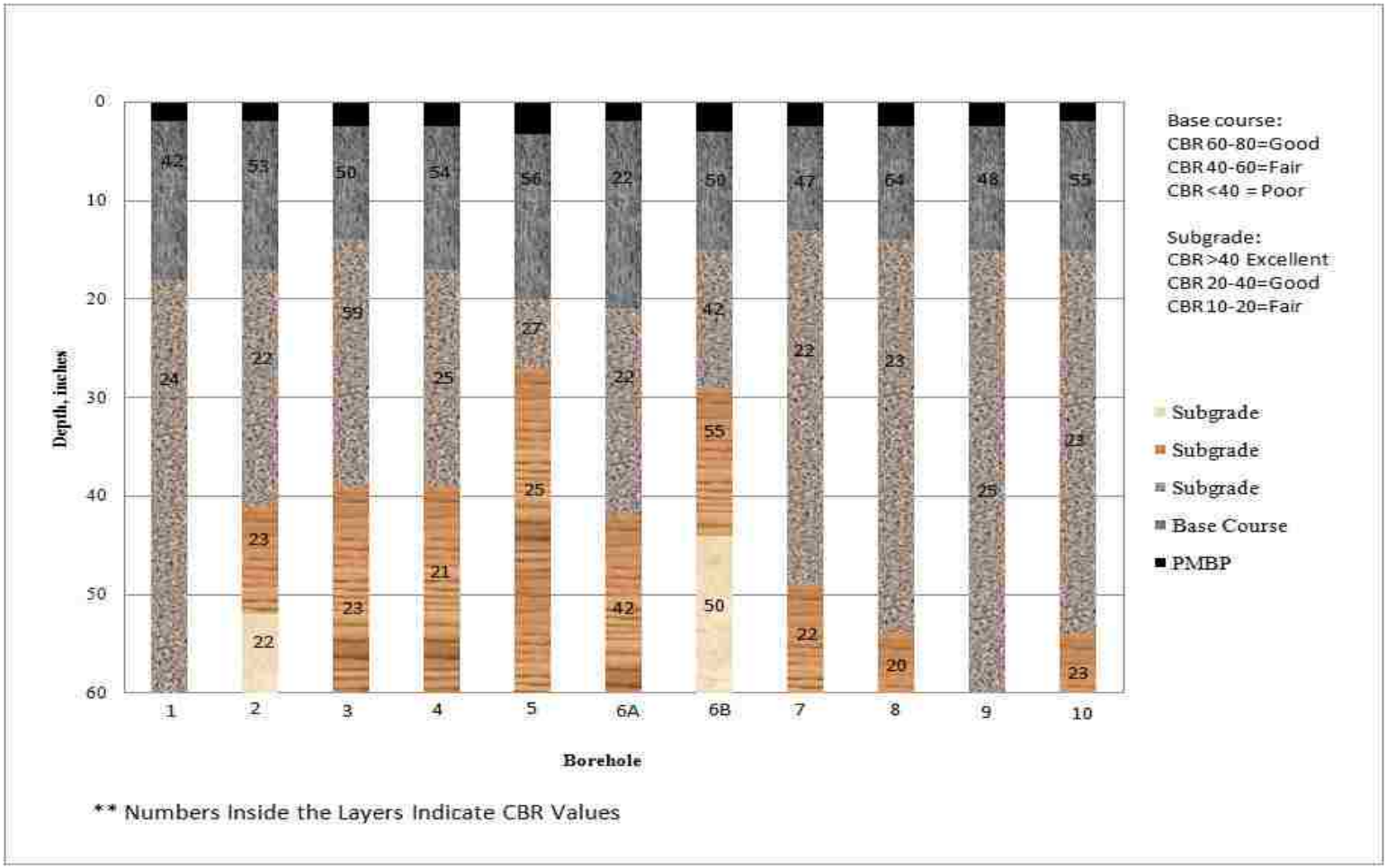

Figure 14 Soil Profile of Runway 2-20 and Runway 12-30 at Clayton Municipal Airport with CBR Values

APPENDIX IV

Table 1 Results of the Resilient Modulus Test of Runway 4-22 at Double Eagle II

Project	Location	Bag No.	Core No.	Sitting load, lb (P_o)	Repeated load, lb (P)	Horizontal Deflection 10^{-6} inches (H)	Average Thickness inches (t)	Resilient Modulus Mr = 0.62[(P-P_o)/Ht] psi	Average Resilient Modulus, psi
Double Eagle II	RW 4-22	N-82	A	2	41	45	2.03	264696	274635
		N-82	B	4	42	43	2.00	273953	
		N-82	C	3	43	42	2.07	285254	
		S-28	A	4	42	39	2.28	264957	262282
		S-28	B	5	41	42	2.31	230056*	
		S-28	C	4	38	35	2.32	259606	

(Poisson's Ratio assumed to be 0.35)

(* values not used for averaging)

Table 2 Results of the Indirect Tensile Test of Runway 4-22 at Double Eagle II

Project	Location	Bag No.	Core No.	Diameter inches (D)	Maximum load, lbf (P)	Average Thickness inches (t)	IDT Strength S_t = [(2 P)/(π D t)] psi	Average IDT Strength psi
Double Eagle II	RW 4-22	N-82	A	4.0	3090.3	2.03	242.3	246.2
		N-82	B	4.0	3100.6	2.00	246.7	
		N-82	C	4.0	3249.1	2.07	249.8	
		S-28	A	4.0	3300.7	2.28	230.4	236.0
		S-28	B	4.0	3458.2	2.31	238.2	
		S-28	C	4.0	3490.0	2.32	239.4	

Table 3 Results of the G_{mb} Test of Runway 4-22 at Double Eagle II Airport

Project	Location	Bag No.	Core No.	Weight in air, (g) (A)	Weight in water, (g) (B)	Weight surface dry, (g) (C)	G_{mb} = [A/(C-B)]	Average G_{mb}
Double Eagle II	RW 4-22	N-82	A	853.3	456.5	854.1	2.146	2.138
		N-82	B	842.7	450.9	845.5	2.136	
		N-82	C	860.8	459.4	863.2	2.132	
		S-28	A	980.7	509.8	985	2.064	2.069
		S-28	B	1001.2	529.2	1009.4	2.085	
		S-28	C	1030.1	533.9	1034.2	2.059	

Table 4 Results of the G_{mm} Test of Runway 4-22 at Double Eagle II

Project	Location	Bag No.	Wt. of Sample in air g (A)	Wt. of Flask with water g (B)	Wt. of Flask with Water and Sample g (C)	G_{mm} = A/(A+B-C)
DE II	RW 4-	N-82	1004.7	2565.1	3138.5	2.329
		S-28	1063.6	2565.1	3164.7	2.292

Table 5 Void Ratio of Runway 4-22 at Double Eagle II Airport

Project	Location	Bag No.	G_{mm}	G_{mb}	% Voids = 100* (G_{mm} - G_{mb})/ G_{mm}
DE II	RW 4-	N-82	2.329	2.138	8.23
		S-28	2.292	2.069	9.73

Table 6 Results of the Asphalt Content Test of Runway 4-22 at Double Eagle II

Project	Location	Bag No.	Sample Weight (g)	Weight Loss (g)	Percent Loss %	Temp Comp %	Bitumen Ratio %	Calibrated Asphalt Content %
DE II	RW 4-	N-82	2517	152.6	6.06	0.12	6.34	5.94
		S-28	3027	196.0	6.48	0.10	6.82	6.38

Values taken directly from the printout of NCAT Asphalt Content Tester

Table 7 Results of Resilient Modulus Test of Runway 12-30 at Sierra Blanca Regional

Project	Location	Bag No.	Core No.	Sitting load lb (P_o)	Repeated load, lb (P)	Horizontal Deflection 10^{-6} inches (H)	Average Thickness inches (t)	Resilient Modulus Mr = 0.62[(P-P_o)/Ht] psi	Average Resilient Modulus psi
Sierra Blanca	RW 12-30	P-600	A	7	42	35	2.53	245059*	276534
		P-600	B	2	41	34	2.52	282213	
		P-600	C	2	44	38	2.53	270855	
		L-6	A	2	40	42	2.49	225282	227074
		L-6	B	2	45	40	2.49	267671*	
		L-6	C	7	47	43	2.52	228867	

(Poisson's Ratio assumed to be 0.35)

(* Values not used for averaging)

Table 8 Results of Indirect Tensile Test of Runway 12-30 at Sierra Blanca Regional

Project	Location	Bag No.	Core No.	Diameter inches (D)	Maximum load, lbf (P)	Average Thickness inches (t)	IDT Strength $S_t = [(2 P)/(\pi D t)]$ psi	Average IDT Strength psi
Sierra Blanca	RW 12-30	P-600	A	4.0	4868.9	2.53	306.2	306.1
		P-600	B	4.0	4846.1	2.52	306.0	
		P-600	C	4.0	4973.2	2.53	312.8*	
		L-6	A	4.0	3812.3	2.49	243.6	237.3
		L-6	B	4.0	3613.5	2.49	230.9	
		L-6	C	4.0	3378.9	2.52	213.4*	

(* Values not used for averaging)

Table 9 Results of the Gmb Test of Runway 12-30 at Sierra Blanca Regional

Project	Location	Bag No.	Core No.	Weight in air, (g) (A)	Weight in water, (g) (B)	Weight surface dry, (g) (C)	$G_{mb} = [A/(C-B)]$	Average G_{mb}
Sierra Blanca	RW 12-30	P-600	A	1189.4	670.8	1192.9	2.278	2.270
		P-600	B	1183.3	667.1	1184.1	2.289*	
		P-600	C	1154.5	650.6	1160.8	2.263	
		L-6	A	1086.7	592.9	1093.6	2.170	2.170
		L-6	B	1082	591.8	1090.3	2.171	
		L-6	C	1105.8	603.4	1113.4	2.168	

(* Values not used for averaging)

Table 10 Results of the Gmm Test of Runway 12-30 at Sierra Blanca Regional

Project	Location	Bag No.	Wt. of Sample in air g (A)	Wt. of Flask with water g (B)	Wt. of Flask with Water and Sample g (C)	G_{mm} = A/(A+B-C)
SB	RW 17-	P-600	1023.2	2565.1	3153.6	2.354
		L-6	1229.0	2565.1	3262.7	2.313

Table 11 Void Ratio of Runway 12-30 at Sierra Blanca Regional

Project	Location	Bag No.	G_{mm}	G_{mb}	% Voids = 100* (G_{mm} - G_{mb})/ G_{mm}
SB	RW 17-30	P-600	2.354	2.270	3.56
		L-6	2.313	2.170	6.17

Table 12 Results of Asphalt Content Test of Runway 12-30 at Sierra Blanca Regional

Project	Location	Bag No.	Sample Weight (g)	Weight Loss (g)	Percent Loss %	Temp Comp %	Bitumen Ratio %	Calibrated Asphalt Content %
SB	RW	P-600	2685	178.0	6.63	0.11	6.99	6.52
		L-6	2583	164.6	6.37	0.12	6.69	6.26

Values taken directly from the printout of NCAT Asphalt Content Tester

Table 13 Results of the Resilient Modulus Test of Runway 2-20 at Raton Municipal

Project	Location	Bag No.	Core No.	Sitting load lb (P_o)	Repeated load, lb (P)	Horizontal Deflection 10^{-6} inches (H)	Average Thickness inches (t)	Resilient Modulus Mr = 0.62[(P-P_o)/Ht] psi	Average Resilient Modulus psi
Raton Municipal	RW 02-20	V 18	A	7	49	39	2.61	255821	243639
		V 18	B	6	42	42	2.53	210051*	
		V 18	C	6	44	39	2.61	231457	
		F 19	A	2	48	37	3.00	256937	262871
		F 19	B	1	44	38	2.61	268804	
		F 19	C	6	48	38	3.00	228421	

(Poisson's Ratio assumed to be 0.35)

(* Values not used for averaging)

Table 14 Results of the Indirect Tensile Test of Runway 2-20 at Raton Municipal

Project	Location	Bag No.	Core No.	Diameter inches (D)	Maximum load, lbf (P)	Average Thickness inches (t)	IDT Strength S_t = [(2 P)/(π D t)] psi	Average IDT Strength psi
Raton Municipal	RW 02-20	V 18	A	4.0	2371.2	2.61	144.6	146.1
		V 18	B	4.0	3420.6	2.53	215.2*	
		V 18	C	4.0	2420.1	2.61	147.6	
		F 19	A	4.0	3967.1	3.00	210.4*	183.4
		F 19	B	4.0	2851	2.61	173.8	
		F 19	C	4.0	3638.8	3.00	193.0	

(* Values not used for averaging)

Table 15 Results of the G_{mb} Test of Runway 2-20 at Raton Municipal Airport

Project	Location	Bag No.	Core No.	Weight in air, (g) (A)	Weight in water, (g) (B)	Weight surface dry, (g) (C)	G_{mb} = [A/(C-B)]	Average G_{mb}
Raton Municipal	RW 02-20	V 18	A	1176.5	657.1	1178.2	2.258	2.250
		V 18	B	1159.8	646.7	1162.6	2.248	
		V 18	C	1177.7	653.8	1178.9	2.243	
		F 19	A	1388.9	773.7	1391.7	2.247	2.264
		F 19	B	1247.0	708.5	1247.6	2.313	
		F 19	C	1374.4	768.4	1384.5	2.231	

Table 16 Results of the Gmm Test of Runway 2-20 at Raton Municipal

Project	Location	Bag No.	Wt. of Sample in air g (A)	Wt. of Flask with water g (B)	Wt. of Flask with Water and Sample g (C)	G_{mm} = A/(A+B-C)
Raton	RW 02-	V 18	1003.0	2565.1	3139.0	2.337
		F 19	1059.2	2565.1	3181.2	2.390

Table 17 Void Ratio of Runway 2-20 at Raton Municipal Airport

Project	Location	Bag No.	G_{mm}	G_{mb}	% Voids = 100* (G_{mm} - G_{mb})/ G_{mm}
Raton	RW 02-20	V 18	2.337	2.250	3.74
		F 19	2.390	2.264	5.29

Table 18 Results of the Asphalt Content Test of Runway 2-20 at Raton Municipal

Project	Location	Bag No.	Sample Weight (g)	Weight Loss (g)	Percent Loss %	Temp Comp %	Bitumen Ratio %	Calibrated Asphalt Content %
Rat	RW	V 18	3456	278.0	8.04	0.09	8.66	7.96
		F 19	3955	311.8	7.88	0.08	8.48	7.81

Values taken directly from the printout of NCAT Asphalt Content Tester

Table 19 Results of the Resilient Modulus Test of Runway 7-25 at Raton Municipal

Project	Location	Bag No.	Core No.	Sitting load lb (P_o)	Repeated load, lb (P)	Horizontal Deflection 10^{-6} inches (H)	Average Thickness inches (t)	Resilient Modulus Mr = 0.62[(P-P_o)/Ht] psi	Average Resilient Modulus psi
Raton Municipal	RW 07-25	U 68	A	6	45	41	2.30	256416	255471
		U 68	B	7	46	38	2.50	254526	
		U 68	C	5	42	45	2.52	202293*	
		R 60	A	3	45	37	2.80	251351*	270965
		R 60	B	3	41	39	2.22	272118	
		R 60	C	2	45	41	2.41	269811	

(Poisson's Ratio assumed to be 0.35)

(* Values not used for averaging)

Table 20 Results of the Indirect Tensile Test of Runway 7-25 at Raton Municipal

Project	Location	Bag No.	Core No.	Diameter inches (D)	Maximum load, lbf (P)	Average Thickness inches (t)	IDT Strength $S_t = [(2 P)/(\pi D t)]$ psi	Average IDT Strength psi
Raton Municipal	RW 07-25	U 68	A	4.0	1891.4	2.30	130.9	155.2
		U 68	B	4.0	3390.3	2.50	215.8*	
		U 68	C	4.0	2842.9	2.52	179.5	
		R 60	A	4.0	3647.7	2.80	207.3	207.0
		R 60	B	4.0	2882.8	2.22	206.6	
		R 60	C	4.0	3023.7	2.41	199.7	

(* Values not used for averaging)

Table 21 Results of the G_{mb} Test of Runway 7-25 at Raton Municipal Airport

Project	Location	Bag No.	Core No.	Weight in air, (g) (A)	Weight in water, (g) (B)	Weight surface dry, (g) (C)	$G_{mb} = [A/(C-B)]$	Average G_{mb}
Raton Municipal	RW 07-25	U 68	A	1029.8	559.9	1031.6	2.183	2.137
		U 68	B	1053.1	564.4	1060.8	2.121	
		U 68	C	1042.7	556.2	1050.9	2.108	
		R 60	A	1271.8	682.9	1278.2	2.136	2.153
		R 60	B	1035.5	570.1	1040.8	2.200	
		R 60	C	1082.7	576.6	1086.4	2.124	

Table 22 Results of the Gmm Test of Runway 7-25 at Raton Municipal

Project	Location	Bag No.	Wt. of Sample in air g (A)	Wt. of Flask with water g (B)	Wt. of Flask with Water and Sample g (C)	G_{mm} = A/(A+B-C)
Raton	RW 07-	U 68	1020.1	2565.1	3150.3	2.346
		R 60	1049.5	2565.1	3182.3	2.428

Table 23 Void Ratio of Runway 7-25 at Raton Municipal Airport

Project	Location	Bag No.	G_{mm}	G_{mb}	% Voids = 100* (G_{mm} - G_{mb})/ G_{mm}
Raton	RW 07-25	U 68	2.278	2.137	8.89
		R 60	2.390	2.153	11.32

Table 24 Results of the Asphalt Content Test of Runway 7-25 at Raton Municipal

Project	Location	Bag No.	Sample Weight (g)	Weight Loss (g)	Percent Loss %	Temp Comp %	Bitumen Ratio %	Calibrated Asphalt Content %
Rat	RW	U68	3084	286.5	9.29	0.10	7.40	6.87
		R 60	3387	372.2	10.99	0.09	6.60	6.17

Values taken directly from the printout of NCAT Asphalt Content Tester

Table 25 Results of the Resilient Modulus Test of Runway 8-26 at Moriarty Municipal

Project	Location	Bag No.	Core No.	Sitting load lb (P_o)	Repeated load, lb (P)	Horizontal Deflection 10^{-6} inches (H)	Average Thickness inches (t)	Resilient Modulus Mr = 0.62[(P-P_o)/Ht] psi	Average Resilient Modulus psi
Moriarty Municipal	RW 08-26	L 41	A	3	42	44	2.50	219818	220578
		L 41	B	3	42	36	2.58	260336*	
		L 41	C	8	43	38	2.58	221338	
		L 56	A	3	43	38	2.58	252958*	222972
		L 56	B	2	41	44	2.53	217212	
		L 56	C	8	42	36	2.56	228733	

(Poisson's Ratio assumed to be 0.35)

(* Values not used for averaging)

Table 26 Results of the Indirect Tensile Test of Runway 8-26 at Moriarty Municipal

Project	Location	Bag No.	Core No.	Diameter inches (D)	Maximum load, lbf (P)	Average Thickness inches (t)	IDT Strength S_t = [(2 P)/(π D t)] psi	Average IDT Strength psi
Moriarty Municipal	RW 08-26	L 41	A	4.0	3965.5	2.50	252.4	247.2
		L 41	B	4.0	3923.9	2.58	242.0	
		L 41	C	4.0	1793.6	2.58	110.6	
		L 56	A	4.0	5062.8	2.58	312.3	240.9
		L 56	B	4.0	3376.5	2.53	212.4	
		L 56	C	4.0	4333.7	2.56	269.4	

Table 27 Results of the G_{mb} Test of Runway 8-26 at Moriarty Municipal

Project	Location	Bag No.	Core No.	Weight in air, (g) (A)	Weight in water, (g) (B)	Weight surface dry, (g) (C)	G_{mb} = [A/(C-B)]	Average G_{mb}
Moriarty Municipal	RW 08-26	L 41	A	1215	696.5	1217	2.334	2.328
		L 41	B	1254.5	721.4	1256	2.347	
		L 41	C	1217.3	694.5	1223.3	2.302	
		L 56	A	1235.3	708.2	1240.2	2.322	2.322
		L 56	B	1226.9	706.5	1231.2	2.338	
		L 56	C	1218.6	693.8	1222.1	2.307	

Table 28 Results of the G_{mm} Test of Runway 8-26 at Moriarty Municipal

Project	Location	Bag No.	Wt. of Sample in air g (A)	Wt. of Flask with water g (B)	Wt. of Flask with Water and Sample g (C)	G_{mm} = A/(A+B-C)
Moriart	RW 08-	L 41	1774.6	2565.1	3599.7	2.398
		L 56	1200.1	2565.1	3259.2	2.372

Table 29 Void Ratio of Runway 8-26 at Moriarty Municipal

Project	Location	Bag No.	G_{mm}	G_{mb}	% Voids = 100* (G_{mm} - G_{mb})/ G_{mm}
Moriarty	RW 08-26	L 41	2.398	2.328	2.92
		L 56	2.347	2.322	2.10

Table 30 Results of the Asphalt Content Test of Runway 8-26 at Moriarty Municipal

Project	Location	Bag No.	Sample Weight (g)	Weight Loss (g)	Percent Loss %	Temp Comp %	Bitumen Ratio %	Calibrated Asphalt Content %
Mor	RW	L 41	3659	212.0	5.79	0.08	6.07	5.71
		L 56	2496	145.7	5.84	0.12	6.08	5.72

Values taken directly from the printout of NCAT Asphalt Content Tester

Table 31 Results of the Resilient Modulus Test of Runway 8-26 at Las Cruces

Project	Location	Bag No.	Core No.	Sitting load lb (P_o)	Repeated load, lb (P)	Horizontal Deflection 10^{-6} inches (H)	Average Thickness inches (t)	Resilient Modulus Mr = 0.62[(P-P_o)/Ht] psi	Average Resilient Modulus psi
Las Cruces	RW 08-26	H 48	A	2	44	38	2.72	251935*	276969
		H 48	B	2	44	35	2.68	277612	
		H 48	C	2	45	36	2.68	276327	
		H 37	A	7	48	43	2.69	219763*	255611
		H 37	B	2	47	39	2.75	260140	
		H 37	C	2	46	41	2.65	251081	

(Poisson's Ratio assumed to be 0.35)

(* Values not used for averaging)

Table 32 Results of the Indirect Tensile Test of Runway 8-26 at Las Cruces

Project	Location	Bag No.	Core No.	Diameter inches (D)	Maximum load, lbf (P)	Average Thickness inches (t)	IDT Strength $S_t = [(2 P)/(\pi D t)]$ psi	Average IDT Strength psi
Las Cruces International	RW 08-26	H 48	A	4.0	4891	2.72	286.1	289.8
		H 48	B	4.0	4943	2.68	293.5	
		H 48	C	4.0	4677	2.68	277.7*	
		H 37	A	4.0	3479	2.69	205.8	211.2
		H 37	B	4.0	3744	2.75	216.7	
		H 37	C	4.0	3075	2.65	184.7*	

(* Values not used for averaging)

Table 33 Results of the G_{mb} Test of Runway 8-26 at Las Cruces International

Project	Location	Bag No.	Core No.	Weight in air, (g) (A)	Weight in water, (g) (B)	Weight surface dry, (g) (C)	$G_{mb} = [A/(C-B)]$	Average G_{mb}
Las Cruces International	RW 08-26	H 48	A	1228.2	675.4	1231.6	2.208	2.225
		H 48	B	1249.7	693.6	1251	2.242	
		H 48	C	1229.7	680	1232.8	2.224	
		H 37	A	1166.4	634.5	1181.9	2.131	2.126
		H 37	B	1184.5	638.6	1196.7	2.122	
		H 37	C	1134	610.8	1150.1	2.103*	

(* Values not used for averaging)

Table 34 Results of the G_{mm} Test of Runway 8-26 at Las Cruces

Project	Location	Bag No.	Wt. of Sample in air g (A)	Wt. of Flask with water g (B)	Wt. of Flask with Water and Sample g (C)	G_{mm} = A/(A+B-C)
Cruces	RW 08-	H 48	1093.7	2565.1	3199.6	2.382
		H 37	1066.7	2565.1	3179.4	2.358

Table 35 Void Ratio of Runway 8-26 at Las Cruces International

Project	Location	Bag No.	G_{mm}	G_{mb}	% Voids = 100* (G_{mm} - G_{mb})/ G_{mm}
Cruces	RW 08-26	H 48	2.382	2.225	6.59
		H 37	2.358	2.126	9.83

Table 36 Results of the Asphalt Content Test of Runway 8-26 at Las Cruces

Project	Location	Bag No.	Sample Weight (g)	Weight Loss (g)	Percent Loss %	Temp Comp %	Bitumen Ratio %	Calibrated Asphalt Content %
Cru	RW	H 48	2480	252.7	10.19	0.12	11.23	10.07
		H 37	2254	129.6	5.75	0.13	5.97	5.62

Values taken directly from the printout of NCAT Asphalt Content Tester

Table 37 Results of the Resilient Modulus Test of Runway 12-30 at Las Cruces

Project	Location	Bag No.	Core No.	Sitting load lb (P_o)	Repeated load, lb (P)	Horizontal Deflection 10^{-6} inches (H)	Average Thickness inches (t)	Resilient Modulus Mr = 0.62[(P-P_o)/Ht] psi	Average Resilient Modulus psi
Las Cruces	RW 12-30	WT 656	A	2	39	39	2.72	216252*	231991
		WT 656	B	2	38	35	2.75	231896	
		WT 656	C	2	37	34	2.75	232086	
		H 21	A	2	46	32	2.74	311131*	284254
		H 21	B	2	39	31	2.74	270073	
		H 21	C	6	50	33	2.77	298436	

(Poisson's Ratio assumed to be 0.35)

(* Values not used for averaging)

Table 38 Results of the Indirect Tensile Test of Runway 12-30 at Las Cruces

Project	Location	Bag No.	Core No.	Diameter inches (D)	Maximum load, lbf (P)	Average Thickness inches (t)	IDT Strength S_t = [(2 P)/(π D t)] psi	Average IDT Strength psi
Las Cruces	RW 12-30	WT 656	A	4.0	4490	2.72	262.7	262.9
		WT 656	B	4.0	4548	2.75	263.2	
		WT 656	C	4.0	4294	2.75	248.5*	
		H 21	A	4.0	4232	2.74	245.8*	263.3
		H 21	B	4.0	4606	2.74	267.5	
		H 21	C	4.0	4510	2.77	259.1	

(* Values not used for averaging)

Table 39 Results of the G_{mb} Test of Runway 12-30 at Las Cruces International

Project	Location	Bag No.	Core No.	Weight in air, (g) (A)	Weight in water, (g) (B)	Weight surface dry, (g) (C)	G_{mb} = [A/(C-B)]	Average G_{mb}
Las Cruces International	RW 12-30	WT 656	A	1189.1	636	1191.9	2.139	2.144
		WT 656	B	1214.4	651.7	1215.6	2.154	
		WT 656	C	1195.8	641.7	1200.8	2.139	
		H 21	A	1207.1	651.7	1212.7	2.152	2.152
		H 21	B	1200.6	646.3	1206.6	2.143	
		H 21	C	1211.1	654.7	1215.2	2.161	

Table 40 Results of the G_{mm} Test of Runway 12-30 at Las Cruces

Project	Location	Bag No.	Wt. of Sample in air g (A)	Wt. of Flask with water g (B)	Wt. of Flask with Water and Sample g (C)	G_{mm} = A/(A+B-C)
Cruces	RW 17-	WT 656	1002.1	2565.1	3146.8	2.384
		H 21	996.7	2565.1	3144.1	2.386

Table 41 Void Ratio of Runway 12-30 at Las Cruces

Project	Location	Bag No.	G_{mm}	G_{mb}	% Voids = 100* (G_{mm} - G_{mb})/ G_{mm}
Cruces	RW 17-30	WT 656	2.384	2.144	10.06
		H 21	2.386	2.152	9.82

Table 42 Results of the Asphalt Content Test of Runway 12-30 at Las Cruces

Project	Location	Bag No.	Sample Weight (g)	Weight Loss (g)	Percent Loss %	Temp Comp %	Bitumen Ratio %	Calibrated Asphalt Content %
Cru	RW	WT 656	2582	162.9	6.31	0.12	6.62	6.19
		H 21	2469	145.4	5.89	0.12	6.14	5.77

Values taken directly from the printout of NCAT Asphalt Content Tester

Table 43 Results of the Resilient Modulus Test of Runway 8-26 at Grant County

Project	Location	Bag No.	Core No.	Sitting load lb (P_o)	Repeated load, lb (P)	Horizontal Deflection 10^{-6} inches (H)	Average Thickness inches (t)	Resilient Modulus Mr = 0.62[(P-P_o)/Ht] psi	Average Resilient Modulus psi
Grant County	RW 08-26	1 B	A	7	44	36	2.44	261157	245721
		1 B	B	4	43	37	2.3	284136*	
		1 B	C	4	43	42	2.5	230286	
		G 20	A	4	43	37	2.69	242942	243005
		G 20	B	4	45	42	2.49	243068	
		G 20	C	5	44	42	2.52	228458*	

(Poisson's Ratio assumed to be 0.35)

(* Values not used for averaging)

Table 44 Results of the Indirect Tensile Test of Runway 8-26 at Grant County

Project	Location	Bag No.	Core No.	Diameter inches (D)	Maximum load, lbf (P)	Average Thickness inches (t)	IDT Strength $S_t = [(2P)/(\pi D t)]$ psi	Average IDT Strength psi
Grant County	RW 08-26	1 B	A	4.0	3146	2.44	205.2	206.0
		1 B	B	4.0	2990	2.3	206.9	
		1 B	C	4.0	3091	2.5	196.8*	
		G 20	A	4.0	3832	2.69	226.7	223.8
		G 20	B	4.0	3458	2.49	221.0	
		G 20	C	4.0	3372	2.52	212.9*	

(* Values not used for averaging)

Table 45 Results of the G_{mb} Test of Runway 8-26 at Grant County Airport

Project	Location	Bag No.	Core No.	Weight in air, (g) (A)	Weight in water, (g) (B)	Weight surface dry, (g) (C)	$G_{mb} = [A/(C-B)]$	Average G_{mb}
Grant County	RW 08-26	1 B	A	1078.88	602.2	1079.9	2.258	2.261
		1 B	B	1057.0	589.9	1057.9	2.259	
		1 B	C	1097.7	613.8	1098.5	2.265	
		G 20	A	1177.1	647.3	1177.8	2.219	2.215
		G 20	B	1093.3	601.2	1094.4	2.217	
		G 20	C	1109.5	607.8	1110.3	2.208	

Table 46 Results of the G_{mm} Test of Runway 8-26 at Grant County

Project	Location	Bag No.	Wt. of Sample in air g (A)	Wt. of Flask with water g (B)	Wt. of Flask with Water and Sample g (C)	G_{mm} = A/(A+B-C)
Grant	RW 08-	1 B	1027.1	2565.1	3162.8	2.392
		G 20	1006.9	2565.1	3144.3	2.354

Table 47 Void Ratio of of Runway 8-26 at Grant County

Project	Location	Bag No.	G_{mm}	G_{mb}	% Voids = 100* (G_{mm} - G_{mb})/ G_{mm}
Grant	RW 08-26	1 B	2.392	2.261	5.49
		G 20	2.354	2.215	5.93

Table 48 Results of the Asphalt Content Test of Runway 8-26 at Grant County

Project	Location	Bag No.	Sample Weight (g)	Weight Loss (g)	Percent Loss %	Temp Comp %	Bitumen Ratio %	Calibrated Asphalt Content %
Gra	RW	1 B	2143	162.2	7.57	0.14	8.05	7.45
		G 20	2311	178.5	7.72	0.13	8.24	7.59

Values taken directly from the printout of NCAT Asphalt Content Tester

Table 49 Results of the Resilient Modulus Test of Runway 4-22 at Deming Municipal

Project	Location	Bag No.	Core No.	Sitting load lb (P_o)	Repeated load, lb (P)	Horizontal Deflection 10^{-6} inches (H)	Average Thickness inches (t)	Resilient Modulus Mr = 0.62[(P-P_o)/Ht] psi	Average Resilient Modulus psi
Deming Municipal	RW 04-22	A 112	A	3	50	34	2.86	299671*	265932
		A 112	B	4	44	32	2.88	269097	
		A 112	C	3	43	33	2.86	262768	
		Q 52	A	3	43	36	2.88	239198*	244865
		Q 52	B	3	42	34	2.91	244391	
		Q 52	C	2	40	33	2.91	245340	

(Poisson's Ratio assumed to be 0.35)

(* Values not used for averaging)

Table 50 Results of the Indirect Tensile Test of Runway 4-22 at Deming Municipal

Project	Location	Bag No.	Core No.	Diameter inches (D)	Maximum load, lbf (P)	Average Thickness inches (t)	IDT Strength S_t = [(2 P)/(π D t)] psi	Average IDT Strength psi
Deming Municipal	RW 04-22	A 112	A	4.0	4763	2.86	265.0*	203.9
		A 112	B	4.0	3698	2.88	204.3	
		A 112	C	4.0	3658	2.86	203.5	
		Q 52	A	4.0	3233	2.88	178.6	176.3
		Q 52	B	4.0	3214	2.91	175.8	
		Q 52	C	4.0	3192	2.91	174.6	

(* Values not used for averaging)

Table 51 Results of the G_{mb} Test of Runway 4-22 at Deming Municipal Airport

Project	Location	Bag No.	Core No.	Weight in air, (g) (A)	Weight in water, (g) (B)	Weight surface dry, (g) (C)	G_{mb} = [A/(C-B)]	Average G_{mb}
Deming	RW 04-22	A 112	A	1285.2	690.7	1286	2.159	2.147
		A 112	B	1291.8	689.6	1292.6	2.142	
		A 112	C	1263.5	675.4	1266.1	2.139	
		Q 52	A	1258.2	666.7	1259.7	2.122	2.113
		Q 52	B	1254.7	661.4	1256.3	2.109	
		Q 52	C	1253.8	660.9	1255.3	2.109	

Table 52 Results of the G_{mm} Test of Runway 4-22 at Deming Municipal

Project	Location	Bag No.	Wt. of Sample in air g (A)	Wt. of Flask with water g (B)	Wt. of Flask with Water and Sample g (C)	G_{mm} = A/(A+B-C)
Deming	RW 04-	A 112	1003.6	2565.1	3137.7	2.329
		Q 52	1062.3	2565.1	3166.7	2.306

Table 53 Void Ratio of Runway 4-22 at Deming Municipal Airport

Project	Location	Bag No.	G_{mm}	G_{mb}	% Voids = 100* (G_{mm} - G_{mb})/ G_{mm}
Deming	RW 04-22	A 112	2.329	2.147	7.81
		Q 52	2.306	2.113	8.35

Table 54 Results of the Asphalt Content Test of Runway 4-22 at Deming Municipal

Project	Location	Bag No.	Sample Weight (g)	Weight Loss (g)	Percent Loss %	Temp Comp %	Bitumen Ratio %	Calibrated Asphalt Content %
De	RW	A 112	2372	205.2	8.65	0.13	8.25	7.59
		Q 52	2328	199.6	8.57	0.13	7.74	7.16

Values taken directly from the printout of NCAT Asphalt Content Tester

Table 55 Results of the Resilient Modulus Test of Runway 8-26 at Deming Municipal

Project	Location	Bag No.	Core No.	Sitting load lb (P_o)	Repeated load, lb (P)	Horizontal Deflection 10^{-6} inches (H)	Average Thickness inches (t)	Resilient Modulus Mr = 0.62[(P-P_o)/Ht] psi	Average Resilient Modulus psi
Deming	RW 08-26	M 399	A	2	47	35	2.99	266603	
		M 399	B	2	47	37	3.08	244823*	
		M 399	C	1	48	36	3.02	268028	267315
		L 86	A	1	49	41	2.93	247732*	
		L 86	B	2	49	39	2.86	261252	260027
		L 86	C	2	48	38	2.9	258802	

(Poisson's Ratio assumed to be 0.35)

(* Values not used for averaging)

Table 56 Results of the Indirect Tensile Test of Runway 8-26 at Deming Municipal

Project	Location	Bag No.	Core No.	Diameter inches (D)	Maximum load, lbf (P)	Average Thickness inches (t)	IDT Strength $S_t = [(2P)/(\pi D t)]$ psi	Average IDT Strength psi
Deming Municipal	RW 08-26	M 399	A	4.0	4699	2.99	250.1	254.2
		M 399	B	4.0	5000	3.08	258.3	
		M 399	C	4.0	5195	3.02	273.7*	
		L 86	A	4.0	4224	2.93	229.4	223.9
		L 86	B	4.0	3674	2.86	204.4*	
		L 86	C	4.0	3978	2.9	218.3	

(* Values not used for averaging)

Table 57 Results of the G_{mb} Test of Runway 8-26 at Deming Municipal

Project	Location	Bag No.	Core No.	Weight in air, (g) (A)	Weight in water, (g) (B)	Weight surface dry, (g) (C)	$G_{mb} = [A/(C-B)]$	Average G_{mb}
Deming Municipal	RW 08-26	M 399	A	1407.9	786.1	1408.7	2.261	2.265
		M 399	B	1430.3	800.2	1431	2.267	
		M 399	C	1435.1	802.9	1435.9	2.267	
		L 86	A	1306.6	715.8	1313.3	2.187	2.188
		L 86	B	1273.4	696.1	1277.8	2.189	
		L 86	C	1276.2	698.9	1287.8	2.167*	

(* Values not used for averaging)

Table 58 Results of the G_{mm} Test of Runway 8-26 at Deming Municipal

Project	Location	Bag No.	Wt. of Sample in air g (A)	Wt. of Flask with water g (B)	Wt. of Flask with Water and Sample g (C)	G_{mm} = A/(A+B-C)
Deming	RW 08-	M 399	1038.5	2565.1	3166.4	2.375
		L 86	1034.8	2565.1	3165.2	2.380

Table 59 Void Ratio of Runway 8-26 at Deming Municipal

Project	Location	Bag No.	G_{mm}	G_{mb}	% Voids = 100* (G_{mm} - G_{mb})/ G_{mm}
Deming	RW 08-26	M 399	2.375	2.265	4.63
		L 86	2.380	2.188	8.09

Table 60 Results of the Asphalt Content Test of Runway 8-26 at Deming Municipal

Project	Location	Bag No.	Sample Weight (g)	Weight Loss (g)	Percent Loss %	Temp Comp %	Bitumen Ratio %	Calibrated Asphalt Content %
De	RW	M 399	2464	197.8	8.03	0.12	8.61	7.91
		L 86	2401	187.8	7.82	0.12	8.36	7.70

Values taken directly from the printout of NCAT Asphalt Content Tester

Table 61 Results of the Resilient Modulus Test of Runway 3-21 at Roswell International

Project	Location	Bag No.	Core No.	Sitting load lb (P_o)	Repeated load, lb (P)	Horizontal Deflection 10^{-6} inches (H)	Average Thickness inches (t)	Resilient Modulus Mr = 0.62[(P-P_o)/Ht] psi	Average Resilient Modulus psi
Roswell International	RW 03-21	WT-IE	B	6	41	42	3.00	172222	177943
		WT-IE	C	7	44	43	2.99	178424	
		WT-IE	D	7	46	44	3.00	183182	
		WT 310	A	6	45	41	2.99	197243	191034
		WT 310	B	6	41	39	2.88	193198	
		WT 310	D	7	42	40	2.97	182660	
		Y 93	B	4	38	43	2.81	174460	181992
		Y 93	C	6	39	44	2.72	170956	
		Y 93	D	3	40	43	2.66	200560	

(Poisson's Ratio assumed to be 0.35)

Table 62 Results of the Indirect Tensile Test of Runway 3-21 at Roswell International

Project	Location	Bag No.	Core No.	Diameter inches (D)	Maximum load, lbf (P)	Average Thickness inches (t)	IDT Strength S_t = [(2 P)/(π D t)] psi	Average IDT Strength psi
Roswell International	RW 03-21	WT-IE	B	4	5769	3.00	306.0	293.7
		WT-IE	C	4	5279	2.99	281.4	
		WT-IE	D	4	4898	3.00	259.8	
		WT 310	A	4	5113	2.99	272.6	289.7
		WT 310	B	4	5548	2.88	306.9	
		WT 310	D	4	5536	2.97	296.6	
		Y 93	B	4	6096	2.81	345.2	338.9
		Y 93	C	4	5686	2.72	332.7	
		Y 93	D	4	5949	2.66	355.9	

Table 63 Results of the G_{mb} Test of Runway 3-21 at Roswell International

Project	Location	Bag No.	Core No.	Weight in air, (g) (A)	Weight in water, (g) (B)	Weight surface dry, (g) (C)	G_{mb} = [A/(C-B)]	Average G_{mb}
Roswell International	RW 03-21	WT-IE	B	1339.5	749.8	1340.8	2.266	2.256
		WT-IE	C	1341.0	740.1	1343.1	2.224	
		WT-IE	D	1378.1	773.8	1379.0	2.277	
		WT 310	A	1324.7	744.5	1327.0	2.274	2.240
		WT 310	B	1298.6	719.0	1300.6	2.233	
		WT 310	D	1298.7	716.1	1303.0	2.213	
		Y 93	B	1324.5	746.5	1327	2.282	2.281
		Y 93	C	1289.3	723.6	1291.6	2.270	
		Y 93	D	1300.6	735.4	1303.1	2.291	

Table 64 Results of G_{mm} Test of Runway 3-21 at Roswell International

Project	Location	Bag No.	Wt. of Sample in air g (A)	Wt. of Flask with water g (B)	Wt. of Flask with Water and Sample g (C)	G_{mm} = A/(A+B-C)
Roswell	RW 03-	WT IE	1029.9	2568	3158.8	2.345
		WT 310	1124.4	2568	3221.5	2.388
		Y 93	1175.2	2568	3252.0	2.393

Table 65 Void Ratio of Runway 3-21 at Roswell International

Project	Location	Bag No.	G_{mm}	G_{mb}	% Voids = 100* (G_{mm} - G_{mb})/ G_{mm}
Roswell	RW 03-21	WT IE	2.345	2.256	3.81
		WT 310	2.388	2.240	6.19
		Y 93	2.393	2.281	4.66

Table 66 Results of the Asphalt Content Test of Runway 3-21 at Roswell International

Project	Location	Bag No.	Sample Weight (g)	Weight Loss (g)	Percent Loss %	Temp Comp %	Bitumen Ratio %	Calibrated Asphalt Content %
Roswel	RW	WT IE	1808	116.0	6.42	0.17	6.69	6.25
		WT 310	2081	139.6	6.71	0.14	7.05	6.56
		Y 93	2315	146.6	6.33	0.13	6.63	6.20

Values taken directly from the printout of NCAT Asphalt Content Tester

Table 67 Results of the Resilient Modulus Test of Runway 03-21 at Belen Municipal

Project	Location	Bag No.	Core No.	Sitting load lb (P_o)	Repeated load, lb (P)	Horizontal Deflection 10^{-6} inches (H)	Average Thickness inches (t)	Resilient Modulus Mr = 0.62[(P-P_o)/Ht] psi	Average Resilient Modulus psi
Belen Municipal	RW 03-21	R99	A	8	46	46	2.25	227633	235332
		R99	B	8	46	43	2.25	243514	
		R99	C	7	45	44	2.28	234848	
		WT CX	A	7	41	39	2.25	240228	245009
		WT CX	B	8	43	40	2.20	246591	
		WT CX	C	7	45	42	2.26	248209	

(Poisson's Ratio assumed to be 0.35)

Table 68 Results of the Indirect Tensile Test of Runway 03-21 at Belen Municipal

Project	Location	Bag No.	Core No.	Diameter inches (D)	Maximum load, lbf (P)	Average Thickness inches (t)	IDT Strength S_t = [(2 P)/(π D t)] psi	Average IDT Strength psi
Belen Municipal	RW 03-21	R99	A	4	3132	2.25	221.5	214.5
		R99	B	4	2935	2.25	207.6	
		R99	C	4	2956	2.28	206.3	
		WT CX	A	4	3857	2.25	272.8	274.0
		WT CX	B	4	3805	2.20	275.2	
		WT CX	C	4	3724	2.26	262.2	

Table 69 Results of the G_{mb} Test of Runway 03-21 at Belen Municipal

Project	Location	Bag No.	Core No.	Weight in air, (g) (A)	Weight in water, (g) (B)	Weight surface dry, (g) (C)	G_{mb} = [A/(C-B)]	Average G_{mb}
Belen Municipal	RW 03-21	R99	A	1058.0	590.1	1058.9	2.257	2.262
		R99	B	1057.0	590.6	1057.8	2.262	
		R99	C	1064.2	595.5	1064.9	2.267	
		WT CX	A	1104.9	614.7	1105.4	2.252	2.260
		WT CX	B	1098.0	613.6	1098.8	2.263	
		WT CX	C	1110.6	620.7	1111.1	2.265	

Table 70 Results of the G_{mm} Test of Runway 03-21 at Belen Municipal

Project	Location	Bag No.	Wt. of Sample in air g (A)	Wt. of Flask with water g (B)	Wt. of Flask with Water and Sample g (C)	G_{mm} = A/(A+B-C)
Belen	RW 03-21	R 99	1101.6	2568	3197.0	2.331
		WT CX	1189.9	2568	3246.1	2.325

Table 71 Void Ratio of Runway 03-21 at Belen Municipal

Project	Location	Bag No.	G_{mm}	G_{mb}	% Voids = 100* (G_{mm} - G_{mb})/ G_{mm}
Belen	RW 03-21	R 99	2.331	2.262	2.96
		WT CX	2.325	2.260	2.79

Table 72 Results of the Asphalt Content Test of Runway 03-21 at Belen Municipal

Project	Location	Bag No.	Sample Weight (g)	Weight Loss (g)	Percent Loss %	Temp Comp %	Bitumen Ratio %	Calibrated Asphalt Content %
Bel	RW 03-	R 99	1921	116.6	6.07	0.16	6.31	5.91
		WT CX	2406	109.2	5.34	0.15	5.49	5.19

Values taken directly from the printout of NCAT Asphalt Content Tester

Table 73 Results of the Resilient Modulus Test of Runway 12-30 at Clayton Municipal

Project	Location	Bag No.	Core No.	Sitting load lb (P_o)	Repeated load, lb (P)	Horizontal Deflection 10^{-6} inches (H)	Average Thickness inches (t)	Resilient Modulus Mr = 0.62[(P-P_o)/Ht] psi	Average Resilient Modulus psi
Clayton Municipal	RW 12-30	Y 56	B	6	47	36	1.94	363975	353456
		Y 56	C	5	46	37	2.22	309472	
		Y 56	D	5	51	39	1.89	386922	
		I 66	A	9	46	43	2.32	229952	242449
		I 66	B	8	47	41	2.31	255306	
		I 66	D	8	47	44	2.27	242091	
		V 67	B	9	44	40	2.00	271250	295054
		V 67	C	8	43	39	1.88	295963	
		V 67	D	8	45	39	1.85	317949	

(Poisson's Ratio assumed to be 0.35)

Table 74 Results of the Indirect Tensile Test of Runway 12-30 at Clayton Municipal

Project	Location	Bag No.	Core No.	Diameter inches (D)	Maximum load, lbf (P)	Average Thickness inches (t)	IDT Strength $S_t = [(2 P)/(\pi D t)]$ psi	Average IDT Strength psi
Clayton Municipal	RW 12-30	Y 56	B	4	3287	1.94	269.6	250.8
		Y 56	C	4	3235	2.22	231.9	
		Y 56	D	4	3467	1.89	291.9	
		I 66	A	4	4456	2.32	305.6	296.9
		I 66	B	4	4183	2.31	288.2	
		I 66	D	4	4185	2.27	293.4	
		V 67	B	4	2491	2.00	198.2	214.3
		V 67	C	4	2723	1.88	230.5	
		V 67	D	4	2376	1.85	204.4	

Table 75 Results of the G_{mb} Test of Runway 12-30 at Clayton Municipal

Project	Location	Bag No.	Core No.	Weight in air, (g) (A)	Weight in water, (g) (B)	Weight surface dry, (g) (C)	$G_{mb} = [A/(C-B)]$	Average G_{mb}
Clayton Municipal	RW 12-30	Y 56	B	1009.8	587.4	1013.1	2.372	2.377
		Y 56	C	1060.3	617.8	1063.0	2.382	
		Y 56	D	1023.4	595.5	1026.1	2.377	
		I 66	A	1149.1	684.7	1150.4	2.467	2.470
		I 66	B	1146.0	682.5	1147.0	2.467	
		I 66	D	1122.6	670.8	1124.2	2.476	
		V 67	B	968.2	557.4	971.4	2.339	2.339
		V 67	C	927.2	531.9	929.9	2.330	
		V 67	D	930.1	535.8	931.7	2.349	

Table 76 Results of the G_{mm} Test of Runway 12-30 at Clayton Municipal

Project	Location	Bag No.	Wt. of Sample in air g (A)	Wt. of Flask with water g (B)	Wt. of Flask with Water and Sample g (C)	G_{mm} = A/(A+B-C)
Clayton	RW 12-30	Y 56	969.9	2553.9	3136.1	2.502
		I 66	860.0	2553.9	3082.6	2.596
		V 67	980.4	2553.9	3140.3	2.488

Table 77 Void Ratio of Runway 12-30 at Clayton Municipal

Project	Location	Bag No.	G_{mm}	G_{mb}	% Voids = 100* (G_{mm} - G_{mb})/ G_{mm}
Clayton	RW 12-30	Y 56	2.502	2.377	4.98
		I 66	2.596	2.470	4.85
		V 67	2.488	2.339	6.00

Table 78 Results of the Asphalt Content Test of Runway 12-30 at Clayton Municipal

Project	Location	Bag No.	Sample Weight (g)	Weight Loss (g)	Percent Loss %	Temp Comp %	Bitumen Ratio %	Calibrated Asphalt Content %
Clayton	RW 12-30	Y 56	1553	95.3	6.14	0.19	6.34	5.94
		I 66	1394	95.6	6.86	0.22	7.15	6.64
		V 67	1751	108.1	6.17	0.17	6.41	6.00

Values taken directly from the printout of NCAT Asphalt Content Tester

Table 79 Results of the Resilient Modulus Test of Runway 2-20 at Clayton Municipal

Project	Location	Bag No.	Core No.	Sitting load lb (P_o)	Repeated load, lb (P)	Horizontal Deflection 10^{-6} inches (H)	Average Thickness inches (t)	Resilient Modulus Mr = 0.62[(P-P_o)/Ht] psi	Average Resilient Modulus psi
Clayton Municipal	RW 2-20	V 662	A	9	45	37	2.41	250308	276951
		V 662	B	10	44	36	1.99	294249	
		V 662	C	9	43	37	1.99	286296	
		Y 79	B	10	44	35	2.19	275016	278773
		Y 79	C	9	43	34	2.38	260504	
		Y 79	D	9	43	32	2.19	300799	
		U 23	A	9	44	35	1.99	311558	304956
		U 23	B	8	43	37	2.03	288910	
		U 23	D	8	43	34	2.03	314402	

(Poisson's Ratio assumed to be 0.35)

Table 80 Results of the Indirect Tensile Test of Runway 2-20 at Clayton Municipal

Project	Location	Bag No.	Core No.	Diameter inches (D)	Maximum load, lbf (P)	Average Thickness inches (t)	IDT Strength S_t = [(2 P)/(π D t)] psi	Average IDT Strength psi
Clayton Municipal	RW 2-20	V 662	A	4	4014	2.41	265.0	249.5
		V 662	B	4	2925	1.99	233.9	
		V 662	C	4	3326	1.99	266.0	
		Y 79	B	4	4696	2.19	341.2	326.5
		Y 79	C	4	4664	2.38	311.8	
		Y 79	D	4	4522	2.19	328.6	
		U 23	A	4	2598	1.99	207.8	207.9
		U 23	B	4	2654	2.03	208.1	
		U 23	D	4	2478	2.03	194.3	

Table 81 Results of the G_{mb} Test of Runway 2-20 at Clayton Municipal

Project	Location	Bag No.	Core No.	Weight in air, (g) (A)	Weight in water, (g) (B)	Weight surface dry, (g) (C)	G_{mb} = [A/(C-B)]	Average G_{mb}
Clayton Municipal	RW 2-20	V 662	A	1154.2	649.8	1156.5	2.278	2.237
		V 662	B	887.6	488.5	888.9	2.217	
		V 662	C	883.6	487.3	885.9	2.217	
		Y 79	B	1050.1	592.6	1052.6	2.283	2.275
		Y 79	C	1175.5	661.6	1177.5	2.279	
		Y 79	D	995.0	557.6	996.9	2.265	
		U 23	A	919.2	537.0	931.8	2.328	2.349
		U 23	B	958.3	563.0	968.2	2.365	
		U 23	D	933.1	550.4	946.8	2.354	

Table 82 Results of the G_{mm} Test of Runway 2-20 at Clayton Municipal

Project	Location	Bag No.	Wt. of Sample in air g (A)	Wt. of Flask with water g (B)	Wt. of Flask with Water and Sample g (C)	G_{mm} = A/(A+B-C)
Clayton	RW 2-20	V 662	949.1	2553.9	3108.3	2.405
		Y 79	1025.7	2553.9	3150.6	2.391
		U 23	1146.1	2553.9	3240.0	2.492

Table 83 Void Ratio of Runway 2-20 at Clayton Municipal

Project	Location	Bag No.	G_{mm}	G_{mb}	% Voids = 100* (G_{mm} - G_{mb})/ G_{mm}
Clayton	RW 2-20	V 662	2.405	2.237	6.97
		Y 79	2.391	2.375	4.85
		U 23	2.492	2.349	5.72

Table 84 Results of the Asphalt Content Test of Runway 2-20 at Clayton Municipal

Project	Location	Bag No.	Sample Weight (g)	Weight Loss (g)	Percent Loss %	Temp Comp %	Bitumen Ratio %	Calibrated Asphalt Content %
Clayto	RW 2-20	V 662	1975	127.5	6.46	0.15	6.75	6.30
		Y 79	2000	129.5	6.48	0.15	6.77	6.33
		U 23	1644	85.2	5.18	0.18	5.28	5.00

Values taken directly from the printout of NCAT Asphalt Content Tester

APPENDIX V

Table 1 Gradation Results of Sample N 82 of Runway 4-22 at Double Eagle II

Sieve Size, mm	Sieve Wt., g	Sieve Wt. with Soil, g	Soil Wt. g	% Retained	Cumulative % Passing
19	495.3	525.3	30.0	1.3	98.7
9.5	482.3	993.2	510.9	21.6	77.2
4.75	531.4	1052.6	521.2	22.0	55.2
2.00	463.9	796.2	332.3	14.0	41.1
0.425	368.8	709.2	340.4	14.4	26.7
0.150	414.0	832.5	418.5	17.7	9.1
0.075	513.0	658.8	145.8	6.2	2.9
Pan	376.6	445.0	68.4	2.9	
		Total	2367.5		

Sample Weight (g): 2368.3

Table 2 Gradation Results of Sample S 28 of Runway 4-22 at Double Eagle II

Sieve Size, mm	Sieve Wt., g	Sieve Wt. with Soil, g	Soil Wt. g	% Retained	Cumulative % Passing
19	495.3	522.1	26.8	0.9	99.1
9.5	482.3	1049.7	567.4	20.1	79.0
4.75	531.4	1098.8	567.4	20.1	58.9
2.00	463.9	874.1	410.2	14.5	44.4
0.425	368.8	830.5	461.7	16.3	28.1
0.150	414.0	912.5	498.5	17.6	10.4
0.075	513.0	712.0	199.0	7.0	3.4
Pan	376.6	470.8	94.2	3.3	
		Total	2825.2		

Sample Weight (g): 2826.7

Table 3 Gradation Results of Sample P 600 of Runway 12-30 at Sierra Blanca Regional

Sieve Size, mm	Sieve Wt., g	Sieve Wt. with Soil, g	Soil Wt. g	% Retained	Cumulative % Passing
19	495.3	547.3	52.0	2.1	97.9
9.5	482.3	1022.1	539.8	21.6	76.3
4.75	531.4	957.0	425.6	17.0	59.3
2.00	463.9	1015.3	551.4	22.1	37.3
0.425	368.8	879.1	510.3	20.4	16.9
0.150	414.0	603.7	189.7	7.6	9.3
0.075	513.0	596.2	83.2	3.3	5.9
Pan	376.6	523.9	147.3	5.9	
		Total	2499.3		

Sample Weight (g): 2500.5

Table 4 Gradation Results of Sample L 6 of Runway 12-30 at Sierra Blanca Regional

Sieve Size, mm	Sieve Wt., g	Sieve Wt. with Soil, g	Soil Wt. g	% Retained	Cumulative % Passing
19	495.3	495.3	0.0	0.0	100.0
9.5	482.3	1034.1	551.8	22.9	77.1
4.75	531.4	1002.4	471.0	19.5	57.6
2.00	463.9	967.0	503.1	20.9	36.7
0.425	368.8	834.4	465.6	19.3	17.4
0.150	414.0	602.9	188.9	7.8	9.6
0.075	513.0	595.7	82.7	3.4	6.2
Pan	376.6	524.6	148.0	6.1	
		Total	2411.1		

Sample Weight (g): 2412.4

Table 5 Gradation Results of Sample V 18 of Runway 2-20 at Raton Municipal

Sieve Size, mm	Sieve Wt., g	Sieve Wt. with Soil, g	Soil Wt. g	% Retained	Cumulative % Passing
19	495.3	626.8	131.5	4.1	95.9
9.5	482.3	1053.4	571.1	18.0	77.9
4.75	531.4	1256.1	724.7	22.8	55.1
2.00	463.9	956.5	492.6	15.5	39.6
0.425	368.8	977.4	608.6	19.1	20.5
0.150	414.0	772.1	358.1	11.3	9.2
0.075	327.3	456.5	129.2	4.1	5.2
Pan	376.6	540.6	164.0	5.2	
		Total	3179.8		

Sample Weight (g): 3180.5

Table 6 Gradation Results of Sample F 19 of Runway 2-20 at Raton Municipal

Sieve Size, mm	Sieve Wt., g	Sieve Wt. with Soil, g	Soil Wt. g	% Retained	Cumulative % Passing
19	495.3	576.5	81.2	2.2	97.8
9.5	482.3	1053.2	570.9	15.7	82.0
4.75	531.4	1477.4	946.0	26.0	56.0
2.00	463.9	1220.5	756.6	20.8	35.2
0.425	368.8	994.0	625.2	17.2	18.0
0.150	414.0	767.8	353.8	9.7	8.2
0.075	327.3	461.4	134.1	3.7	4.5
Pan	376.6	539.4	162.8	4.5	
		Total	3630.6		

Sample Weight (g): 3632.7

Table 7 Gradation Results of Sample U 68 of Runway 7-25 at Raton Municipal

Sieve Size, mm	Sieve Wt., g	Sieve Wt. with Soil, g	Soil Wt. g	% Retained	Cumulative % Passing
19	495.3	495.3	0.0	0.0	100.0
9.5	482.3	811.9	329.6	11.5	88.5
4.75	531.4	1433.6	902.2	31.4	57.1
2.00	463.9	1073.6	609.7	21.2	35.9
0.425	368.8	846.8	478.0	16.6	19.3
0.150	414.0	695.7	281.7	9.8	9.5
0.075	327.3	455.9	128.6	4.5	5.0
Pan	376.6	518.5	141.9	4.9	
		Total	2871.7		

Sample Weight (g): 2872.9

Table 8 Gradation Results of Sample R 60 of Runway 7-25 at Raton Municipal

Sieve Size, mm	Sieve Wt., g	Sieve Wt. with Soil, g	Soil Wt. g	% Retained	Cumulative % Passing
19	495.3	495.3	0.0	0.0	100.0
9.5	482.3	908.1	425.8	13.5	86.5
4.75	531.4	1506.3	974.9	31.0	55.4
2.00	463.9	1080.3	616.4	19.6	35.8
0.425	368.8	902.4	533.6	17.0	18.9
0.150	414.0	723.8	309.8	9.9	9.0
0.075	327.3	455.8	128.5	4.1	4.9
Pan	376.6	528.8	152.2	4.8	
		Total	3141.2		

Sample Weight (g): 3143.2

Table 9 Gradation Results of Sample L 41 of Runway 8-26 at Moriarty Municipal

Sieve Size, mm	Sieve Wt., g	Sieve Wt. with Soil, g	Soil Wt. g	% Retained	Cumulative % Passing
19	495.3	630.8	135.5	3.9	96.1
9.5	482.3	1665.9	1183.6	34.5	61.6
4.75	531.4	1194.6	663.2	19.3	42.3
2.00	463.9	959.2	495.3	14.4	27.8
0.425	368.8	799.6	430.8	12.5	15.3
0.150	414.0	589.1	175.1	5.1	10.2
0.075	514.4	656.2	141.8	4.1	6.1
Pan	376.6	582.6	206.0	6.0	
		Total	3431.3		

Sample Weight (g): 3433.0

Table 10 Gradation Results of Sample L 56 of Runway 8-26 at Moriarty Municipal

Sieve Size, mm	Sieve Wt., g	Sieve Wt. with Soil, g	Soil Wt. g	% Retained	Cumulative % Passing
19	495.3	545.0	49.7	2.1	97.9
9.5	482.3	1205.0	722.7	30.7	67.2
4.75	531.4	1042.4	511.0	21.7	45.5
2.00	463.9	838.6	374.7	15.9	29.5
0.425	368.8	675.9	307.1	13.1	16.5
0.150	414.0	536.3	122.3	5.2	11.3
0.075	514.4	614.5	100.1	4.3	7.0
Pan	376.6	533.7	157.1	6.7	
		Total	2344.7		

Sample Weight (g): 2352.9

Table 11 Gradation Results of Sample H 48 of Runway 8-26 at Las Cruces International

Sieve Size, mm	Sieve Wt., g	Sieve Wt. with Soil, g	Soil Wt. g	% Retained	Cumulative % Passing
19	494.8	494.8	0.0	0.0	100.0
9.5	481.7	1128.6	646.9	27.6	72.4
4.75	530.6	1081.2	550.6	23.5	48.9
2.00	661.0	1033.7	372.7	15.9	33.0
0.425	368.6	751.0	382.4	16.3	16.7
0.150	413.8	624.9	211.1	9.0	7.7
0.075	344.8	397.6	52.8	2.3	5.5
Pan	473.1	601.2	128.1	5.5	
		Total	2344.6		

Sample Weight (g): 2344.8

Table 12 Gradation Results of Sample H 37 of Runway 8-26 at Las Cruces International

Sieve Size, mm	Sieve Wt., g	Sieve Wt. with Soil, g	Soil Wt. g	% Retained	Cumulative % Passing
19	494.8	494.8	0.0	0.0	100.0
9.5	481.7	937.6	455.9	21.5	78.5
4.75	530.6	1061.2	530.6	25.1	53.4
2.00	661.0	1036.2	375.2	17.7	35.7
0.425	368.6	745.8	377.2	17.8	17.9
0.150	413.8	625.4	211.6	10.0	7.9
0.075	344.8	395.7	50.9	2.4	5.5
Pan	473.1	588.5	115.4	5.4	
		Total	2116.8		

Sample Weight (g): 2117.5

Table 13 Gradation Results of Sample WT 656 of Runway 12-30 at Las Cruces Int'l

Sieve Size, mm	Sieve Wt., g	Sieve Wt. with Soil, g	Soil Wt. g	% Retained	Cumulative % Passing
19	494.8	495.3	0.5	0.0	100.0
9.5	481.7	801.8	320.1	13.3	86.7
4.75	530.6	1199.9	669.3	27.8	58.9
2.00	661.0	1093.6	432.6	17.9	41.0
0.425	368.6	712.2	343.6	14.3	26.7
0.150	413.8	761.5	347.7	14.4	12.3
0.075	344.8	537.0	192.2	8.0	4.4
Pan	473.1	577.4	104.3	4.3	
		Total	2410.3		

Sample Weight (g): 2411.0

Table 14 Gradation Results of Sample H 21 of Runway 12-30 at Las Cruces International

Sieve Size, mm	Sieve Wt., g	Sieve Wt. with Soil, g	Soil Wt. g	% Retained	Cumulative % Passing
19	494.8	552.8	58.0	2.5	97.5
9.5	481.7	915.5	433.8	18.7	78.9
4.75	530.6	1070.0	539.4	23.2	55.7
2.00	661.0	1042.6	381.6	16.4	39.3
0.425	368.6	682.1	313.5	13.5	25.8
0.150	413.8	731.4	317.6	13.7	12.1
0.075	344.8	523.7	178.9	7.7	4.4
Pan	473.1	575.5	102.4	4.4	
		Total	2325.2		

Sample Weight (g): 2325.8

Table 15 Gradation Results of Sample 1 B of Runway 8-26 at Grant County

Sieve Size, mm	Sieve Wt., g	Sieve Wt. with Soil, g	Soil Wt. g	% Retained	Cumulative % Passing
19	494.8	535.3	40.5	2.0	98.0
9.5	481.7	977.7	496.0	25.0	73.0
4.75	530.6	809.6	279.0	14.1	58.9
2.00	661.0	940.2	279.2	14.1	44.9
0.425	368.6	877.8	509.2	25.6	19.2
0.150	413.8	629.7	215.9	10.9	8.3
0.075	344.8	430.7	85.9	4.3	4.0
Pan	473.1	552.1	79.0	4.0	
		Total	1984.7		

Sample Weight (g): 1985.3

Table 16 Gradation Results of Sample G 20 of Runway 8-26 at Grant County

Sieve Size, mm	Sieve Wt., g	Sieve Wt. with Soil, g	Soil Wt. g	% Retained	Cumulative % Passing
19	494.8	536.8	42.0	1.9	98.1
9.5	481.7	983.8	502.1	23.3	74.8
4.75	530.6	833.6	303.0	14.1	60.7
2.00	661.0	947.9	286.9	13.3	47.4
0.425	368.6	952.4	583.8	27.1	20.3
0.150	413.8	674.0	260.2	12.1	8.2
0.075	514.4	568.8	54.4	2.5	5.7
Pan	473.1	595.3	122.2	5.7	
		Total	2154.6		

Sample Weight (g): 2155.4

Table 17 Gradation Results of Sample A 112 of Runway 4-22 at Deming Municipal

Sieve Size, mm	Sieve Wt., g	Sieve Wt. with Soil, g	Soil Wt. g	% Retained	Cumulative % Passing
19	495.0	495.0	0.0	0.0	100.0
9.5	481.9	696.5	214.6	9.9	90.1
4.75	531.0	997.4	466.4	21.6	68.5
2.00	661.2	1142.7	481.5	22.3	46.2
0.425	368.5	939.9	571.4	26.4	19.8
0.150	413.8	674.2	260.4	12.0	7.7
0.075	513.9	541.2	27.3	1.3	6.5
Pan	473.3	612.5	139.2	6.4	
		Total	2160.8		

Sample Weight (g): 2161.1

Table 18 Gradation Results of Sample Q 52 of Runway 4-22 at Deming Municipal

Sieve Size, mm	Sieve Wt., g	Sieve Wt. with Soil, g	Soil Wt. g	% Retained	Cumulative % Passing
19	495.0	495.0	0.0	0.0	100.0
9.5	481.9	749.2	267.3	12.6	87.4
4.75	531.0	1010.8	479.8	22.5	64.9
2.00	661.2	1129.6	468.4	22.0	42.9
0.425	368.5	878.8	510.3	24.0	18.9
0.150	413.8	656.0	242.2	11.4	7.5
0.075	513.9	598.6	84.7	4.0	3.5
Pan	473.3	547.9	74.6	3.5	
		Total	2127.3		

Sample Weight (g): 2128.1

Table 19 Gradation Results of Sample M 399 of Runway 8-26 at Deming Municipal

Sieve Size, mm	Sieve Wt., g	Sieve Wt. with Soil, g	Soil Wt. g	% Retained	Cumulative % Passing
19	494.8	494.8	0.0	0.0	100.0
9.5	481.7	859.7	378.0	16.7	83.3
4.75	530.6	1092.5	561.9	24.8	58.6
2.00	661.0	1101.4	440.4	19.4	39.1
0.425	368.6	798.3	429.7	18.9	20.2
0.150	413.8	632.8	219.0	9.7	10.5
0.075	344.8	455.1	110.3	4.9	5.7
Pan	473.1	601.5	128.4	5.7	
		Total	2267.7		

Sample Weight (g): 2267.9

Table 20 Gradation Results of Sample L 86 of Runway 8-26 at Deming Municipal

Sieve Size, mm	Sieve Wt., g	Sieve Wt. with Soil, g	Soil Wt. g	% Retained	Cumulative % Passing
19	494.8	526.7	31.9	1.4	98.6
9.5	481.7	946.5	464.8	21.1	77.5
4.75	530.6	1084.6	554.0	25.1	52.4
2.00	661.0	1043.2	382.2	17.3	35.1
0.425	368.6	738.7	370.1	16.8	18.3
0.150	413.8	620.7	206.9	9.4	9.0
0.075	514.4	600.1	85.7	3.9	5.1
Pan	473.1	583.9	110.8	5.0	
		Total	2206.4		

Sample Weight (g): 2207.8

Table 21 Gradation Results of Sample WT 310 of Runway 3-21 at Roswell International

Sieve Size, mm	Sieve Wt., g	Sieve Wt. with Soil, g	Soil Wt. g	% Retained	Cumulative % Passing
19	495.0	495.0	0.0	0.0	100.0
9.5	481.9	766.5	284.6	14.9	85.1
4.75	531.0	1005.9	474.9	24.8	60.3
2.00	661.2	1036.7	375.5	19.6	40.7
0.425	368.5	680.7	312.2	16.3	24.4
0.150	413.8	647.5	233.7	12.2	12.1
0.075	344.8	471.9	127.1	6.6	5.5
Pan	473.3	576.2	102.9	5.4	
		Total	1910.9		

Sample Weight (g): 1913.2

Table 22 Gradation Results of Sample Y 93 of Runway 3-21 at Roswell International

Sieve Size, mm	Sieve Wt., g	Sieve Wt. with Soil, g	Soil Wt. g	% Retained	Cumulative % Passing
19	495.0	495.0	0.0	0.0	100.0
9.5	481.9	621.7	139.8	13.4	86.6
4.75	531.0	791.7	260.7	24.9	61.7
2.00	661.2	852.8	191.6	18.3	43.4
0.425	368.5	554.9	186.4	17.8	25.6
0.150	413.8	551.0	137.2	13.1	12.5
0.075	344.8	411.8	67.0	6.4	6.1
Pan	473.3	534.3	61.0	5.8	
		Total	1043.7		

Sample Weight (g): 1046.9

Table 23 Gradation Results of Sample WT IE of Runway 3-21 at Roswell International

Sieve Size, mm	Sieve Wt., g	Sieve Wt. with Soil, g	Soil Wt. g	% Retained	Cumulative % Passing
19	495.0	506.5	11.5	1.1	98.9
9.5	481.9	671.3	189.4	18.1	80.8
4.75	531.0	838.8	307.8	29.4	51.4
2.00	661.2	880.6	219.4	21.0	30.4
0.425	368.5	511.7	143.2	13.7	16.7
0.150	413.8	496.3	82.5	7.9	8.8
0.075	344.8	392.3	47.5	4.5	4.3
Pan	473.3	516.3	43.0	4.1	
		Total	1044.3		

Sample Weight (g): 1046.1

Table 24 Gradation Results of Sample R 99 of Runway 3-21 at Belen Municipal

Sieve Size, mm	Sieve Wt., g	Sieve Wt. with Soil, g	Soil Wt. g	% Retained	Cumulative % Passing
19	495.0	495.0	0.0	0.0	100.0
9.5	481.9	765.3	283.4	22.7	77.3
4.75	531.0	771.6	240.6	19.3	58.1
2.00	661.2	826.7	165.5	13.2	44.8
0.425	368.5	618.1	249.6	20.0	24.9
0.150	413.8	610.3	196.5	15.7	9.1
0.075	344.8	413.2	68.4	5.5	3.7
Pan	473.3	516.2	42.9	3.4	
		Total	1246.9		

Sample Weight (g): 1249.8

Table 25 Gradation Results of Sample WT CX of Runway 3-21 at Belen Municipal

Sieve Size, mm	Sieve Wt., g	Sieve Wt. with Soil, g	Soil Wt. g	% Retained	Cumulative % Passing
19	495.0	495.0	0.0	0.0	100.0
9.5	481.9	820.9	339.0	29.3	70.7
4.75	531.0	852.8	321.8	27.8	42.9
2.00	661.2	834.6	173.4	15.0	27.9
0.425	368.5	541.1	172.6	14.9	13.0
0.150	413.8	487.7	73.9	6.4	6.6
0.075	344.8	375.8	31.0	2.7	3.9
Pan	473.3	515.2	41.9	3.6	
		Total	1153.6		

Sample Weight (g): 1157.0

Table 26 Gradation Results of Sample Y 56 of Runway 3-21 at Belen Municipal

Sieve Size, mm	Sieve Wt., g	Sieve Wt. with Soil, g	Soil Wt. g	% Retained	Cumulative % Passing
19	494.6	494.6	0.0	0.0	100.0
9.5	481.4	823.9	342.5	23.9	76.1
4.75	530.2	886.0	355.8	24.9	51.2
2.00	660.8	877.5	216.7	15.1	36.1
0.425	368.6	684.0	315.4	22.0	14.0
0.150	413.3	527.0	113.7	7.9	6.1
0.075	344.0	378.9	34.9	2.4	3.6
Pan	472.5	524.0	51.5	3.6	
		Total	1430.5		

Sample Weight (g): 1430.9

Table 27 Gradation Results of Sample I 66 of Runway 3-21 at Belen Municipal

Sieve Size, mm	Sieve Wt., g	Sieve Wt. with Soil, g	Soil Wt. g	% Retained	Cumulative % Passing
19	494.6	494.6	0.0	0.0	100.0
9.5	481.4	730.0	248.6	19.7	80.3
4.75	530.2	847.6	317.4	25.1	55.2
2.00	660.8	864.7	203.9	16.1	39.1
0.425	368.6	667.4	298.8	23.6	15.5
0.150	413.3	513.8	100.5	7.9	7.5
0.075	344.0	381.3	37.3	3.0	4.6
Pan	472.5	530.3	57.8	4.6	
		Total	1264.3		

Sample Weight (g): 1264.4

Table 28 Gradation Results of Sample V 67 of Runway 3-21 at Belen Municipal

Sieve Size, mm	Sieve Wt., g	Sieve Wt. with Soil, g	Soil Wt. g	% Retained	Cumulative % Passing
19	494.6	494.6	0.0	0.0	100.0
9.5	481.4	734.4	253.0	18.8	81.2
4.75	530.2	887.5	357.3	26.6	54.6
2.00	660.8	873.9	213.1	15.9	38.8
0.425	368.6	671.0	302.4	22.5	16.3
0.150	413.3	526.6	113.3	8.4	7.8
0.075	344.0	383.0	39.0	2.9	4.9
Pan	472.5	538.3	65.8	4.9	
		Total	1343.9		

Sample Weight (g): 1344.4

Table 29 Gradation Results of Sample V 662 of Runway 2-20 at Clayton Municipal

Sieve Size, mm	Sieve Wt., g	Sieve Wt. with Soil, g	Soil Wt. g	% Retained	Cumulative % Passing
19	494.6	494.6	0.0	0.0	100.0
9.5	481.4	668.7	187.3	19.6	80.4
4.75	530.2	719.2	189.0	19.8	60.6
2.00	660.8	803.6	142.8	15.0	45.6
0.425	368.6	546.1	177.5	18.6	27.0
0.150	413.3	559.8	146.5	15.4	11.6
0.075	344.0	392.7	48.7	5.1	6.5
Pan	472.5	534.5	62.0	6.5	
		Total	953.8		

Sample Weight (g): 954.0

Table 30 Gradation Results of Sample Y 79 of Runway 2-20 at Clayton Municipal

Sieve Size, mm	Sieve Wt., g	Sieve Wt. with Soil, g	Soil Wt. g	% Retained	Cumulative % Passing
19	494.6	494.6	0.0	0.0	100.0
9.5	481.4	741.7	260.3	19.8	80.2
4.75	530.2	824.0	293.8	22.3	58.0
2.00	660.8	870.6	209.8	15.9	42.0
0.425	368.6	598.1	229.5	17.4	24.6
0.150	413.3	592.9	179.6	13.6	11.0
0.075	344.0	403.6	59.6	4.5	6.5
Pan	472.5	557.5	85.0	6.4	
		Total	1317.6		

Sample Weight (g): 1317.9

Table 31 Gradation Results of Sample U 23 of Runway 2-20 at Clayton Municipal

Sieve Size, mm	Sieve Wt., g	Sieve Wt. with Soil, g	Soil Wt. g	% Retained	Cumulative % Passing
19	494.6	494.6	0.0	0.0	100.0
9.5	481.4	874.6	393.2	35.9	64.1
4.75	530.2	869.1	338.9	30.9	33.2
2.00	660.8	763.8	103.0	9.4	23.8
0.425	368.6	470.0	101.4	9.2	14.6
0.150	413.3	463.9	50.6	4.6	10.0
0.075	344.0	378.7	34.7	3.2	6.8
Pan	472.5	546.7	74.2	6.8	
		Total	1096.0		

Sample Weight (g): 1096.6